

AD-A121 369

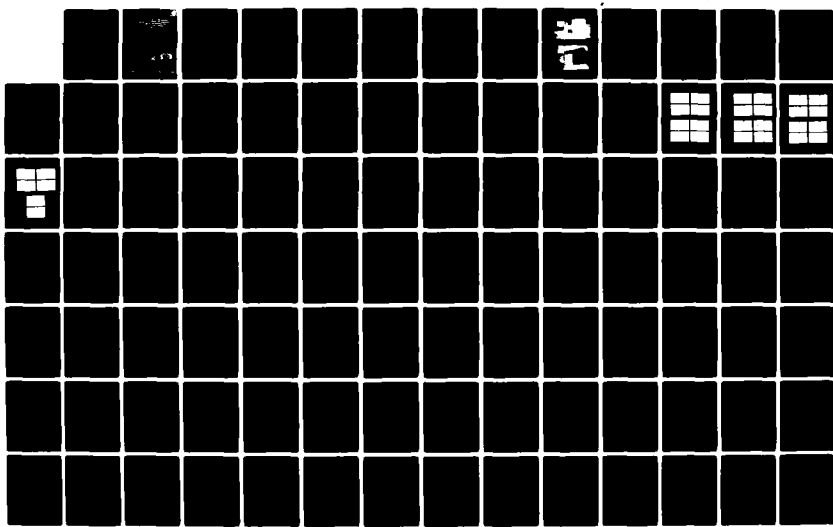
RESULTS OF LASER-CALIBRATED HIGH-RESOLUTION  
TRANSMISSION MEASUREMENTS AND .(U) NAVAL RESEARCH LAB  
WASHINGTON DC J A DOWLING ET AL. 30 SEP 82 NRL-8618

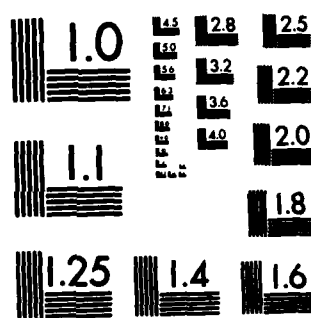
F/G 4/1

1/2

NL

UNCLASSIFIED





MICROCOPY RESOLUTION TEST CHART  
NATIONAL BUREAU OF STANDARDS-1963-A

AD A121369

REPORT DOCUMENTATION PAGE		READ INSTRUCTIONS BEFORE COMPLETING FORM
1. REPORT NUMBER NRL Report 8618	2. GOVT ACCESSION NO. AD-A121 389	3. RECIPIENT'S CATALOG NUMBER
4. TITLE (and Subtitle) <b>RESULTS OF LASER-CALIBRATED HIGH-RESOLUTION TRANSMISSION MEASUREMENTS AND COMPARISONS WITH BROADBAND TRANSMISSOMETER DATA: SAN NICOLAS ISLAND, CALIFORNIA, MAY 1979</b>		5. TYPE OF REPORT & PERIOD COVERED Final report on one phase of an NRL Problem.
7. AUTHOR(s) J. A. Dowling,* S. T. Hanley,* J. A. Curcio, G. L. Trusty, T. H. Cosden,† K. M. Haught,‡ C. O. Gott, F. A. Tidball,† G. B. Matthews,§ and A. Ackermann¶	6. PERFORMING ORG. REPORT NUMBER	
9. PERFORMING ORGANIZATION NAME AND ADDRESS Naval Research Laboratory Washington, DC 20375	10. PROGRAM ELEMENT, PROJECT, TASK AREA & WORK UNIT NUMBERS Program Element: 62759N Task Area: SF59551697 Work Unit: A0314A.307	
11. CONTROLLING OFFICE NAME AND ADDRESS Naval Ocean Systems Center San Diego, CA 92152	12. REPORT DATE September 30, 1982	
14. MONITORING AGENCY NAME & ADDRESS (if different from Controlling Office)	13. NUMBER OF PAGES 98	
16. DISTRIBUTION STATEMENT (of this Report)	15. SECURITY CLASS. (of this report) <b>UNCLASSIFIED</b>	
	18a. DECLASSIFICATION/DOWNGRADING SCHEDULE	
17. DISTRIBUTION STATEMENT (of the abstract entered in Block 20, if different from Report)		
18. SUPPLEMENTARY NOTES Present addresses: *OptiMetrics, Inc., 106 East Idaho Avé., Suite G, Las Cruces, NM 88001 †Sachs-Freeman Associates, 14300 Gallant Fox Lane, Bowie, MD 20360 (Continued)		
19. KEY WORDS (Continue on reverse side if necessary and identify by block number)		
Atmospheric transmission Laser propagation Infrared	Infrared aerosol extinction Marine atmosphere <i>(+ or -)</i>	
20. ABSTRACT (Continue on reverse side if necessary and identify by block number)	Atmospheric transmission was measured along a 4.07 km overwater path in May 1979 at San Nicolas Island (SNI), California. A deuterium fluoride (DF) laser and a high-resolution Fourier transform spectrometer (FTS) system were used to generate high-quality transmission spectra of the 4.07 km path accurate to $\pm 3$ to 5% in absolute transmission. Details and procedures used and results obtained in the absolute transmission calibration of the spectra are presented. Path-integrated values for water vapor density have been derived from the FTS spectra.	

**DD FORM 1 JAN 73 1473 EDITION OF 1 NOV 68 IS OBSOLETE**  
**S/N 0102-014-6601**

SECURITY CLASSIFICATION OF THIS PAGE (When Data Entered)

18. Supplementary Notes (Continued)

#Naval Sea Systems Command, PMS 405-42, Washington, DC 20360

\*Pacific Missile Test Center, Point Mugu, CA 93041

20. ABSTRACT (Continued)

and show good agreement with fixed-location dew-point hygrometer measurements. Comparisons of measured DF laser extinction coefficients with calculated molecular absorption values are presented which suggest modifications to existing water vapor continuum absorption models and which also provide a measure of infrared aerosol extinction. The aerosol extinction values thus derived have been found to show little correlation with concurrent measurements of visibility, windspeed, and relative humidity. Comparisons of spectral-band-averaged FTS data with Pacific Missile Test Center broadband transmissometer measurements show good average agreement with significant scatter in the data attributable in part to sizable fluctuations in transmission occurring during the time scales used to acquire the FTS data.

## CONTENTS

1. INTRODUCTION .....	1
2. EXPERIMENTAL EQUIPMENT AND PROCEDURES .....	2
3. EXPERIMENTAL RESULTS .....	6
3.1 Laser Extinction Measurements .....	6
3.2 High Resolution Fourier Transform Spectroscopy and Absolute Transmission Calibration .....	14
3.3 Path Integral Water Vapor Concentrations .....	24
3.4 Micrometeorological Measurements .....	34
3.5 Visibility Measurements .....	65
4. COMPARISONS OF MEASURED AND CALCULATED TRANSMISSION VALUES .....	65
4.1 Laser Extinction Measurements .....	65
4.2 Fourier Transform Spectrometer and Broadband Transmissometer Values .....	69
5. CONCLUSIONS AND RECOMMENDATIONS .....	78
6. ACKNOWLEDGMENTS .....	79
7. REFERENCES .....	79
APPENDIX — Aerosol Spectrometer Data .....	81

Accession For	
Funding GRA&I	
TAB	
Compound	
Specification	
Distribution	
Availability Codes	
Dist	Avail and/or Special
A	

ORIC  
COPY  
INSP 2

## RESULTS OF LASER-CALIBRATED HIGH-RESOLUTION TRANSMISSION MEASUREMENTS AND COMPARISONS WITH BROADBAND TRANSMISSOMETER DATA: SAN NICOLAS ISLAND, CALIFORNIA, MAY 1979

### 1. INTRODUCTION

This report contains the results of an experiment performed in May 1979 at San Nicolas Island (SNI), California by the Optical Radiation Branch of the Naval Research Laboratory (NRL) and by the Electromagnetic Systems Division of the Pacific Missile Test Center (PMTC). Atmospheric transmission was measured over a 4.07 km overwater path using a low-power deuterium fluoride (DF) laser together with a blackbody infrared source and a high-resolution Fourier transform spectrometer (FTS) system. The portable instrumentation facility used for these measurements is designated the Infrared Mobile Optical Radiation Laboratory (IMORL) and is described in greater detail in Section 2 of this report where additional references are given for further information. Results of laser extinction and FTS measurements are presented in Sections 3.1 and 3.2.

The measurements were performed using a 4.07 km overwater path between two shore locations on the northwest coast of SNI. Figure 1 shows the location of SNI 55 nmi from Point Mugu off the California coastline. The inset shows the relative locations of the three sites A, B, and C used in the PMTC optical transmission measurements. The NRL long-path transmission measurements described herein were performed using the 4.07 km path between sites A and C.

Meteorological measurements were performed by two NRL groups, Codes 4320 and 6530. Data were collected by Code 4320 during the experimental period as part of an extensive ongoing micrometeorological characterization of the island and are contained in a separate report. The data collected by Code 6530 are presented in Section 3.4. Visibility was measured during the experiment by use of a telemeter technique described in Section 3.5 which also contains a tabulation of results.

The measurements and analysis described in this report were supported by the Navy Electro-Optical Meteorology Program as part of an extensive program to characterize the maritime environment at SNI. An ongoing transmission measurement program conducted by PMTC under sponsorship of the Navy Optical Signatures Program used the same measurement path between sites A and C described above. Part of the measurements described in this report involved a cross-comparison of data taken with the NRL IMORL system to the PMTC transmissometer measurements so that results obtained with the two independent transmission measurement systems and procedures could be compared. These comparisons are presented and discussed in Section 4.2. Results of path-integrated water vapor density measurements derived from the NRL long-path FTS data and comparisons to point-sampled dew-point hygrometer results are presented and discussed in Section 3.3.

The data and analyses in this report show that the 3- to 5- $\mu\text{m}$  water vapor continuum absorption models when compared with the infrared transmission data show consistent disagreement. Procedures and results are described showing that high-accuracy ( $\pm 3$  to 5%) absolute transmission spectra of the overwater path at SNI can be measured with the IMORL system.

Atmospheric aerosol extinction coefficients at DF laser wavelengths obtained from the long-path transmission data show a wide range of variation and do not exhibit significant correlations with visibility, windspeed, or relative humidity.

\*Manuscript submitted April 23, 1982.

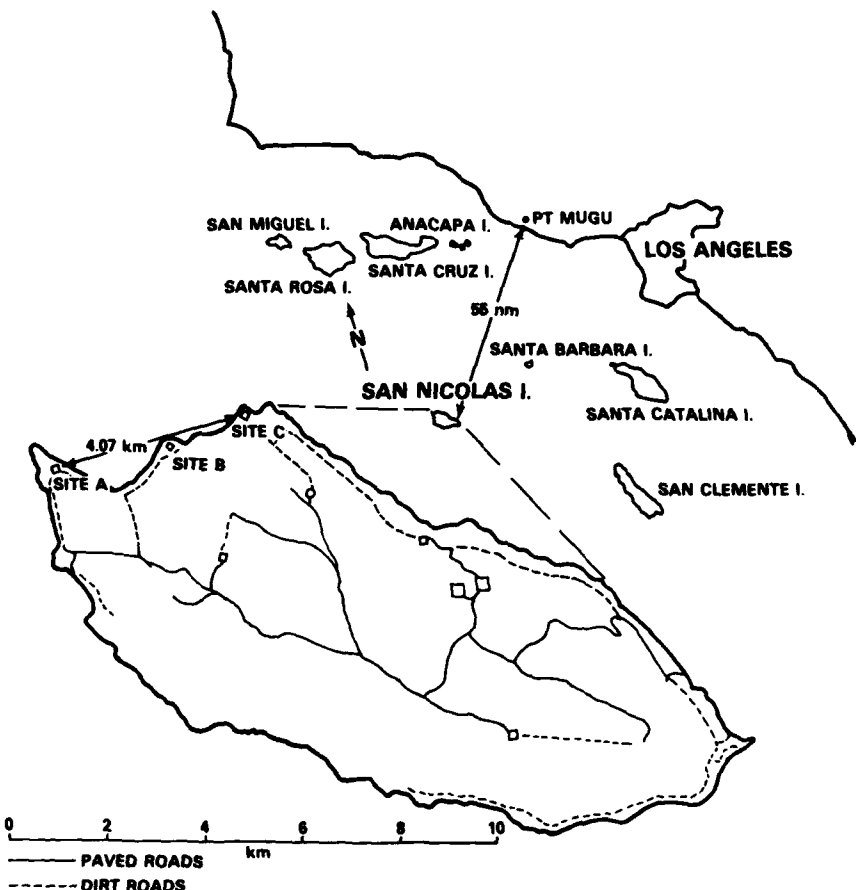


Fig. 1 — San Nicolas Island, California measurement site

Based on the results obtained in the work described in this report, it is recommended that additional long-path field measurements of laser extinction and high-resolution transmission spectra be used to improve existing atmospheric molecular absorption models, particularly for the 3- to 5- $\mu\text{m}$  water vapor continuum absorption. The need to improve the agreement between infrared aerosol extinction data derived from overwater transmission measurements, and that obtained from aerosol spectrometer measurements, is demonstrated by results presented in this report.

The importance of path-integrated measures of water vapor density and aerosol extinction coefficients for use in atmospheric transmission model evaluation is discussed, and it is recommended that measurements of this type be included in future experiments.

## 2. EXPERIMENTAL EQUIPMENT AND PROCEDURES

The Infrared Mobile Optical Radiation Laboratory (IMORL) has been developed at NRL as a field laboratory for precision atmospheric propagation measurements. Detailed descriptions of the electro-optical instrumentation contained in the IMORL facility are presented in Refs. 1 and 2. Only the essential features of the IMORL system are reviewed in the present report.

The IMORL system, used to collect laser-calibrated high-resolution atmospheric transmission spectra, comprises several infrared laser and backbody sources, large stable telescope optics, a Fourier transform spectrometer (FTS) system, and various support equipment, all of which are transported in and operated from several large semitrailers. The usual measurement configuration consists of an optical transmitter trailer housing HeNe, Nd-YAG, DF, CO, and CO<sub>2</sub> single-line cw laser sources, relay optics, and a large, stably mounted, precisely pointed, 91-cm aperture, f/35, Cassegrainian collimating telescope. The small cw combustion-driven DF laser used for much of the laser extinction work requires a large 755 l/s (1600 cfm) vacuum system for operation. This pump is housed in a separate trailer. A 20-cm-diameter vacuum line is installed once the two trailers are properly located at the measurement site. Two additional trailers contain office space, meteorological signal-processing and recording electronics, and bottled gas and other consumable supplies used during an experiment.

The FTS system and apparatus used for laser extinction measurements are housed in a receiver trailer that contains a 120-cm aperture, f/5 Newtonian telescope. The large receiver telescope aperture ensures that the entire laser beam used during long-path (typically 5 km) extinction measurements can be entirely collected, thereby providing reliable absolute transmission calibrations for the FTS measurements. High-resolution transmission spectra are taken by substituting a 1300 K blackbody source for the laser source in the transmitter optical system and adjusting the receiver optical system so as to couple the FTS system to the 120-cm collecting telescope. Repeated calibrations and extensive experience with this measurement system in field experiments have demonstrated that absolute transmission can be reliably measured for long atmospheric paths with an uncertainty less than  $\pm 3\%$ .

Figure 2 shows the transmitter trailer at site A (SNI) during the recent experiment. At the right in the figure can be seen the optical transmitter trailer. The 91-cm aperture telescope mirror and telescope frame may be seen through the open doors. The vacuum pump trailer is shown to the left in the figure; the demountable vacuum line connecting the two trailers can be seen supported about 1 m above ground level. Figure 3 shows the receiver trailer at site C (SNI), shown with the rear door open. The Newtonian telescope secondary mirror support can be seen immediately inside the open door. The inside diameter of this support frame matches the full 1.2-m diameter of the primary mirror.

Figure 4 depicts the experimental arrangement used for laser extinction measurements. The output beam from any of the several laser sources used is first collimated by auxiliary optics to a diameter of approximately 18 mm. The beam is then focused via the off-axis parabolic mirror shown in the upper left in Fig. 4 and then diverged to fill the 91-cm transmitter telescope aperture. A 37 Hz, 50% duty cycle chopper modulates the beam near the focus formed by the off-axis parabola. The beam is alternately transmitted through the telescope and reflected onto the stationary detector as shown. The mobile detector shown in Fig. 4 is placed in the "XMTR" position for calibration measurements in which the relative response of the two detectors is measured. The mobile detector is then placed near the focus of the 120-cm aperture receiver telescope for (a) calibrations of the large telescope optical efficiencies or (b) long path extinction measurements. The calibrations are measured with the transmitter and receiver trailers immediately opposite one another, i.e., for  $\sim$  zero atmospheric path. When the trailers are separated for long path measurements, the two types of calibration data are then used to determine absolute atmospheric transmission for the several laser lines studied. As shown in Fig. 4 the signal produced by the mobile detector in the receiver trailer at one end of the measurement path is relayed to the transmitter by means of a pulse-rate-modulated (PRM) GaAs-laser-based data link. This signal, proportional to laser power at the receiver, is connected to the numerator input of a special purpose analog ratiometer [2]. The stationary detector signal, proportional to the transmitted laser power, is connected to the denominator input of the ratiometer. Thus, a real-time measure of transmission for the laser line being studied is available at the transmitter site. The ratiometer reading must be corrected for the relative response of the two detectors for that laser line (monitored daily) and the efficiency of the large optical elements beyond the chopper in order to obtain absolute transmission

J. A. DOWLING ET AL.

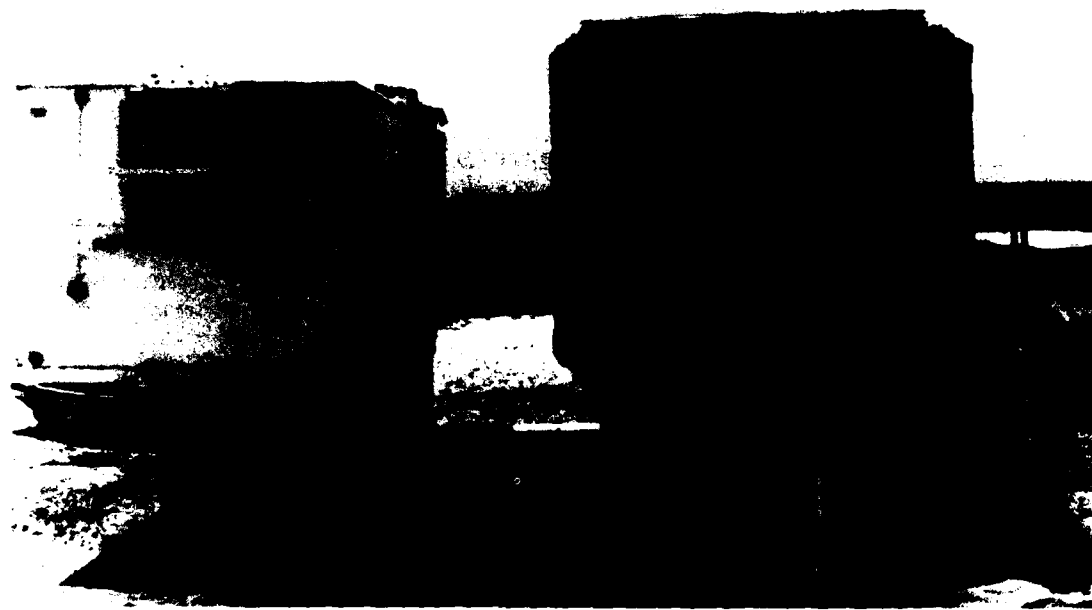


Fig. 2 - NRL-IMORL optical transmitter and vacuum pump trailers at Site A, SNI

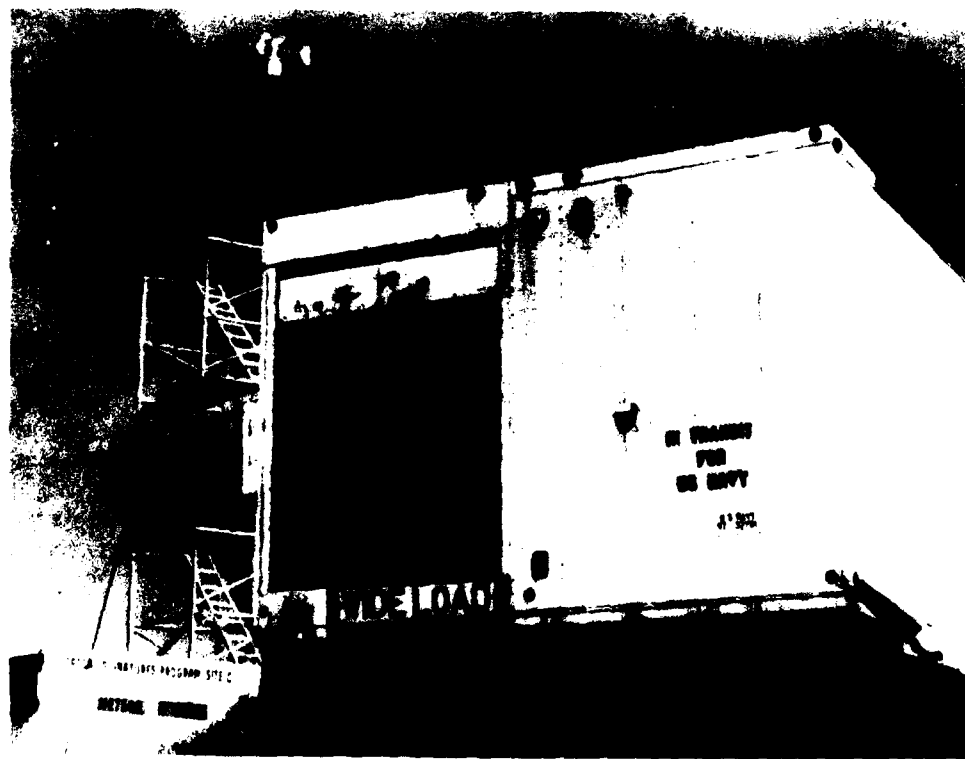


Fig. 3 - NRL-IMORL optical receiver trailer at Site C, SNI

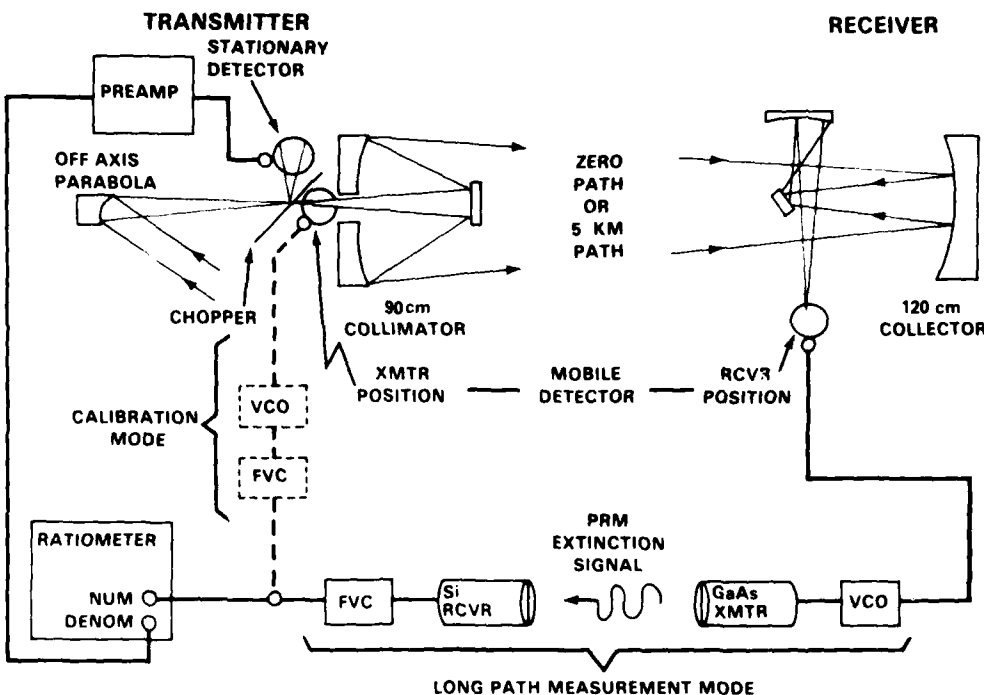


Fig. 4 — Laser extinction measurement schematic

readings. As shown in Fig. 4, the voltage-controlled oscillator (VCO) and frequency-to-voltage converter (FVC) used with the GaAs data link are also connected in the numerator circuit of the ratiometer when the mobile detector is used in the "XMTR" position, so that their combined transfer function is normalized out of the final extinction ratio. Additional information concerning the measurement instrumentation and procedures is contained in Refs. 1 and 3.

Local meteorological measurements are usually performed at each end of the measurement path to monitor absolute humidity, air temperature and pressure, and wind conditions in order to document local conditions during a series of measurements. The period required to make both laser extinction and FTS measurements in turn is typically about 1 hour. Extensive measurements using an aerosol spectrometer system have been performed during some experiments. In some cases infrared aerosol extinction estimates based on Mie scattering calculations utilizing the measured particle distributions have shown good agreement with results derived from infrared extinction measurements at DF laser wavelengths [3], especially for those situations where aerosol sampling occurs at locations representative of conditions along the entire optical path.

During this measurement on SNI we relied primarily on the NRL Aerosol Van (Code 6532) for meteorological and aerosol measurements although some meteorological values tabulated below came from the NRL Micrometeorological Tower (Code 4320). The equipment associated with the tower is described elsewhere [4]. Both facilities were located near Site A of Fig. 1. We briefly describe the Aerosol Van here.

An EG&G Model 110 system provided air temperature and dewpoint readings. An R.M. Young Gill propeller vane gave values for wind speed and wind direction. All the aerosol-particle size distributions referenced here come from two Particle Measuring Systems (PMS) particle spectrometers. The Active Scattering Aerosol Spectrometer Probe (ASAP) measured the small particles (0.13 to 0.75  $\mu\text{m}$ ),

and the High-Volume version of the Classical Scattering Aerosol Spectrometer Probe (CSASP-HV) measured the larger particles (0.75 to 15  $\mu\text{m}$ ). (All particle sizes referenced here are in terms of radius.) A data acquisition system accessed both probes and the air temperature/dew point/wind vector set simultaneously with 1-s time resolution. More details of the Aerosol Van description are in Ref. 5.

### 3. EXPERIMENTAL RESULTS

#### 3.1 Laser Extinction Measurements

Laser extinction was measured using the 4.07 km path between sites A and C on the northwest coast of SNI. The measurements were performed in conjunction with high-resolution spectroscopic measurements to provide a means for absolute transmission normalization of the FTS data. A multi-band Barnes transmissometer system was operated simultaneously by the Pacific Missile Test Center (PMTc); cross-comparisons of the two independent transmission measurements are described in Section 4.2.

Long-path laser extinction was measured on 8 days between 1 and 10 May 1979. The majority of measurements were performed using several deuterium-fluoride (DF) laser lines. A few measurements using the  $P_{20}$  (001  $\rightarrow$  010) line of the CO<sub>2</sub> laser at 10.591  $\mu\text{m}$  were possible on 8 to 10 March, since the laser was inoperable during the first several days of the experimental period.

Table 1 summarizes the transmission values measured for the series of lines in the 2  $\rightarrow$  1 DF vibrational band available from the cw DF laser source used in the experiment. The P2-8 (2  $\rightarrow$  1, P-8) line at 2631.067 cm<sup>-1</sup> was measured three times during a "run" or measurement sequence in order to ascertain constancy and repeatability of the transmission measurements. Columns 7 and 8 of Table 1 respectively list the measured transmissions T and corresponding extinction coefficients  $\alpha$  in units of km<sup>-1</sup>. Column 9 lists the calculated molecular absorption (CMA) in km<sup>-1</sup> corresponding to the meteorological conditions documented in Section 3.4. Column 10 contains the difference values, DIFF =  $\alpha - \text{CMA}$ .

The transmission values listed in Table 1 require that the zero path optical system efficiency for the extinction measurement system be known since it is part of the calibration procedure (see Refs. 1 and 3 for detailed descriptions and examples of this procedure). Due to space constraints at site A (the IMORL transmitter location) and experimental schedule requirements while the equipment was on the island, the zero-path calibrations for the data contained in this report were performed once the IMORL system was returned to the Chesapeake Bay Detachment (CBD) of NRL near Washington, D.C. Table 2 and Fig. 5 summarize the results of the optical system efficiency measurements obtained from this calibration carried out during 1 to 2 July 1979. The slight dependence of  $T_0$  on wavenumber apparent in Fig. 5 was not included in the reduction of data for this experiment since the peak-to-peak excursions represent less than  $\pm 1\%$  of the average value of  $T_0$  and are comparable in magnitude to the experimental uncertainty on each measurement of  $T_0$ . Accordingly the values shown in Table 2 were simply averaged without regard to wavelength. Using the single average value of  $T_0 = 0.722 \pm 0.0044$  greatly simplified the reduction of the long path data without introducing any significant additional error.

The values tabulated in Table 1 show that for most of the DF laser lines measured transmissions between 0.5 and 0.7 were observed. The P2-10 line, which is located on the shoulder of an atmospheric N<sub>2</sub>O absorption line, showed consistently lower transmission. The locations of the DF laser lines listed in Table 1 relative to atmospheric absorption lines are shown in detail in Section 3.2. The measurements performed on DAY 124 centered around 0133 Greenwich Mean Time (GMT) (5-3-79, 1833

## NRL REPORT 8618

Table 1 — Laser Extinction Measurement Summary

Day (GMT)	Time (GMT)	Date (PDT)	Time (PDT)	Laser Line	$\nu$ (cm $^{-1}$ )	T	$\alpha$ (km $^{-1}$ )	CMA (km $^{-1}$ )	DIFF (km $^{-1}$ )
121	1656	5-1-79	0956	P2-8	2631.067	.836	.044	.044	.000
	1657		0957	P2-7	2655.863	.660	.102	.099	.003
	1658		0958	P2-6	2680.179	.740	.074	.078	-.004
	1659		0959	P2-5	2703.999	.836	.044	.057	-.013
	1701		1001	P2-4	2727.309	.797	.058	.078	-.020
	1704		1004	P2-8	2631.067	.841	.043	.044	-.001
	1705		1005	P2-9	2605.806	.756	.069	.057	.012
	1707		1007	P2-10	2580.096	.638	.110	.083	.027
	1708		1008	P2-8	2631.067	.796	.056	.044	.012
121	2038	5-1-79	1338	P2-8	2631.067	.732	.077	.044	.033
	2040		1340	P2-7	2655.863	.603	.124	.099	.025
	2041		1341	P2-6	2680.179	.674	.097	.078	.019
	2042		1342	P2-5	2703.999	.742	.073	.057	.016
	2043		1343	P2-4	2727.309	.702	.087	.078	.009
	2044		1344	P2-8	2631.067	.739	.074	.044	.030
	2046		1346	P2-9	2605.806	.697	.089	.057	.032
	2047		1347	P2-10	2580.096	.580	.134	.083	.049
	2050		1350	P2-8	2631.067	.721	.080	.044	.036
122	0147	5-1-79	1847	P2-8	2631.067	.576	.136	.037	.099
	0148		1848	P2-7	2655.863	.462	.190	.082	.108
	0149		1849	P2-6	2680.179	.545	.149	.065	.074
	0150		1850	P2-5	2703.999	.581	.133	.048	.085
	0152		1852	P2-4	2727.309	.574	.136	.065	.061
	0153		1853	P2-8	2631.067	.599	.126	.037	.089
	0154		1854	P2-9	2605.806	.544	.150	.048	.102
	0156		1856	P2-10	2580.096	.490	.175	.077	.098
	0157		1857	P2-8	2631.067	.578	.135	.037	.098
122	1538	5-2-79	0838	P2-8	2631.067	.679	.095	.039	.056
	1540		0840	P2-7	2655.863	.565	.140	.086	.054
	1541		0841	P2-6	2680.179	.640	.110	.069	.041
	1542		0842	P2-5	2703.999	.695	.089	.050	.039
	1544		0844	P2-4	2727.309	.656	.104	.069	.035
	1546		0846	P2-8	2631.067	.692	.091	.039	.052
	1547		0847	P2-9	2605.806	.638	.110	.050	.060
	1549		0849	P2-10	2580.096	.576	.136	.078	.058
	1550		0850	P2-11	2553.952	.605	.124	.045	.079
122	1552	5-2-79	0852	P2-12	2527.391	.662	.101	.047	.054
	1554		0854	P2-8	2631.067	.669	.099	.039	.060
	2154		1454	P2-8	2631.067	.621	.117	.041	.076
	2155		1455	P2-7	2655.863	.473	.184	.091	.093
122	2157	5-2-79	1457	P2-6	2680.179	.557	.144	.073	.071
	2158		1458	P2-5	2703.999	.605	.124	.053	.071
	2202		1502	P2-4	2727.309	.596	.127	.072	.055
	2204		1504	P2-8	2631.067	.641	.120	.041	.079

Table 1 — Laser Extinction Measurement Summary (Continued)

Day (GMT)	Time (GMT)	Date (PDT)	Time (PDT)	Laser Line	$\nu$ (cm $^{-1}$ )	T	$\alpha$ (km $^{-1}$ )	CMA (km $^{-1}$ )	DIFF (km $^{-1}$ )
123	2205	5-2-79	1505	P2-9	2605.806	.578	.135	.053	.072
	2207		1507	P2-10	2580.096	.497	.172	.080	.092
	2208		1508	P2-11	2553.952	.572	.137	.047	.090
	2211		1511	P2-8	2631.067	.588	.131	.041	.090
	0120		1820	P2-8	2631.067	.599	.126	.041	.085
	0122		1822	P2-7	2655.863	.495	.173	.091	.082
	0123		1823	P2-6	2680.179	.532	.155	.073	.082
	0124		1824	P2-5	2703.999	.597	.127	.053	.074
	0125		1825	P2-4	2727.309	.564	.141	.072	.069
	0126		1826	P2-8	2631.067	.605	.124	.041	.083
123	0128	5-3-79	1828	P2-9	2605.806	.581	.133	.053	.080
	0129		1829	P2-10	2580.096	.502	.169	.080	.089
	0134		1834	P2-8	2631.067	.611	.121	.041	.080
	1522		0822	P2-8	2631.067	.673	.097	.041	.056
	1523		0823	P2-7	2655.863	.548	.148	.091	.057
	1525		0825	P2-6	2680.179	.614	.120	.073	.047
	1526		0826	P2-5	2703.999	.680	.095	.053	.042
	1527		0827	P2-4	2727.309	.663	.101	.072	.029
	1528		0828	P2-8	2631.067	.697	.089	.041	.048
	1529		0829	P2-9	2605.806	.665	.100	.053	.047
124	1531	5-3-79	0831	P2-10	2580.096	.577	.135	.080	.055
	1535		0835	P2-8	2631.067	.684	.093	.041	.052
	0127		1827	P2-8	2631.067	.858	.038	.037	.001
	0128		1828	P2-7	2655.863	.717	.082	.082	.000
	0129		1829	P2-6	2680.179	.782	.060	.065	-.005
	0130		1830	P2-5	2703.999	.877	.032	.048	-.016
	0132		1832	P2-4	2727.309	.837	.044	.065	-.021
	0133		1833	P2-8	2631.067	.871	.034	.037	-.003
	0134		1834	P2-9	2605.806	.805	.053	.048	.005
	0136		1836	P2-10	2580.096	.681	.094	.078	.016
124	0138	5-4-79	1838	P2-11	2553.952	.793	.057	.044	.013
	0140		1840	P2-8	2631.067	.844	.042	.037	.005
	1522		0822	P2-8	2631.067	.722	.080	.041	.039
	1523		0823	P2-7	2655.863	.575	.136	.091	.045
	1524		0824	P2-6	2680.179	.637	.111	.073	.038
	1525		0825	P2-5	2703.999	.713	.083	.053	.030
	1527		0827	P2-4	2727.309	.680	.095	.072	.023
	1528		0828	P2-8	2631.067	.723	.080	.041	.039
	1529		0829	P2-9	2605.806	.654	.104	.053	.051
	1531		0831	P2-10	2580.096	.551	.146	.080	.066
	1534		0834	P2-11	2553.952	.650	.106	.047	.059
	1535		0835	P2-8	2631.067	.694	.090	.041	.049

Table 1 — Laser Extinction Measurement Summary (Continued)

Day (GMT)	Time (GMT)	Date (PDT)	Time (PDT)	Laser Line	$\nu$ (cm $^{-1}$ )	T	$\alpha$ (km $^{-1}$ )	CMA (km $^{-1}$ )	DIFF (km $^{-1}$ )
127	2210	5-7-79	1510	P2-8	2631.067	.530	.156	.041	.115
	2211		1511	P2-7	2655.863	.433	.206	.091	.115
	2213		1513	P2-6	2680.179	.503	.169	.073	.096
	2214		1514	P2-5	2703.999	.551	.146	.053	.093
	2215		1515	P2-4	2727.309	.524	.159	.072	.087
	2216		1516	P2-8	2631.067	.516	.163	.041	.122
	2217		1517	P2-9	2605.806	.482	.179	.053	.126
	2219		1519	P2-10	2580.096	.378	.239	.080	.159
	2220		1520	P2-11	2553.952	.454	.194	.047	.147
	2221		1521	P2-8	2631.067	.525	.158	.041	.117
128	0122	5-7-79	1822	P2-8	2631.067	.575	.136	.041	.095
	0125		1825	P2-7	2655.863	.479	.181	.091	.090
	0126		1826	P2-6	2680.179	.544	.150	.073	.077
	0127		1827	P2-5	2703.999	.605	.124	.053	.071
	0128		1828	P2-4	2727.309	.575	.136	.072	.064
	0130		1830	P2-8	2631.067	.522	.160	.041	.119
	0131		1831	P2-9	2605.806	.564	.141	.053	.088
	0132		1832	P2-10	2580.096	.440	.202	.080	.122
	0135		1835	P2-11	2553.952	.471	.185	.047	.138
	0136		1836	P2-8	2631.067	.548	.148	.041	.097
128	1631	5-8-79	0931	P2-8	2631.067	.835	.044	.035	.009
	1633		0933	P2-7	2655.863	.701	.087	.077	.010
	1634		0934	P2-6	2680.179	.769	.065	.061	.004
	1636		0936	P2-5	2703.999	.836	.044	.045	-.001
	1637		0937	P2-4	2727.309	.819	.049	.061	-.012
	1638		0938	P2-8	2631.067	.834	.045	.035	.010
	1638		0938	P2-9	2605.806	.777	.062	.045	.017
	1641		0941	P2-10	2580.096	.667	.100	.076	.024
	1643		0943	P2-11	2553.952	.776	.062	.042	.020
	1642		0944	P2-8	2631.067	.843	.042	.035	.007
129	0348	5-8-79	2048	P2-8	2631.067	.518	.162	.035	.127
	0350		2050	P2-7	2655.863	.432	.206	.077	.129
	0351		2051	P2-6	2680.179	.470	.186	.061	.125
	0352		2052	P2-5	2703.999	.512	.165	.045	.120
	0353		2053	P2-4	2727.309	.453	.195	.061	.134
	0355		2055	P2-8	2631.067	.475	.183	.035	.148
	0356		2056	P2-9	2605.806	.467	.187	.045	.142
	0357		2057	P2-10	2580.096	.378	.239	.076	.163
	0400		2100	P2-8	2631.067	.476	.182	.035	.147
	1518	5-9-79	0818	P2-8	2631.067	.607	.123	.037	.086
	1519		0819	P2-7	2655.863	.528	.157	.082	.075
	1520		0820	P2-6	2680.179	.569	.139	.065	.074
	1521		0821	P2-5	2703.999	.629	.114	.048	.066

Table 1 — Laser Extinction Measurement Summary (Concluded)

Day (GMT)	Time (GMT)	Date (PDT)	Time (PDT)	Laser Line	$\nu$ (cm $^{-1}$ )	T	$\alpha$ (km $^{-1}$ )	CMA (km $^{-1}$ )	DIFF (km $^{-1}$ )
129	1522	5-9-79	0822	P2-4	2727.309	.590	.130	.065	.065
	1523		0823	P2-8	2631.067	.650	.106	.037	.069
	1524		0824	P2-9	2605.806	.600	.126	.048	.078
	1526		0826	P2-10	2580.096	.517	.162	.077	.085
	1528		0828	P2-11	2553.952	.594	.128	.044	.084
	1529		0829	P2-8	2631.067	.654	.104	.037	.067
	2024		1324	P2-8	2631.067	.625	.116	.039	.077
	2026		1326	P2-7	2655.863	.457	.192	.086	.106
	2027		1327	P2-6	2680.179	.501	.170	.069	.101
	2029		1329	P2-5	2703.999	.529	.157	.050	.107
130	2030	5-9-79	1330	P2-4	2727.309	.510	.165	.069	.096
	2031		1331	P2-8	2631.067	.547	.148	.039	.109
	2032		1332	P2-9	2605.806	.497	.172	.050	.122
	2034		1334	P2-10	2580.096	.415	.216	.078	.138
	2035		1335	P2-11	2553.952	.493	.174	.045	.129
	2037		1337	P2-12	2631.067	.532	.155	.039	.116
	0206		1906	P2-8	2631.067	.560	.143	.039	.104
	0208		1908	P2-7	2655.863	.472	.185	.086	.099
	0209		1909	P2-6	2680.179	.512	.165	.069	.096
	0211		1911	P2-5	2703.999	.555	.145	.050	.095
130	0212	5-10-79	1912	P2-4	2727.309	.521	.160	.069	.091
	0214		1914	P2-8	2631.067	.550	.147	.039	.108
	0216		1916	P2-9	2605.806	.511	.165	.050	.115
	0218		1918	P2-10	2580.096	.429	.208	.078	.130
	0220		1920	P2-8	2553.952	.542	.151	.039	.112
	1518		0818	P2-8	2631.067	.375	.241	.047	.194
	1520		0820	P2-7	2655.863	.233	.358	.106	.252
	1521		0821	P2-6	2680.179	.264	.327	.084	.243
	1522		0822	P2-5	2703.999	.276	.316	.062	.254
	1524		0824	P2-4	2727.309	.275	.317	.084	.233
130	1526	5-10-79	0826	P2-8	2631.067	.318	.282	.047	.235
	1527		0827	P2-9	2605.806	.271	.321	.061	.260
	1528		0828	P2-10	2580.096	.245	.346	.086	.260
	1530		0830	P2-8	2631.067	.296	.299	.047	.252
	1709		1009	P2-8	2631.067	.504	.168	.044	.124
	1712		1012	P2-7	2655.863	.428	.211	.099	.112
	1714		1014	P2-6	2680.179	.461	.190	.078	.112
	1715		1015	P2-5	2703.999	.527	.157	.057	.100
	1716		1016	P2-4	2727.309	.516	.163	.078	.085
	1718		1018	P2-8	2631.067	.525	.158	.044	.114
130	1719	5-10-79	1019	P2-9	2605.806	.474	.183	.057	.126
	1721		1021	P2-10	2580.096	.427	.209	.083	.126
	1723		1023	P2-8	2631.067	.502	.169	.044	.125

## NRL REPORT 8618

Table 2 — Optical System Transmission Measurements

Line	$\nu$ (cm $^{-1}$ )	$\bar{T}_0^*$
P2-8	2631.067	.722 ± .001
P2-7	2655.863	.726 ± .003
P2-6	2680.179	.727 ± .003
P2-5	2703.999	.728 ± .003
P2-4	2727.309	.724 ± .009
P2-8	2631.067	.725 ± .001
P2-9	2605.806	.718 ± .002
P2-10	2580.096	.714 ± .006
P2-11	2553.952	.718 ± .012
P2-8	2631.067	.721 ± .004

\*Average of two measurements for each line.

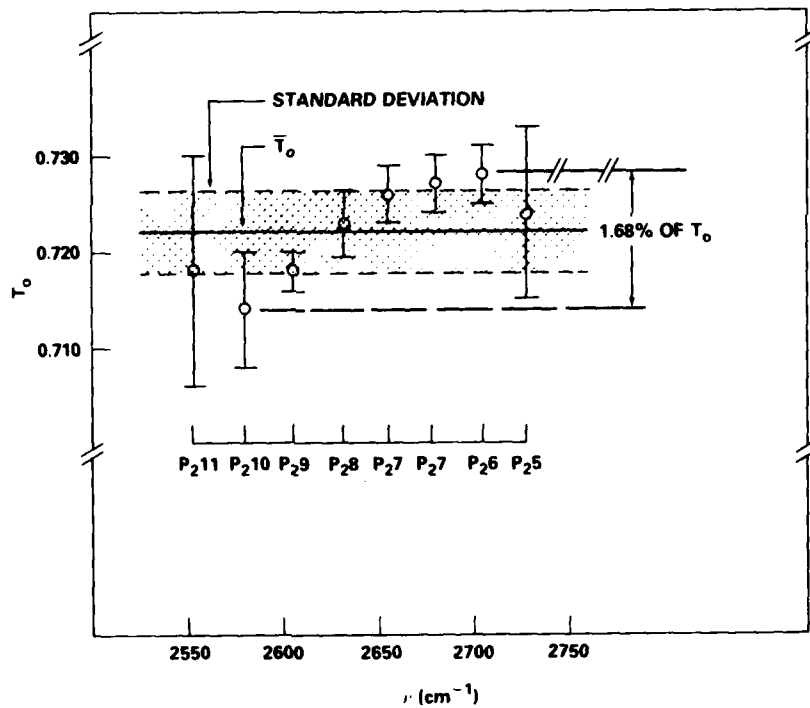


Fig. 5 — Zero-path optical system efficiency measurements

Pacific Daylight Time (PDT)) showed the highest transmission values: 84 to 87% for the P2-8 DF laser line; while data taken on DAY 130, at 1526 GMT showed the lowest transmission values: 30 to 37% at the P2-8 line. The difference values DIFF =  $\alpha$ -CMA listed in column 10 of Table I for each of the "runs" tabulated in Table I are plotted against wavenumber and are shown in Figs. 6 through 10. One expects the difference values to be independent of wavenumber over the interval from 2580 cm $^{-1}$  to 2720 cm $^{-1}$  shown in the figures, however a systematic decrease of ( $\alpha$ -CMA) with increasing wavenumber can be seen.

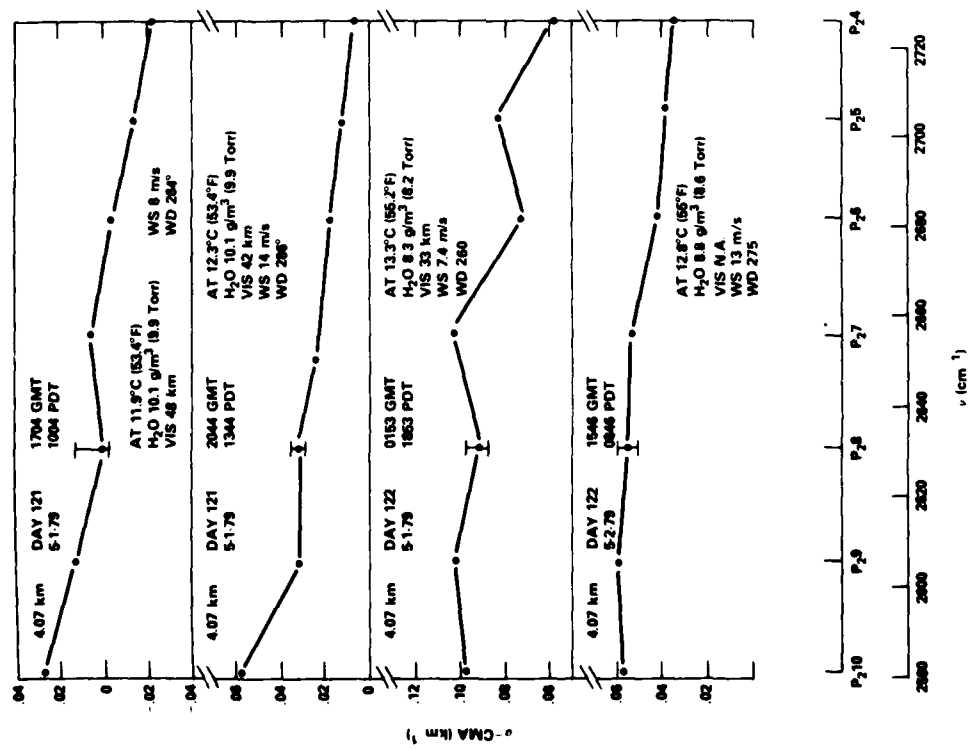


Fig. 6 — Measured extinction coefficients minus calculated molecular absorption coefficients vs wavenumber for NRL measurements at SNI of several DF laser lines

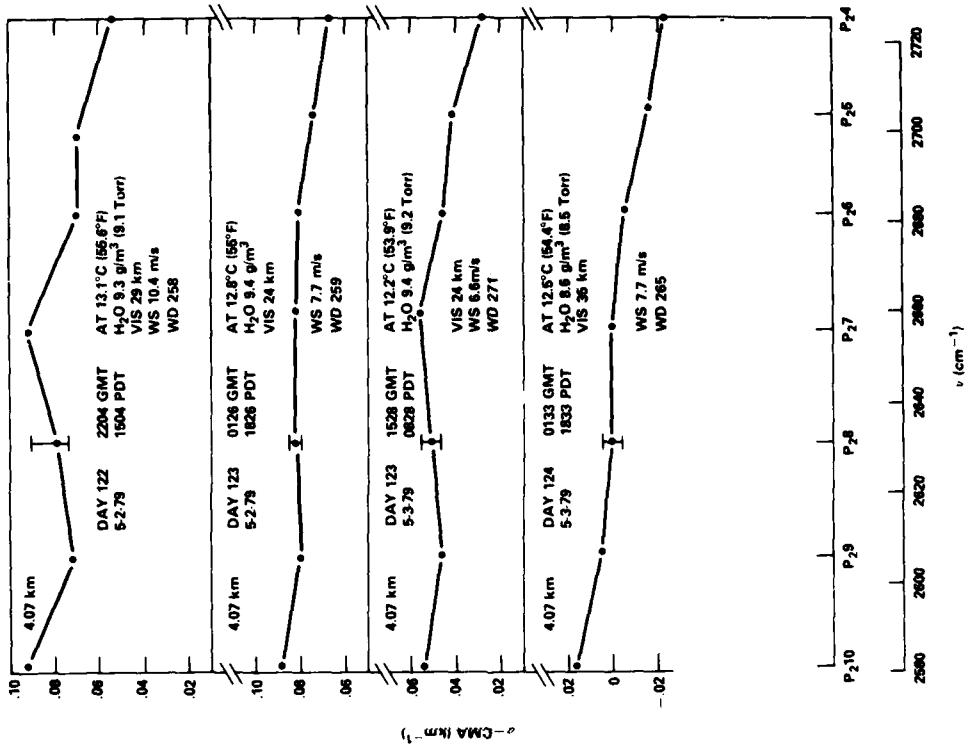


Fig. 7 — Measured extinction coefficients minus calculated molecular absorption coefficients vs wavenumber for NRL measurements at SNI of several DF laser lines

NRL REPORT 8618

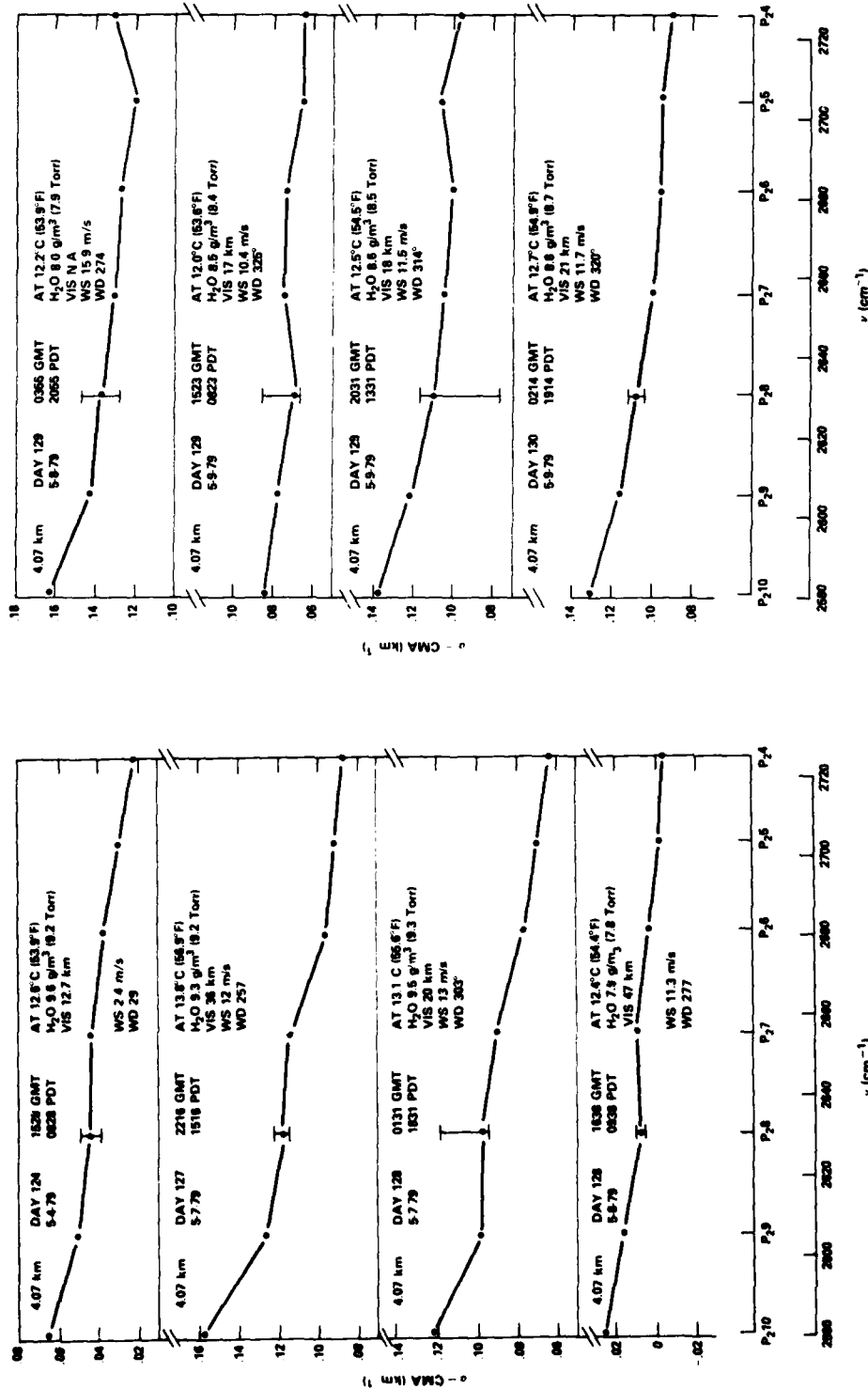


Fig. 8 — Measured extinction coefficients minus calculated molecular absorption coefficients vs wavenumber for NRL measurements at SNI of several DF laser lines

Fig. 9 — Measured extinction coefficients minus calculated molecular absorption coefficients vs wavenumber for NRL measurements at SNI of several DF laser lines

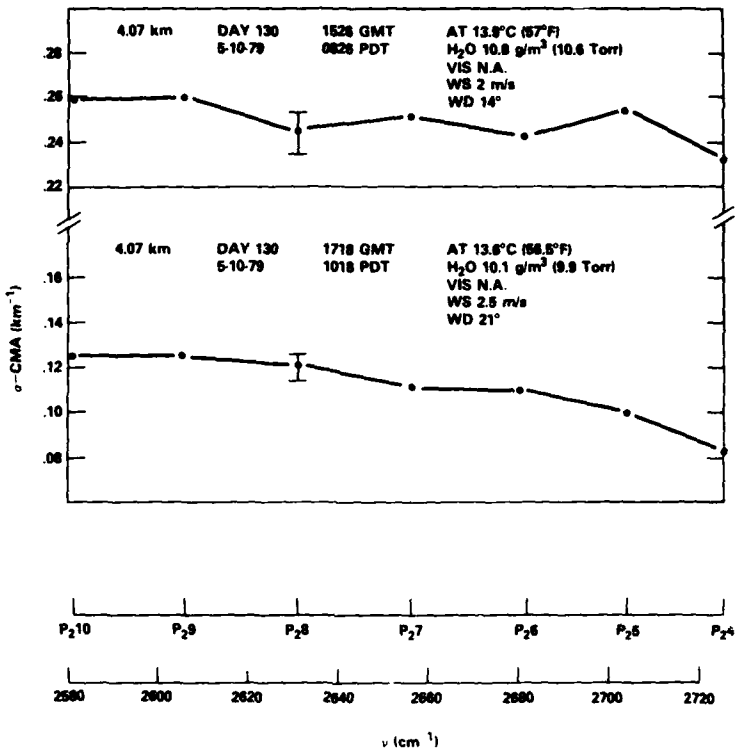


Fig. 10 — Measured extinction coefficients minus calculated molecular absorption coefficients vs wavenumber for NRL measurements at SNI of several DF laser lines

The wavenumber dependence shown is most likely due to the use of a water vapor continuum absorption model in deriving the CMA values which predicts too large an increase of absorption with increasing wavenumber. This observation is consistent with earlier comparisons [6] of long-path field transmission data to the H<sub>2</sub>O continuum model of Watkins and White [7] which represents an improvement over the H<sub>2</sub>O continuum model proposed earlier by Burch et al. [8].

Both GMT and PDT have been listed for each of the runs in Figs. 6 through 10, also the salient meteorological conditions present at the time of the measurements. No correlation can be determined between the size of the ( $\alpha$ -CMA) decrease with increasing wavenumber and meteorological parameters such as absolute humidity, wind speed, or visibility.

### 3.2 High-Resolution Fourier Transform Spectroscopy Measurements and Absolute Transmission Calibration

Twenty-six high-resolution spectra were measured during the period 1 to 10 May 1979. Table 3 summarizes the FTS measurement times, FTS beamsplitter/detector configurations used (determining wavelength range covered), and the corresponding laser extinction measurement times used for absolute transmission normalization of the FTS spectra. Column 8 of Table 3 lists the designations assigned to the ratioed and normalized spectra obtained in the experiment. The spectra acquired over the 4.07 km path are first ratioed to a spectrum obtained using a local source (i.e., one inserted into the receiver

Table 3 — FTS Measurement Summary

FTS Spectrum Iden.	Date (GMT)	Time (GMT)	FTS Config.	#FTS Scans	FTS Measur. Path (km)	Laser Extinct. Meas. Time (GMT)	Normalized FTS Spectrum	Comment
SNI 01	121	1731	HgCdTe/KBr	100	4.07	1704	SNI 1DRN	
SNI 02	121	1807	HgCdTe/KBr	100	4.07	1704	SNI 2DRN	
SNI 04	121	2311	HgCdTe/KBr	100	4.07	0153	SNI 4DRN	
SNI 05	122	0225	HgCdTe/KBr	100	4.07	0153	SNI 5DRN	
SNI 06	122	1637	HgCdTe/KBr	100	4.07	1546	SNI 6DRN	
SNI 07	122	2012	HgCdTe/KBr	100	4.07	2204		Noisy
SNI 08	122	2115	HgCdTe/KBr	100	4.07	2204		Noisy
SNI 09	122	2304	HgCdTe/KBr	100	4.07	0126	SNI 9DRN	
SNI 10	123	0200	HgCdTe/KBr	100	4.07	0126	SNI 10DRN	
SNI 11	123	1600	HgCdTe/KBr	100	4.07	1528	SNI 11DRN	
SNI 12	124	0210	HgCdTe/KBr	100	4.07	0133	SNI 12DRN	
SNI 13	124	1605	HgCdTe/KBr	200	4.07	1528		
SNI 14	127	2139	HgCdTe/KBr	100	4.07	2216	SNI 14DRN	
SNI 15	127	2306	HgCdTe/KBr	200	Local		SNI 15:B	
SNI 16	128	0250	HgCdTe/KBr	200	4.07	0131	SNI 16DRN	
SNI 17	128	1715	HgCdTe/KBr	200	4.07	1638	SNI 17DRN	
SNI 18	129	0217	HgCdTe/KBr	200	4.07	0355		Noisy
SNI 19	129	0329	HgCdTe/KBr	200	4.07	0355		Noisy
SNI 20	129	0430	HgCdTe/KBr	200	4.07	0355		Noisy
SNI 21	129	1636	HgCdTe/KBr	200	4.07	1523		Noisy
SNI 22	129	1739	HgCdTe/KBr	200	4.07	1523		Noisy
SNI 23	129	2145	HgCdTe/KBr	200	4.07	2030	SNI 23DRN	
SNI 24	130	0320	HgCdTe/KBr	200	4.07	0214	SNI 24DRN	
SNI 25	131	1622	HgCdTe/KBr	200	4.07	1526	SNI 25DRN	
SNI 26	131	1750	HgCdTe/KBr	200	4.07	1718	SNI 26DRN	

telescope optical train approximately 3 m from the FTS instrument) to remove detector, blackbody, and beamsplitter response functions. The color temperature of the local source was adjusted to match that of the distant source located in the transmitter trailer by monitoring each with an optical pyrometer. Spectrum SNI 15 was taken using the local source and was used as a denominator in ratioing the long-path spectra. Sixteen of the long-path spectra acquired were suitable for absolute transmission normalization using laser extinction measurements, and these are indicated by the suffix DRN in column 8 of Table 3. The suffix D indicates that only a portion of the 0 to 7900  $\text{cm}^{-1}$  spectrum between 1800  $\text{cm}^{-1}$  and 3200  $\text{cm}^{-1}$  was archived; the R indicates that the spectrum was ratioed (in this case to spectrum SNI 15:B); and the N indicates that the spectrum was normalized for absolute transmission using the independent laser extinction measurements.

The ratioed spectra were converted from relative to absolute transmission by determining the scale factor needed to scale the relative transmission value of a spectrum at a particular laser frequency to the absolute transmission value obtained by means of the independent long path laser extinction measurement. Column 7 of Table 3 lists the time of the laser extinction measurements used for absolute transmission normalization of the several spectra obtained in the experiment. Long-path spectra were obtained usually within 1 hour of the laser extinction measurements used for normalization.

Detailed comparisons of the amplitude of each normalized spectrum to the individual DF laser line transmission measurements used to generate the normalization are contained in Table 4 for each of

the spectra labeled with an "N" suffix in column 7 of Table 3. An average multiplicative factor was determined by averaging the individual factors obtained for the several laser transmission measurements in any particular measurement series. The laser line identification and position in  $\text{cm}^{-1}$  are listed in columns 1 and 2, respectively in Table 4. The next four columns list: (a) the wavenumber of a spectrum sample,  $\nu'$ ; (b) the measured laser transmission,  $\tau$ ; (c) the individual amplitude,  $\tau'$ , of a spectrum sample adjacent to or coincident with (to two decimal places) the appropriate laser line wavenumber; and (d) the difference between the amplitude of the spectrum sample and the actual transmission value measured at the laser frequency,  $\delta$ . The average of the  $\delta$  values and standard deviation are listed at the bottom of each column of  $\delta$  values. Values for  $\tau'$  and  $\delta$  for more than one spectrum normalized by a given set of laser transmission values  $\tau$  are repeated in successive columns in Table 4. As can be seen by examining the comparisons listed in the table, the average  $\delta$  value or residual offset is typically a few tenths of a percent transmission and only slightly larger (<2%) in a few cases. The random error in the normalization procedure approximated by the standard deviation in  $\delta$  is generally less than  $\pm 3\%$  transmission except in the cases where the spectral signal to noise ratio is poorer, e.g., spectra SNI12DRN, SNI16DRN, and SNI17DRN. The measurement accuracy in an individual laser extinction measurement is estimated to be  $\pm 3\%$  under good measurement conditions. Nine or ten individual laser extinction measurements are averaged in arriving at the normalization factor used in scaling a given spectrum in units of absolute transmission, thus redundant laser transmission measurements should combine to produce an average scale factor accurate to about  $\pm 1\%$ . When applied to a given spectrum the resultant absolute transmission calibration should be valid to  $\pm 2\%$  in the best case of a high signal-to-noise ratio spectrum with the accuracy correspondingly degraded to about  $\pm 4$  or 5% in cases where the spectrum signal-to-noise ratio is poorer.

Table 4 — FTS Spectrum Normalization Parameters

Line ID	$\nu$ ( $\text{cm}^{-1}$ )	$\nu'$ ( $\text{cm}^{-1}$ )	Laser Trans. $\tau$	SNI 01DRN		SNI 02DRN	
				Spectrum Amplitude Adjacent Samples, $\tau'$	$\delta$ (S-L)	Spectrum Amplitude Adjacent Samples, $\tau'$	$\delta$ (S-L)
P2-8	2631.067	2631.03	.836	.8282	-.008	.7939	-.043
		2631.09		.8321	-.004	.7948	-.042
P2-7	2655.863	2655.86	.660	.7190	.059*	.7277	.077*
		2680.179	.740	.7225	-.017	.7292	-.011
P2-6	2680.21	2680.15		.6981	-.042	.6992	-.041
		2680.21		.8031	-.033	.8030	-.033
P2-5	2703.999	2703.95	.836	.8007	-.035	.8049	-.031
		2704.01		.7917	-.005	.8276	.030
P2-4	2727.309	2727.27	.797	.7759	-.021	.8111	.014
		2727.33		.7917	-.005	.8276	.030
P2-8	2631.067	2631.03	.841	.8282	-.013	.7939	-.047
		2631.09		.8321	-.008	.7948	-.046
P2-9	2605.806	2605.78	.756	.7476	-.008	.7484	-.008
		2605.84		.7291	-.026	.7394	-.017
P2-10	2580.096	2580.05	.638	.6557	.020*	.5871	-.051*
		2580.11		.7274	.089*	.6797	.042*
P2-8	2631.067	2631.03	.796	.8281	.032	.7939	-.002
		2631.09		.8321	.036	.7948	-.001
AVERAGE STANDARD DEVIATION					.0009 $\pm .0225$	.0206 $\pm .0244$	

\*excluded from average

## NRL REPORT 8618

Table 4 — FTS Spectrum Normalization Parameters (Continued)

Line ID	$\nu$ (cm $^{-1}$ )	$\nu'$ (cm $^{-1}$ )	Laser Trans. $\tau$	SNI 04DRN		Laser Trans. $\tau$	SNI 05DRN		
				Spectrum Amplitude Adjacent Samples, $\tau'$	$\delta$ (S-L)		Spectrum Amplitude Adjacent Samples, $\tau'$	$\delta$ (S-L)	
P2-8	2631.067	2631.03	.654	.6569	.003	.576	.5984	.022	
		2631.09		.6659	.012		.5945	.018	
P2-7	2655.863	2655.86	.5305	.5953	.064*	.462	.5200	.068	
		2680.179		.5993	-.011	.545	.5356	-.009	
P2-6	2680.179	2680.15	.610	.5732	-.037		.5105	-.034	
		2680.21		.6595	-.002	.581	.5770	-.004	
P2-5	2703.999	2703.95	.662	.6464	-.016		.5730	-.008	
		2704.01		.6395	.002	.574	.5658	-.008	
P2-4	2727.309	2727.27	.638	.6353	-.003		.5704	-.004	
		2727.33		.6152	-.006	.544	.5954	-.004	
P2-8	2631.067	2631.03	.669	.6569	-.012	.599	.5984	-.001	
		2631.09		.6659	-.003		.5488	.005	
P2-9	2605.806	2605.78	.621	.6100	-.011		.5414	-.003	
		2605.84		.6088	.066*		.5386	.049*	
P2-10	2580.096	2580.05	.535	.5283	-.007*	.490	.4391	-.050*	
		2580.11		.5714	-.005*				
P2-8	2631.067	2631.03	.650	.6569	.007	.578	.5984	.020	
		2631.09		.6659	.016		.5954	.017	
AVERAGE					-.004			.0005	
STANDARD DEVIATION					$\pm .0132$			$\pm .0150$	

Table 4 — FTS Spectrum Normalization Parameters (Continued)

Line ID	$\nu$ (cm $^{-1}$ )	$\nu'$ (cm $^{-1}$ )	Laser Trans. $\tau$	SNI 06DRN		Laser Trans. $\tau$	SNI 09DRN		SNI 10DRN	
				Spectrum Amplitude Adjacent Samples, $\tau'$	$\delta$ (S-L)		Spectrum Amplitude Adjacent Samples, $\tau'$	$\delta$ (S-L)		
P2-8	2631.067	2631.03	.679	.6833	.004	.621	.6081	-.013	.599	
		2631.09		.6803	.001		.6048	-.017	.6218	
P2-7	2655.863	2655.86	.565	.5845	-.019	.473	.4965	.023	.6244	
		2680.15	.640	.6355	-.004	.557	.5644	.007	.5222	
P2-6	2680.179	2680.21		.6219	-.018		.5371	-.020	.5441	
		2703.95	.695	.6903	-.005	.605	.6082	.003	.5141	
P2-5	2703.999	2704.01		.6841	-.011		.6121	.007	.5850	
		2727.27	.656	.6544	-.002	.596	.5717	-.025	.5869	
P2-4	2727.309	2727.33		.6683	.012		.5745	-.021	.5569	
		2631.03	.692	.6833	-.009	.641	.6081	-.033	.5538	
P2-8	2631.067	2631.09		.6803	-.012		.6048	-.036	.6244	
		2605.78	.638	.6412	.003	.578	.5637	-.014	.5873	
P2-9	2605.806	2605.84		.6262	-.012		.5618	-.016	.5722	
		2580.11		.5714	-.005*		.4974	.000	.5436	
P2-10	2580.096	2580.05	.576	.4908	-.085*	.497	.4709	-.026	.5975	
		2553.952		.5714	-.005*				.041*	
P2-11	2527.391	2527.38	.662	.6389	-.023		.5627	-.009		
		2527.44		.6420	-.020					
P2-8	2631.067	2631.03	.669	.6833	.014	.588	.6081	.020	.6218	
		2631.09		.6803	.011		.6048	.017	.6244	
AVERAGE					-.0034			-.0085	.0051	
STANDARD DEVIATION					$\pm .0139$			$\pm .0181$	$\pm .0164$	

\*excluded from average

Table 4 — FTS Spectrum Normalization Parameters (Continued)

Line ID	SNI 11DRN			SNI 12DRN			SNI 13DRN				
	$\nu$ (cm $^{-1}$ )	$\nu'$ (cm $^{-1}$ )	Laser Trans. $\tau$	Spectrum Amplitude Adjacent Samples, $\tau'$	$\delta$ (S-L)	Laser Trans. $\tau$	Spectrum Amplitude Adjacent Samples, $\tau'$	$\delta$ (S-L)	Laser Trans. $\tau$	Spectrum Amplitude Adjacent Samples, $\tau'$	$\delta$ (S-L)
P2-8	2631.067	2631.03	.673	.7296	.056	.858	.8906	.032	.722	.7261	.004
		2631.09		.7264	.053		.8829	.024		.7346	.013
P2-7	2655.863	2655.86	.548	.6205	.072*	.717	.8099	.092*	.575	.6429	.068*
	2680.179	2680.15	.614	.6156	.001	.782	.7183	-.064	.637	.6311	-.006
P2-6	2680.21			.5872	-.027		.6638	-.119			
	2703.999	2703.95	.680	.6732	-.007	.877	.8508	-.026	.713	.7010	-.012
P2-5	2704.01			.6744	-.006		.8593	-.017		.7014	-.012
	2727.309	2727.27	.663	.6415	-.021	.837	.8377	.001	.680	.6743	-.006
P2-4	2727.33			.6365	-.027		.8281	-.009		.6774	-.003
	2631.067	2631.03	.697	.7296	.031	.871	.8906	.020	.723	.7261	.003
P2-8	2631.09			.7264	.029		.8829	.012		.7346	.011
	2605.806	2605.78	.665	.6768	.011	.805	.7700	-.035	.654	.6753	.021
P2-9	2605.84			.6541	-.011		.7341	-.066		.6620	.008
	2580.096	2580.05	.577	.6696	.092*	.681	.8393	.158*	.551	.6561	.105*
P2-10	2580.11			.7035	.126*		.8490	.168*		.6942	.143*
	2553.952	2553.95					.793	.8549	.061	.7104	.060*
P2-8	2631.067	2631.03	.684	.7296	.045	.844	.8906	.047	.694	.7261	.032
		2631.09		.7264	.042		.8829	.038		.7346	.040
AVERAGE							.0121				.0072
STANDARD DEVIATION							$\pm .0300$				$\pm .0162$

Table 4 — FTS Spectrum Normalization Parameters (Continued)

Line ID	SNI 14DRN			SNI 16DRN			SNI 17DRN				
	$\nu$ (cm $^{-1}$ )	$\nu'$ (cm $^{-1}$ )	Laser Trans. $\tau$	Spectrum Amplitude Adjacent Samples, $\tau'$	$\delta$ (S-L)	Laser Trans. $\tau$	Spectrum Amplitude Adjacent Samples, $\tau'$	$\delta$ (S-L)	Laser Trans. $\tau$	Spectrum Amplitude Adjacent Samples, $\tau'$	$\delta$ (S-L)
P2-8	2631.067	2631.03	.530	.5521	.022	.575	.6016	.027	.835	.8513	.016
		2631.09		.5558	.025		.6017	.027		.8463	.011
P2-7	2655.863	2655.86	.433	.4725	.039	.479	.5200	.031	.701	.7866	.085*
	2680.179	2680.15	.503	.4915	-.011	.544	.5223	-.022	.769	.7229	-.046*
P2-6	2680.21			.4624	-.038		.5087	-.031		.6855	-.083
	2703.999	2703.95	.551	.5388	-.013	.605	.5873	-.018	.836	.8319	-.004
P2-5	2704.01			.5313	-.020		.5831	-.014		.8337	-.002
	2727.309	2727.27	.524	.5093	-.013	.575	.5571	-.018	.819	.8126	-.003
P2-4	2727.33			.5091	-.013		.5596	-.016		.8901	-.010
	2631.067	2631.03	.516	.5551	.039	.522	.6016	.080	.834	.8513	.017
P2-8	2631.09			.5558	.039		.6017	.080		.8463	.012
	2605.806	2605.78	.482	.5215	.039	.564	.5564	-.008	.777	.7612	-.011
P2-9	2605.84			.5068	.024		.5388	-.026		.7368	-.041
	2580.096	2580.05	.378	.4699	.091*	.440	.5067	.066*	.667	.7599	.107*
P2-10	2580.11			.5325	.164*		.5594	.119*		.8261	.159*
	2553.952	2553.95	.454	.5372	.983*	.471	.5853	.114*	.776	.8170	.040
P2-8	2631.067	2631.03	.525	.5551	.030	.548	.6016	.053	.843	.8513	.008
		2631.09		.5558	.030		.6017	.053		.8463	.003
AVERAGE							.0119				-.0031
STANDARD DEVIATION							$\pm .0266$				$\pm .0318$

\*excluded from average

## NRL REPORT 8618

Table 4 — FTS Spectrum Normalization Parameters (Concluded)

Line ID			SNI 24DRN			SNI 25DRN			SNI 26DRN		
	$\nu$ (cm $^{-1}$ )	$\nu'$ (cm $^{-1}$ )	Laser Trans. $\tau$	Spectrum Amplitude Adjacent Samples, $\tau'$	$\delta$ (S-L)	Laser Trans. $\tau$	Spectrum Amplitude Adjacent Samples, $\tau'$	$\delta$ (S-L)	Laser Trans. $\tau$	Spectrum Amplitude Adjacent Samples, $\tau'$	$\delta$ (S-L)
P2-8	2631.067	2631.03	.560	.5554	-.005	.504	.5315	.207	.504	.5236	.020
		2631.09		.5566	-.003		.5341	.030		.5230	.019
P2-7	2655.863	2655.86	.472	.4736	.002	.428	.4518	.024	.428	.4404	.012
	P2-6	2680.179	2680.15	.512	.5010	-.011	.461	.4680	.008	.461	.4658
			2680.21	.4833	-.029		.4479	-.013		.4486	-.013
P2-5	2703.999	2703.95	.555	.5473	-.008	.527	.5205	-.007	.527	.5291	.002
	P2-4	2704.01		.5464	-.009		.5194	-.008		.5253	-.002
		2727.309	2727.27	.521	.5251	.004	.516	.5004	-.016	.516	.4923
			2727.33	.5206	.000		.4965	-.020		.4991	-.017
P2-8	2631.067	2631.03	.550	.5554	.005	.525	.5315	.006	.525	.5236	-.001
	P2-9	2631.09		.5566	.007		.5341	.010		.5230	-.002
		2605.806	2605.78	.511	.5178	.007	.474	.5001	.026	.474	.4982
			2605.84	.5066	-.004		.4903	.016		.4838	.010
P2-10	2580.096	2580.05	.429	.4482	.019*						
	P2-11	2580.11		.4911	.062*						
		2553.952	2553.95			.427	.5241	.097*	.427	.5084	.081*
P2-8	2631.067	2631.03	.542	.5554	.013	.481	.5315	.051	.481	.5236	.043
		2631.09	.5566	.015		.5341	.053		.5330	.052	
AVERAGE					-.0011				.0125		.0086
STANDARD DEVIATION					$\pm .0109$				$\pm .0229$		$\pm .0209$

\*excluded from average

Figures 11 to 18 represent portions of two of the ratioed and normalized spectra listed in Table 3, namely SNI12DRN and SNI26DRN. These figures were reproduced from CRT displays of the spectra obtained with FTS system software. Reading from top to bottom of each column in each of the figures, the location of each of the laser line positions listed in Table 4 is shown. The top photograph shows the atmospheric transmission structure in the vicinity of the individual laser line which is specified at the bottom of each column. The lower photograph in each column shows the same portion of the spectrum at increased dispersion so that individual samples in the spectrum (0.06 cm $^{-1}$ ) are evident. The cursor shown in each photograph marks the spectrum location in cm $^{-1}$  (top number) to two decimal places and the spectrum amplitude at that location to four decimal places. These values are the  $\nu'$  and  $\tau'$  values listed for spectra SNI12DRN and SNI26DRN in Table 4.

Some general observations can be made upon an examination of Figs. 11 through 18. The majority of the 2 — 1 band DF laser lines are located fortuitously at positions which are relatively free of coincidence with atmospheric absorption lines. The P2-10 line located at 2580.096 cm $^{-1}$ , the P2-9 line at 2605.806 cm $^{-1}$ , and the P2-6 line at 2680.179 cm $^{-1}$  being the three notable exceptions (see Figs. 11-18). The P2-10 DF laser line is located on the shoulder of an N<sub>2</sub>O absorption line as can be seen in the figure and consequently is a poor choice for use in obtaining an absolute transmission normalization for the FTS spectra. The P2-9 and P2-6 lines are located near HDO absorption lines where adjacent FTS sampled amplitudes are changing rapidly with wavenumber.

The substantial change in FTS spectrum amplitude values between the two adjacent spectrum samples bracketing the indicated DF laser lines introduces a significant uncertainty into the laser transmission normalization procedure and can introduce additional errors into the procedure due to any misregistration of the laser line position with the FTS spectrum. Both types of problems are minimized when laser line positions free from coincidence with absorption lines are used to derive the absolute

J. A. DOWLING ET AL.

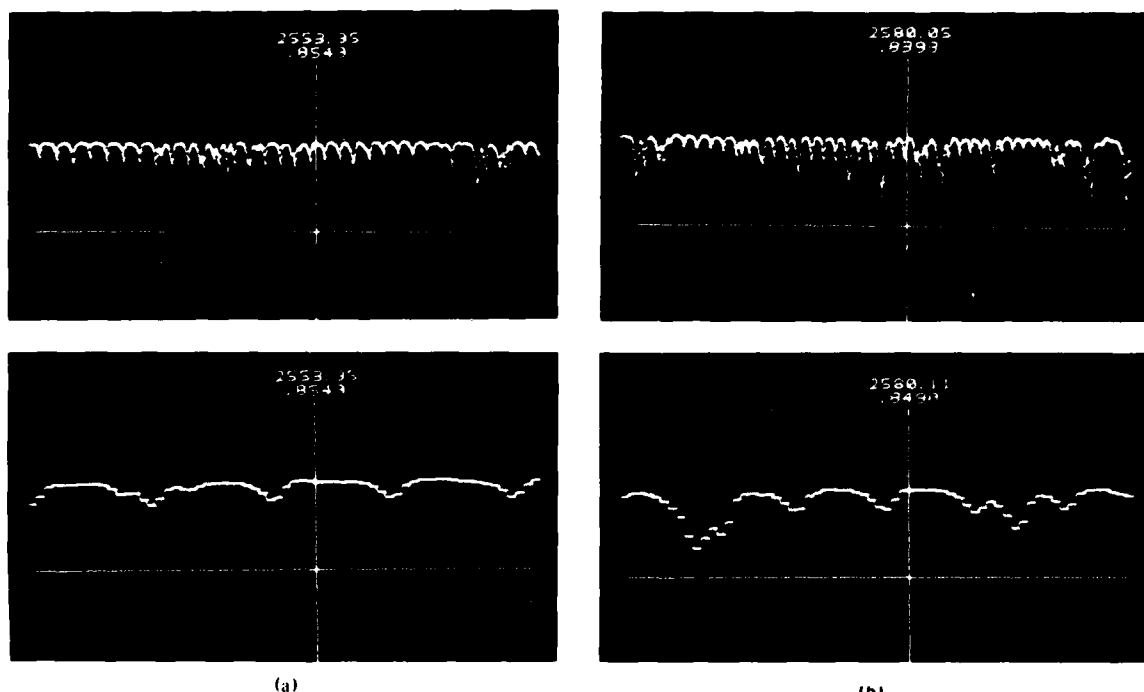


Fig. 11 — Oscilloscope trace showing normalized spectrum structure and absolute transmission amplitude in the vicinity of DF laser lines: Spectrum SNI 12 DRN, (a) P 2-11 and (b) P 2-10.

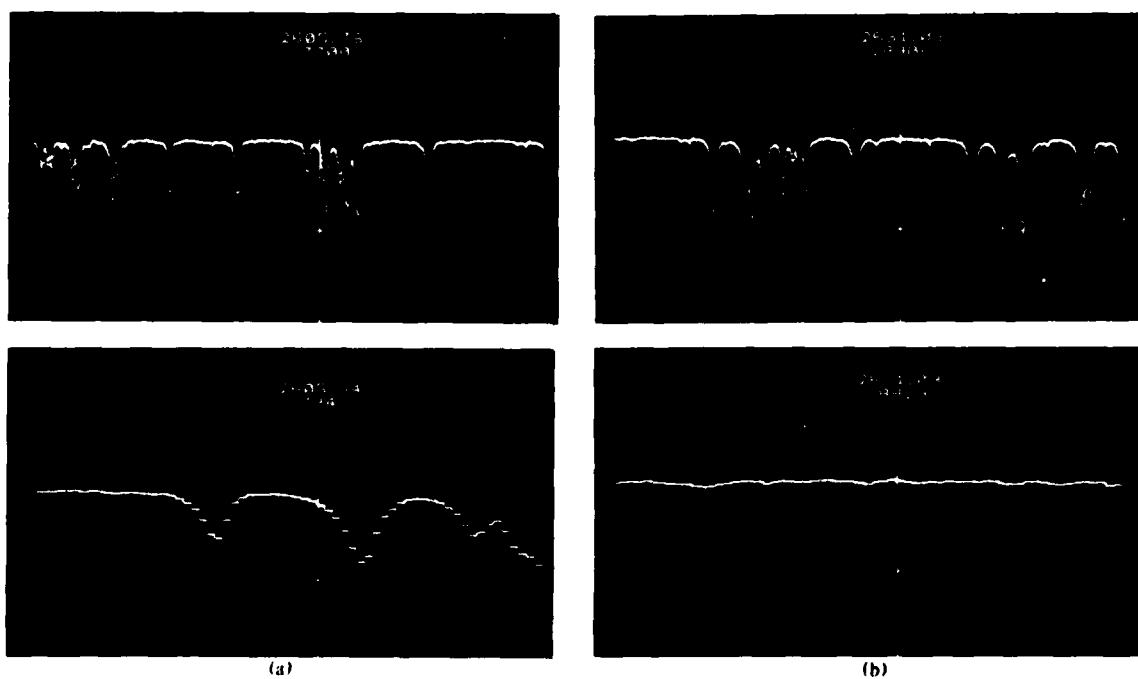


Fig. 12 — Oscilloscope trace showing normalized spectrum structure and absolute transmission amplitude in the vicinity of DF laser lines: Spectrum SNI 12 DRN, (a) P 2-9 and (b) P 2-8.

## NRL REPORT 8618

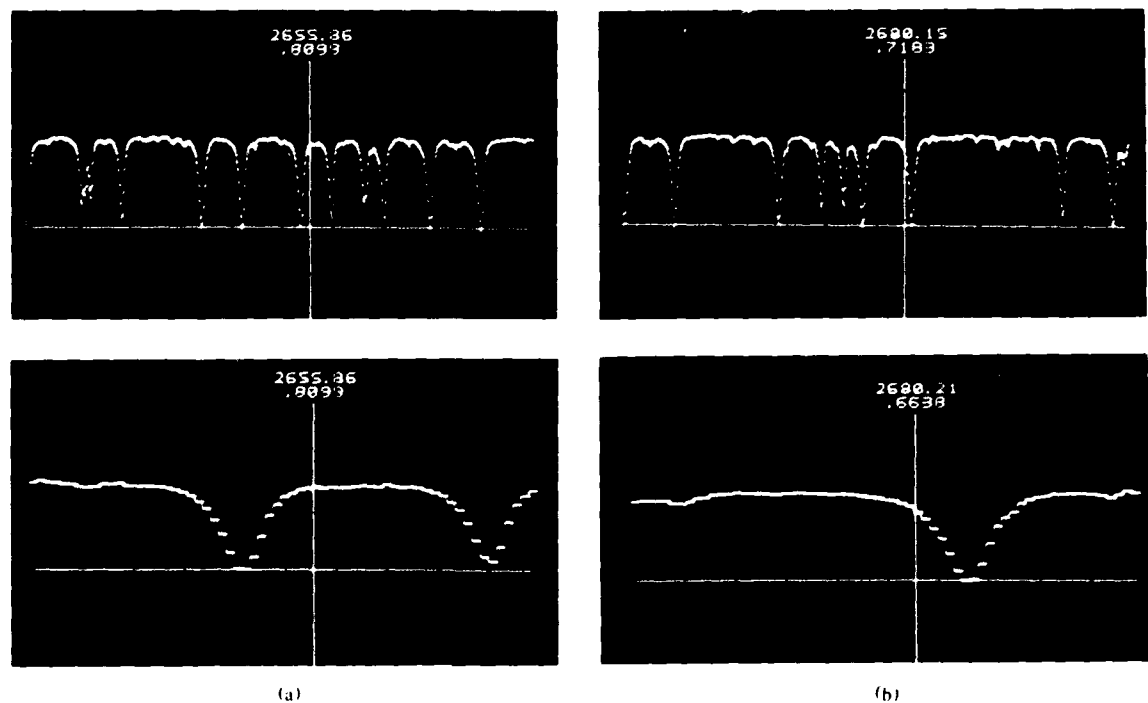


Fig. 13 — Oscilloscope trace showing normalized spectrum structure and absolute transmission amplitude in the vicinity of DF laser lines: Spectrum SNI 12 DRN, (a) P 2-7 and (b) P 2-6

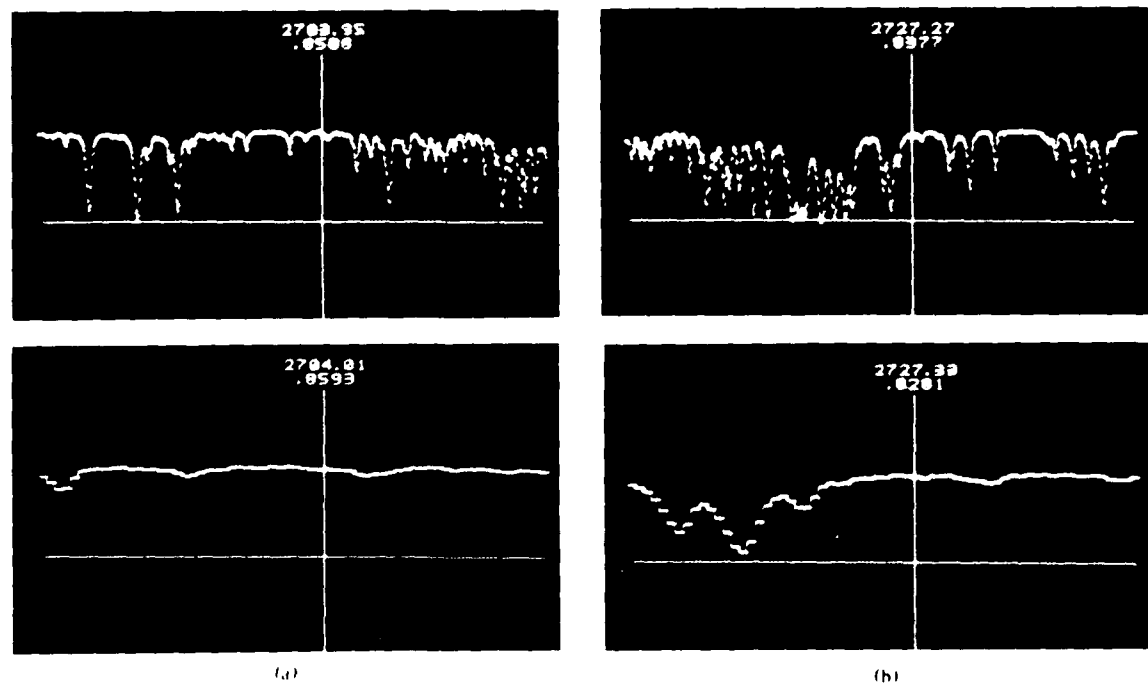


Fig. 14 — Oscilloscope trace showing normalized spectrum structure and absolute transmission amplitude in the vicinity of DF laser lines: Spectrum SNI 12 DRN, (a) P 2-5 and (b) P 2-4

J. A. DOWLING ET AL.

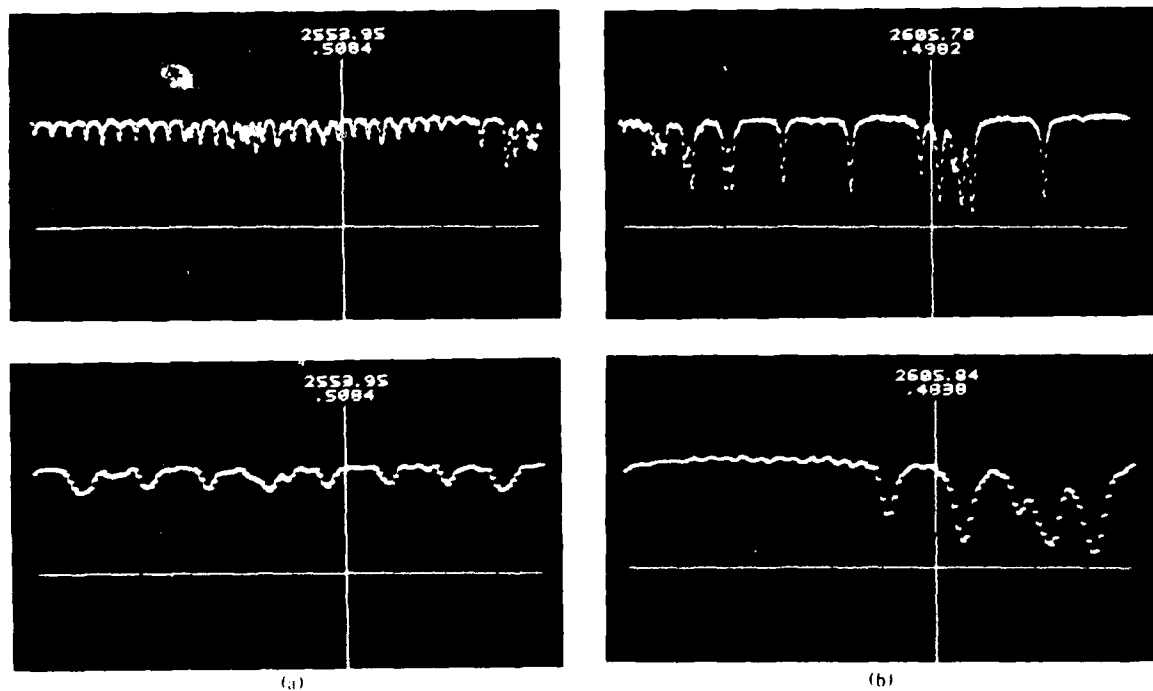


Fig. 15 — Oscilloscope trace showing normalized spectrum structure and absolute transmission amplitude in the vicinity of DE laser lines — Spectrum SNI 26 DRN. (a) P 2-11 and (b) P 2-9

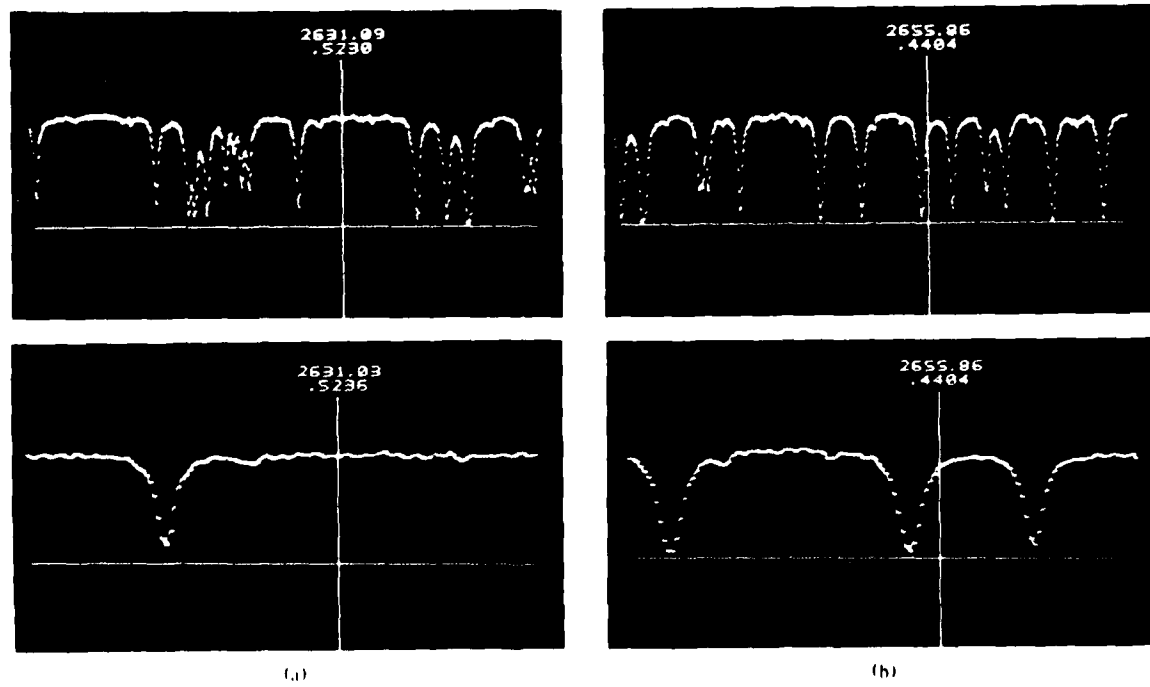


Fig. 16 — Oscilloscope trace showing normalized spectrum structure and absolute transmission amplitude in the vicinity of DE laser lines — Spectrum SNI 26 DRN. (a) P 2-8 and (b) P 2-7

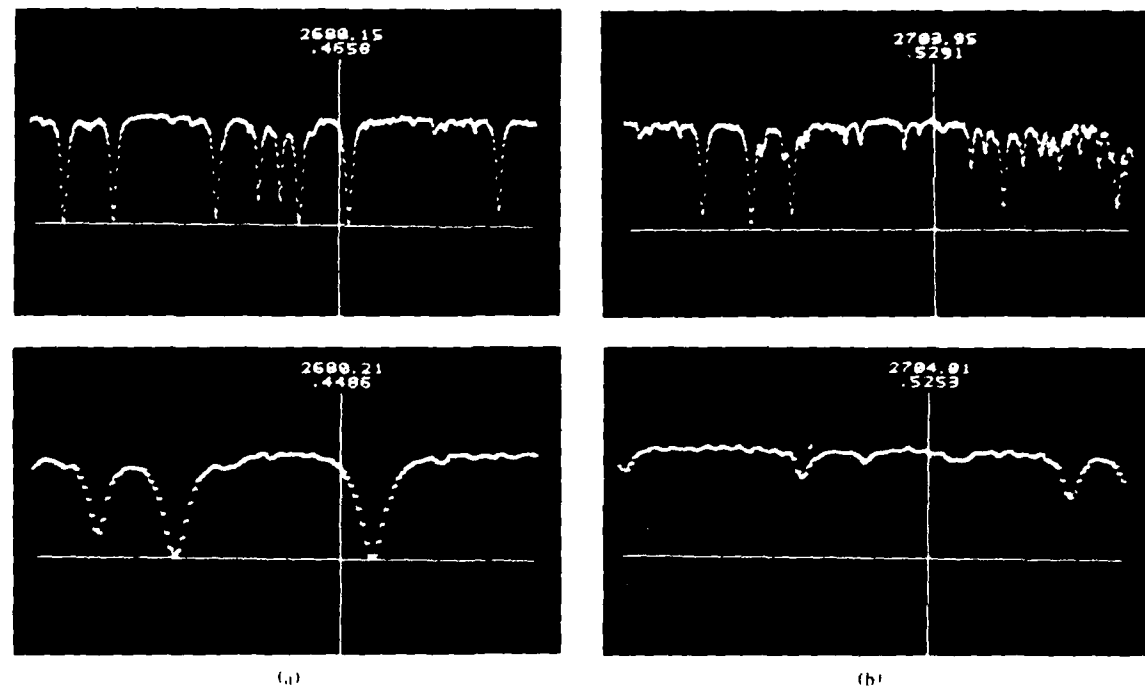


Fig. 17 — Oscilloscope trace showing normalized spectrum structure and absolute transmission amplitude in the vicinity of DF laser lines — Spectrum SNI 26 DRN. (a) P 2-6 and (b) P 2-5

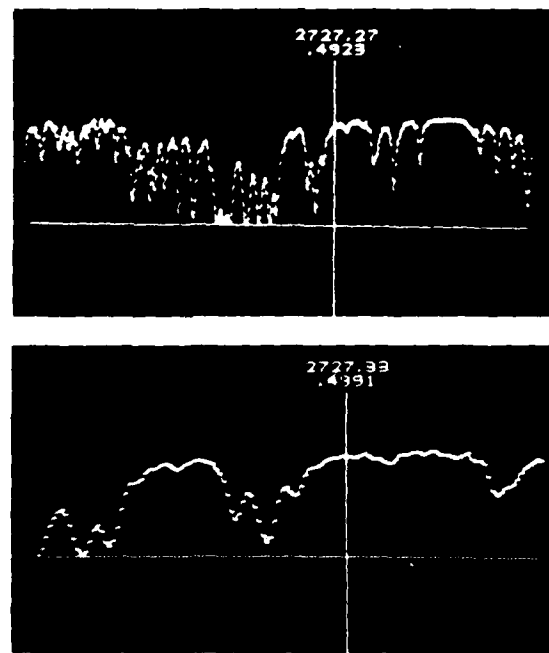


Fig. 18 — Oscilloscope trace showing normalized spectrum structure and absolute transmission amplitude in the vicinity of the P 2-4 DF laser lines

transmission normalization. Examples of the laser lines which are preferable for use in deriving the normalizations are the P2-8, P2-5, and P2-4 lines. The remaining DF laser lines, namely P2-7, P2-6, P2-9, and P2-11 can be seen to be useful in addition for derivation of absolute transmission normalization factors depending upon the particular spectra being studied. Data presented in an earlier report [9] represent a more favorable case than the present one where long-path transmission spectra were measured under higher water vapor partial pressure and higher total atmospheric pressure conditions than in the measurements at White Sands Missile Range discussed in Ref. 9. The P2-7, P2-6, P2-9, and P2-11 laser lines are sufficiently close to atmospheric HDO and H<sub>2</sub>O absorption lines (P2-7, P2-6, and P2-9) and to an atmospheric N<sub>2</sub>O absorption line (P2-11) so that appreciable overlap of the absorption line wing and the laser line position occurs under the higher pressure conditions. For the comparisons listed in Table 4 and shown in Figs. 11 through 18 the amplitude of a spectrum sample value ( $\tau'$  values listed in Table 4) varies usually no more than 1% in absolute transmission between two adjacent samples which bracket the position of the laser line used to normalize the spectrum for absolute transmission. The notable exception is the P2-10 line as previously observed. The average multiplicative normalization factor derived by comparing measured laser transmission to spectrum sample amplitudes at each of the  $\nu'$  values shown in Table 4 did not include the measurements for the P2-10 line and the other lines indicated by an asterisk in the table.

### 3.3 Path Integrated Molecular Absorber Concentrations

Figures 19 and 20 are plots of limited portions of three of the ratioed, normalized spectra listed in Table 3, for the spectral interval 2680 to 2800 cm<sup>-1</sup>. Several reasonably well-isolated HDO absorption lines appear in this region, and absorption profiles of these lines can be used to derive path-integrated average concentrations of this isotope occurring during the measurement times. Using the standard sea-level model atmospheric abundance ratio of 0.03% HDO/H<sub>2</sub>O [10] the path integral HDO measurements can be used to infer values for water vapor concentrations along the path. In the 2680 to 2800 cm<sup>-1</sup> region shown in Figs. 19 and 20 only a few relatively weak H<sub>2</sub>O absorption lines can be identified in contrast to the typical condition of very strong H<sub>2</sub>O absorption lines in almost all other spectral regions of the near infrared. Provided that the accepted value for the sea-level HDO/H<sub>2</sub>O ratio is correct, the spectral region shown in Figs. 19 and 20 is then quite useful for determining average absolute humidities over long atmospheric paths.

In addition to the few weak H<sub>2</sub>O absorption lines that can be identified in the spectral regions shown in Figs. 19 and 20, a few weak, relatively isolated absorption lines of methane and nitrous oxide can also be identified.

Figures 21 and 22 show portions of three spectra recorded in an earlier experiment carried out at White Sands Missile Range (WSMR), New Mexico, shortly before the SNI measurements [9]. The top spectrum shown in these figures (ASL04RN) is annotated with identifications of most of the prominent spectral features in the 2680 to 2800 cm<sup>-1</sup> region which is the same region shown in Figs. 19 and 20.

Table 5 lists the spectral features identified for the three spectra shown in Figs. 21 and 22. Column 1 of the table lists the line position contained in the 1978 edition of the AFGL line atlas [11]. Column 2 contains the observed line position measured from the WSMR spectral records shown in Figs. 21 and 22, generally to a precision of 0.05 cm<sup>-1</sup>. Columns 3, 4, and 5 contain the species identification, line strength, and line half-width respectively as contained in Ref. 11. The same notation for molecular species used in Ref. 10 is used, namely 162 = HDO, 161 = H<sub>2</sub>O, 211 = CH<sub>4</sub>, and 446 = N<sub>2</sub>O. Column 6 of Table 5 lists the transmission at line center (maximum absorption) for each of the prominent absorption lines identified in spectrum ASL04RN. The AFGL line atlas [10,11] lists over 2600 lines in the 2680 to 2800 cm<sup>-1</sup> region whereas Table 5 contains an identification of 165 these for which the product of line strength and concentrations is highest. The observed line positions (column 2 of Table 5) are seen to be consistently about 0.05 to 0.07 cm<sup>-1</sup> less than the AFGL values

NRL REPORT 8618

23

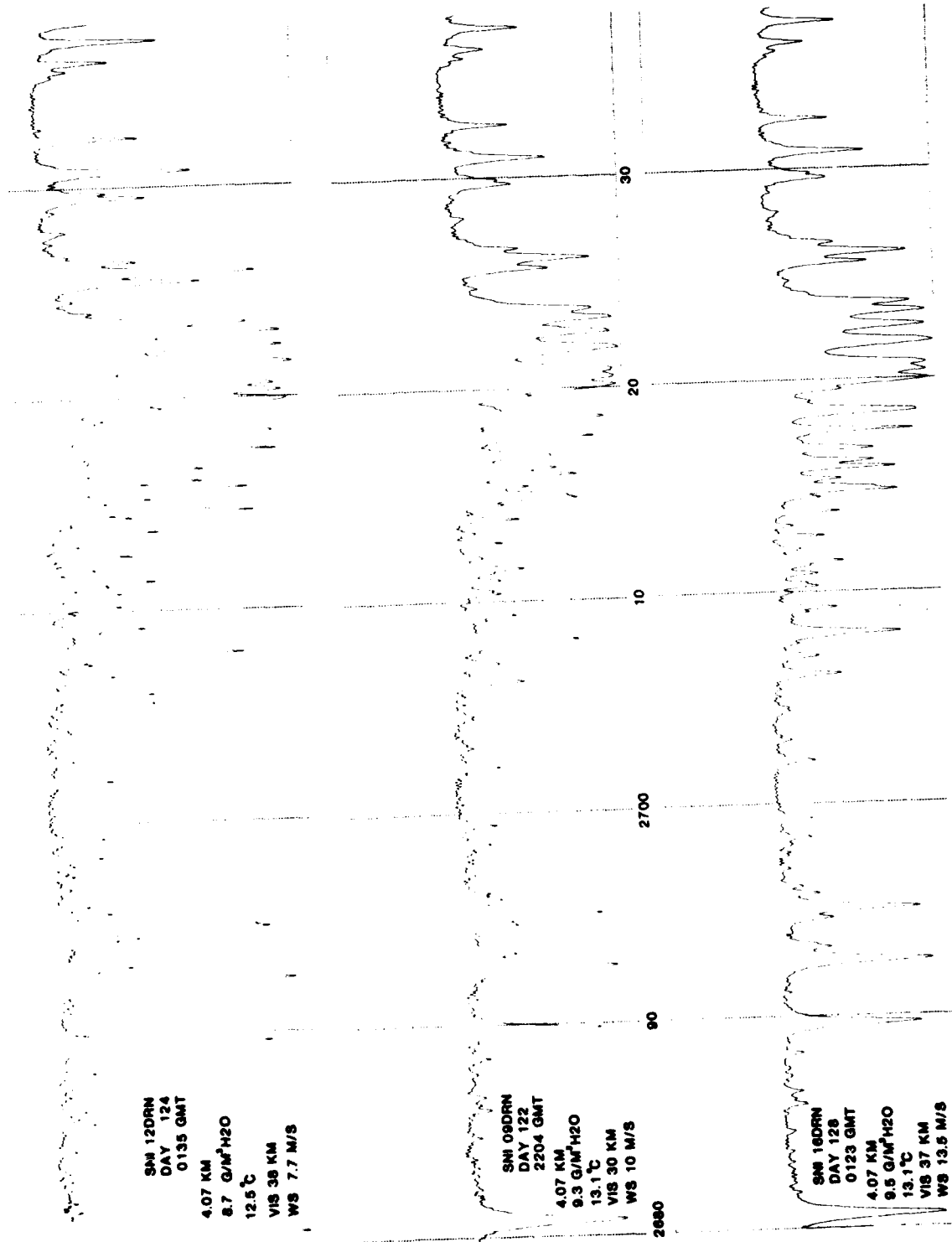


Fig. 19 — Spectra SNI 12 DRN, SNI 09 DRN, and SNI 16 DRN, 2680 cm<sup>-1</sup> to 2740 cm<sup>-1</sup>

J. A. DOWLING ET AL.

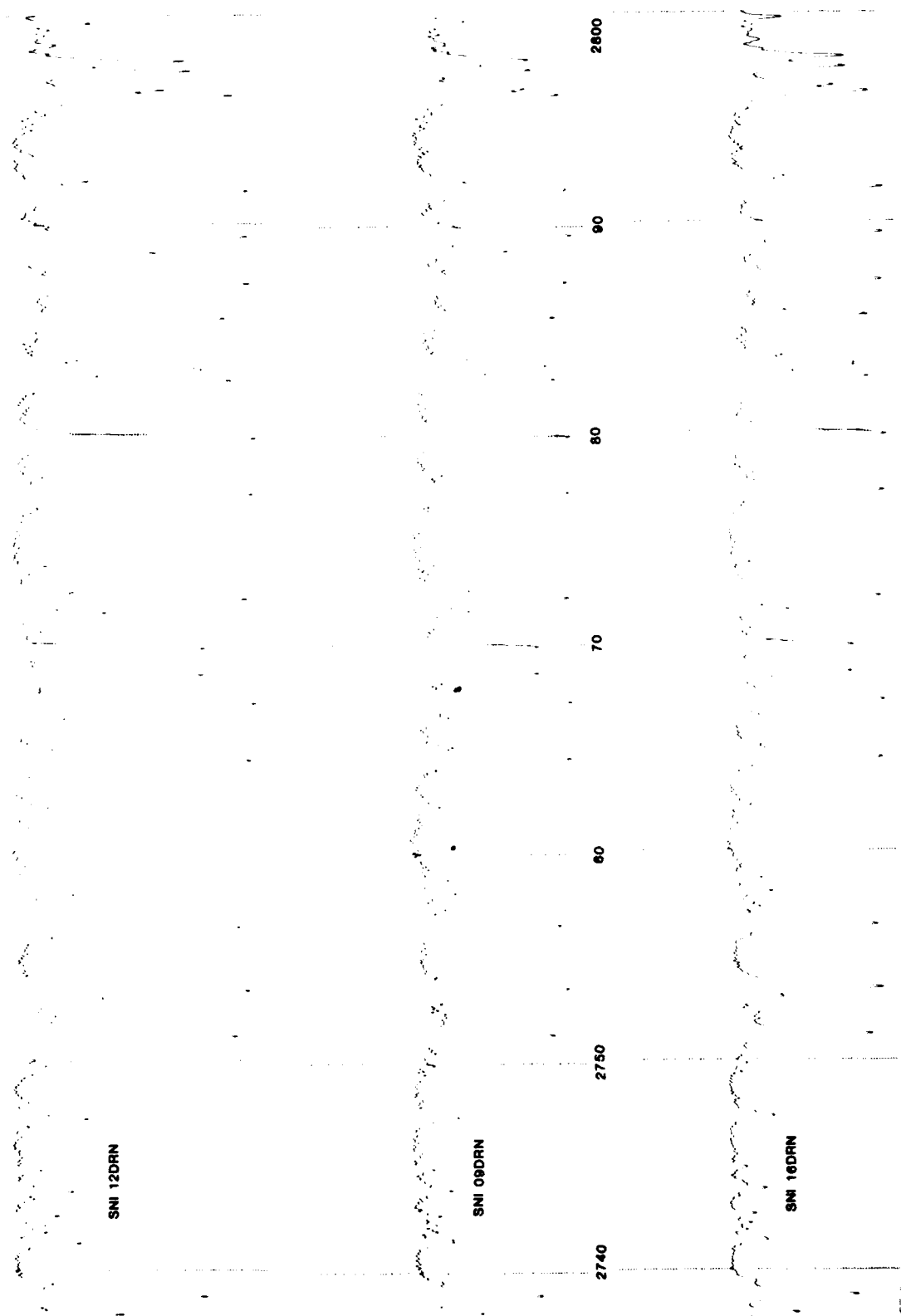


Fig. 20 — Spectra SNI 12 DRN, SNI 09 DRN, and SNI 16 DRN, 2740  $\text{cm}^{-1}$  to 2800  $\text{cm}^{-1}$

NRL REPORT 8618

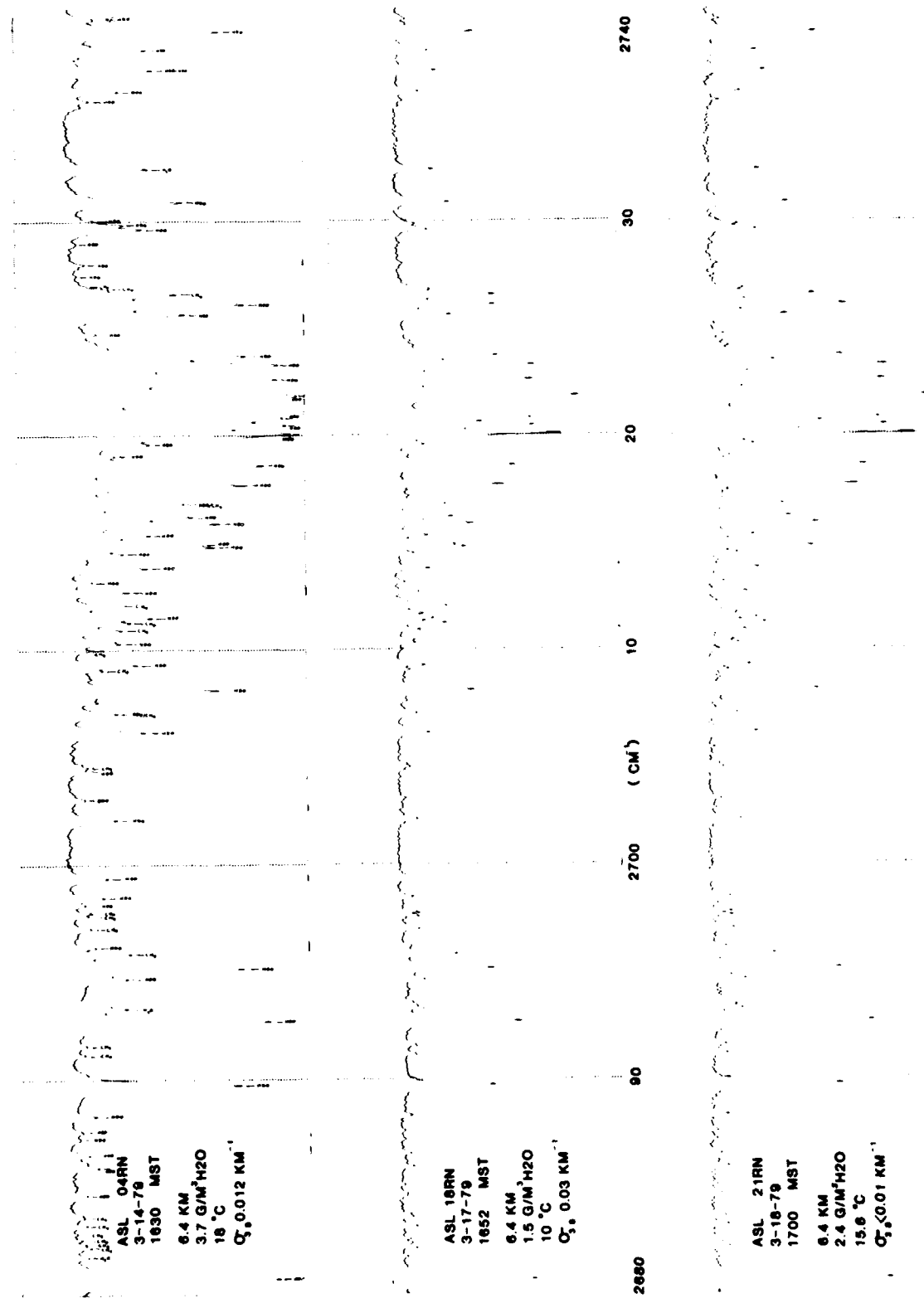


Fig. 21 - Spectra ASL 04 RN, ASL 18 RN, and ASL 21 RN, 2680 cm<sup>-1</sup> to 2740 cm<sup>-1</sup>

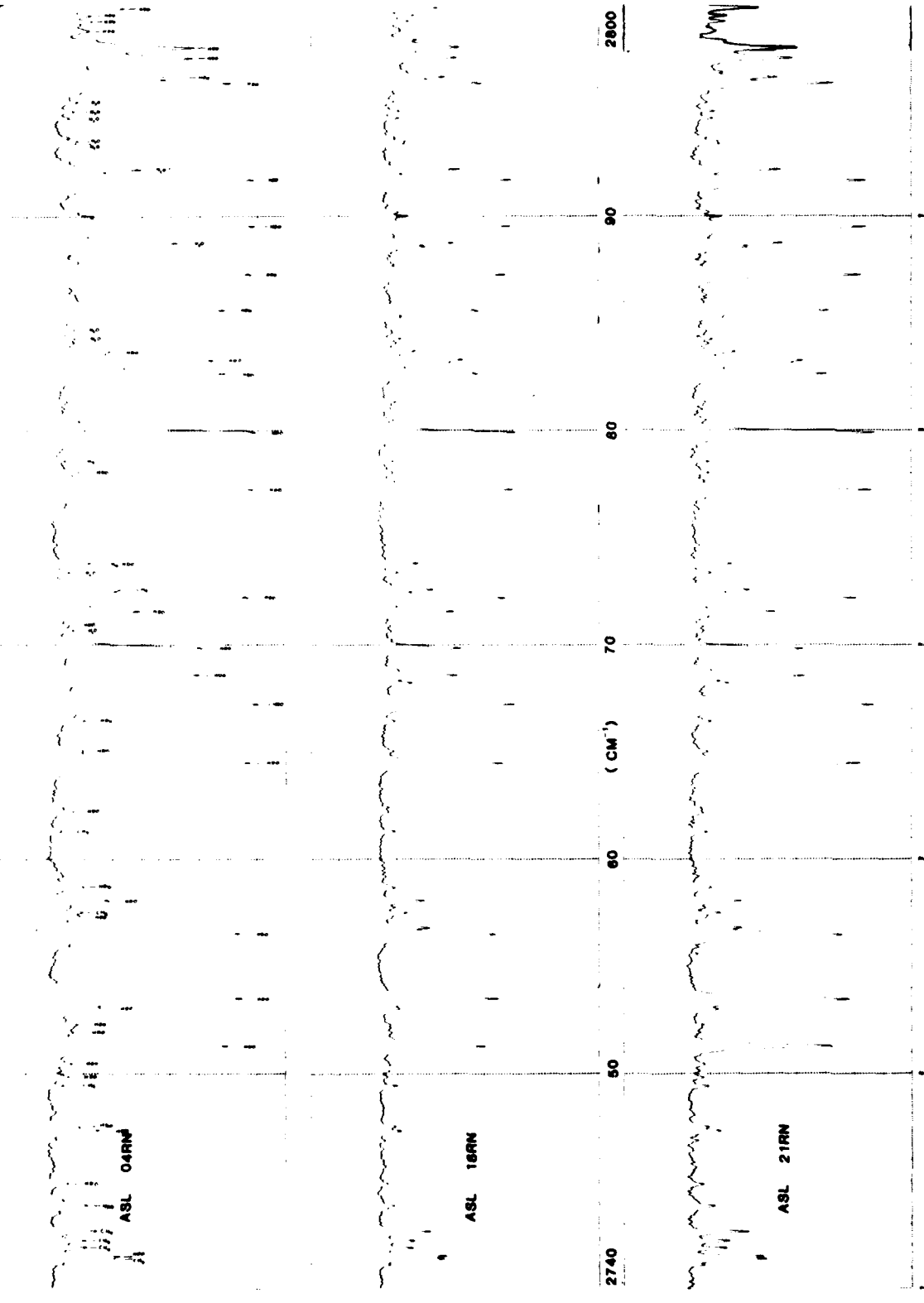


Fig. 22.—Spectra ASL 04 RN, ASL 18 RN, and ASL 21 RN, 2740 cm<sup>-1</sup> to 2800 cm<sup>-1</sup>

Table 5 — FTS Spectral Line Identifications and Measured Transmissions (ASL04RN)

Line Pos. Calculated	Line Pos. Observed	Species*	<i>S</i> (cm <sup>-1</sup> /molecule cm <sup>-2</sup> )	$\alpha$ (cm <sup>-1</sup> )	<i>T</i>
2680.759	2680.70	162	0.776 E-23	0.096	0.103
2681.792	2681.75	161	0.149 E-24	0.046	0.770
2682.230	2682.20	211	0.316 E-21	0.055	0.757
2682.420	2682.35	211	0.228 E-21	0.055	0.775
2682.610	2682.55	211	0.246 E-21	0.055	0.790
2682.860	2682.80	211	0.702 E-22	0.055	0.807
2683.250	2683.20	211	0.263 E-21	0.055	0.772
2683.640	2683.60	211	0.281 E-21	0.055	0.775
2684.686	2684.65	162	0.153 E-24	0.086	0.770
2685.970	2685.90	162	0.303 E-24	0.087	0.728
2682.562	2686.50	162	0.333 E-24	0.089	0.758
2687.267	2687.20	162	0.113 E-24	0.096	0.792
2687.646	2687.55	162	0.130 E-24	0.096	0.782
2688.372	2688.30	162	0.300 E-24	0.084	0.737
2689.785	2689.75	162	0.511 E-23	0.107	0.232
2691.200	2691.15	211	0.281 E-21	0.055	0.772
2691.590	2691.50	211	0.263 E-21	0.055	0.768
2692.750	2692.70	162	0.739 E-23	0.103	0.130
2693.335	2693.30	161	0.425 E-24	0.061	0.624
2694.708	2694.65	162	0.905 E-24	0.094	0.624
2695.208	2695.15	162	0.522 E-23	0.098	0.221
2695.820	B <sup>†</sup>	211	0.694 E-21	0.054	0.610
2696.010		211	0.167 E-24	0.086	0.735
2696.203	2696.15	162	0.351 E-21	0.055	0.750
2697.000	B <sup>†</sup>	211	0.350 E-21	0.054	0.756
2697.120		211	0.386 E-21	0.055	0.745
2697.650	2697.60	211	0.153 E-24	0.098	0.766
2697.810	2697.75	211	0.417 E-24	0.093	0.702
2698.168	2698.10	162	0.682 E-24	0.091	0.688
2698.528	2698.45	162	0.215 E-24	0.094	0.660
2699.420	2699.35	162	0.262 E-24	0.086	0.770
2702.119	2702.10	162	0.198 E-24	0.055	0.758
2703.093	2703.05	162	0.246 E-21	0.097	0.557
2704.458	2704.40	162	0.175 E-22	0.055	0.655
2704.560	2704.50	211	0.417 E-23	0.099	0.300
2706.216	2706.15	162	0.228 E-21	0.055	0.708
2707.150	2707.05	211	0.135 E-23	0.094	0.585
2708.179	2708.15	162	0.175 E-22	0.055	0.745
2709.050	2709.05	211	0.344 E-24	0.044	0.640
2709.340	2709.25	162	0.175 E-21	0.055	0.638
2710.080	2710.00	211	0.422 E-21	0.055	0.608
2710.336	2710.30	162			
2710.960	2710.90	211			
2711.260	2711.25	211			

\* 161 = H<sub>2</sub>O, 162 = HDO, 211 = CH<sub>4</sub>, 446 = N<sub>2</sub>O.<sup>†</sup>B denotes unresolved blend.

Continues

Table 5 — FTS Spectral Line Identifications and Measured Transmissions (ASL04RN) (Continued)

Line Pos. Calculated	Line Pos. Observed	Species*	<i>S</i> (cm <sup>-1</sup> /molecule cm <sup>-2</sup> )	$\alpha$ (cm <sup>-1</sup> )	<i>T</i>
2711.270	2711.50	211	0.333 E-21	0.055	0.528
2711.515	2711.50	162	0.258 E-24	0.061	0.529
2712.060	2712.05	211	0.515 E-21	0.055	0.639
2712.741	2712.70	162	0.708 E-27	0.037	0.606
2713.212	2713.15	162	0.307 E-24	0.075	0.740
2713.866	2713.80	162	0.540 E-24	0.056	0.546
2713.879	2713.80	162	0.540 E-24	0.056	0.546
2714.535	2714.50	162	0.654 E-24	0.071	0.728
2714.853	2714.82	162	0.139 E-23	0.031	0.312
2714.966	2714.92	162	0.270 E-23	0.098	0.355
2715.407	2715.35	162	0.118 E-23	0.085	0.532
2715.958	2715.90	162	0.106 E-23	0.047	0.295
2716.271	2716.20	162	0.255 E-23	0.094	0.390
2716.810	2716.80	162	0.130 E-23	0.070	0.315
2716.840	2716.80	211	0.702 E-22	0.055	0.315
2716.913	2716.80	162	0.130 E-23	0.070	0.315
2716.933	2716.80	162	0.353 E-25	0.081	0.315
2717.751	2717.70	162	0.398 E-23	0.040	0.195
2718.647	2718.60	162	0.245 E-23	0.063	0.145
2718.682	2718.60	162	0.245 E-23	0.063	0.145
2719.007	2719.05	162	0.322 E-25	0.083	0.655
2719.116	2719.05	162	0.322 E-25	0.086	0.655
2719.631	2719.60	162	0.117 E-23	0.085	0.532
2720.132	2720.05	162	0.442 E-23	0.055	0.048
2720.136	2720.05	162	0.442 E-23	0.055	0.048
2720.495	2720.50	162	0.464 E-23	0.095	0.063
2720.553	2720.50	162	0.414 E-23	0.082	0.063
2720.838	2720.80	162	0.562 E-23	0.102	0.075
2720.900	2720.80	162	0.285 E-25	0.093	0.075
2721.877	2721.85	162	0.733 E-23	0.077	0.025
2721.934	2721.85	162	0.733 E-23	0.077	0.025
2722.664	2722.60	162	0.848 E-23	0.096	0.092
2723.338	2723.30	162	0.847 E-23	0.096	0.079
2723.777	2723.75	162	0.461 E-23	0.095	0.200
2724.798	2724.75	162	0.121 E-24	0.094	0.719
2725.682	2725.65	162	0.249 E-23	0.094	0.408
2726.161	2726.10	162	0.558 E-23	0.102	0.207
2726.630	2726.60	211	0.874 E-21	0.057	0.440
2727.528	2725.50	162	0.104 E-24		
2728.060	2728.00	162	0.253 E-24	0.100	0.757
2729.007	2728.95	162	0.105 E-24	0.086	0.790
2729.010	2728.95	162	0.357 E-25	0.096	0.790
2729.675	2729.65	162	0.129 E-23	0.094	0.555

\* 161 = H<sub>2</sub>O, 162 = HDO, 211 = CH<sub>4</sub>, 446 = N<sub>2</sub>O.

Continues

Table 5 — FTS Spectral Line Identifications and Measured Transmissions (ASL04RN) (Continued)

Line Pos. Calculated	Line Pos. Observed	Species*	<i>S</i> (cm <sup>-1</sup> /molecule cm <sup>-2</sup> )	$\alpha$ (cm <sup>-1</sup> )	<i>T</i>
2729.900	2729.80	162	0.559 E-24	0.095	0.620
2730.928	2730.88	162	0.265 E-23	0.098	0.415
2732.491	2732.45	161	0.107 E-23	0.058	0.535
2735.682	2735.65	162	0.295 E-24	0.095	0.738
2736.108	2736.05	162	0.632 E-24	0.091	0.636
2737.121	2737.10	162	0.609 E-24	0.101	0.518
2737.096	2737.10	162	0.485 E-24	0.099	0.518
2738.052	2738.05	162	0.148 E-23	0.097	0.540
2738.923	2738.90	162	0.419 E-23	0.099	0.285
2739.555	2739.50	446	0.770 E-23	0.075	0.720
2739.489	2739.50	162	0.224 E-24	0.100	0.720
2741.478	2741.45	211	0.960 E-21	0.059	0.589
2741.602	2741.55	162	0.998 E-21	0.051	0.572
2741.993	2741.90	211	0.556 E-21	0.059	0.688
2742.314	2742.25	211	0.564 E-21	0.059	0.688
2742.755	2742.70	211	0.872 E-21	0.051	0.652
2743.941	2743.85	162	0.526 E-24	0.096	0.685
2744.965	2744.90	162	0.297 E-24	0.089	0.750
2747.412	2747.35	162	0.851 E-24	0.094	0.645
2747.623	2747.55	162	0.194 E-24	0.097	0.712
2749.490	2749.45	211	0.404 E-21	0.055	0.766
2749.920	2749.85	162	0.239 E-24	0.095	0.750
2750.503	2750.45	162	0.220 E-24	0.094	0.740
2751.342	2751.25	162	0.529 E-23	0.098	0.198
2752.007	2751.95	162	0.199 E-24	0.093	0.733
2752.339	2752.25	162	0.226 E-24	0.096	0.721
2753.112	2753.05	162	0.351 E-24	0.102	0.642
2753.545	2753.50	162	0.746 E-23	0.103	0.149
2756.558	2756.50	162	0.512 E-23	0.102	0.160
2757.377	2757.35	162	0.313 E-24	0.098	0.713
2757.600	2757.55	211	0.449 E-21	0.061	0.703
2758.092	2758.08	162	0.366 E-24	0.098	0.612
2758.751	2758.70	162	0.492 E-24	0.092	0.702
2761.350	2761.30	211	0.421 E-21	0.055	0.779
2762.267	2762.20	162	0.331 E-24	0.102	0.734
2764.551	2764.50	162	0.793 E-23	0.096	0.120
2765.119	2765.05	162	0.257 E-24	0.103	0.705
2766.506	2766.45	162	0.301 E-24	0.099	0.696
2767.277	2767.20	162	0.925 E-23	0.101	0.095
2768.634	2768.60	162	0.381 E-23	0.095	0.295
2769.897	2769.85	162	0.378 E-23	0.096	0.290
2770.717	2770.65	161	0.122 E-24	0.073	0.735
2770.908	2770.90	162	0.886 E-25	0.096	0.751

\* 161 = H<sub>2</sub>O, 162 = HDO, 211 = CH<sub>4</sub>, 446 = N<sub>2</sub>O.

Continues

Table 5 — FTS Spectral Line Identifications and Measured Transmissions (ASL04RN) (Concluded)

Line Pos. Calculated	Line Pos. Observed	Species*	<i>S</i> (cm <sup>-1</sup> /molecule cm <sup>-2</sup> )	$\alpha$ (cm <sup>-1</sup> )	<i>T</i>
2771.614	2771.60	162	0.282 E-24	0.090	0.507
2722.259	2722.20	162	0.739 E-23	0.099	0.131
2722.630	2772.60	211	0.404 E-21	0.055	
2722.657	2722.60	211	0.524 E-21	0.055	
2773.404	2773.40	446	0.454 E-21	0.077	0.752
2773.872	2773.80	211	0.607 E-21	0.063	0.680
2777.301	2777.25	162	0.878 E-23	0.095	0.110
2778.148	2778.10	162	0.197 E-24	0.098	0.720
2778.640	2778.60	211	0.263 E-21	0.055	0.765
2779.969	2779.90	162	0.953 E-23	0.098	0.105
2782.718	2782.70	162	0.526 E-23	0.093	0.207
2783.353	2783.30	162	0.210 E-23	0.081	0.244
2783.722	2783.70	162	0.418 E-24	0.102	0.620
2784.351	2784.30	446	0.153 E-22	0.093	0.732
2784.355	2784.30	446	0.153 E-22	0.110	0.732
2784.748	2784.70	446	0.499 E-23	0.082	0.733
2784.742	2784.70	446	0.499 E-23	0.082	0.733
2785.659	2785.60	162	0.515 E-23	0.095	0.208
2787.333	2787.30	162	0.773 E-23	0.096	0.120
2788.811	2788.75	161	0.121 E-23	0.076	0.377
2789.593	2789.55	162	0.828 E-23	0.094	0.108
2791.759	2791.70	162	0.866 E-23	0.096	0.112
2792.253	2792.20	446	0.555 E-22	0.070	0.503
2793.411	2793.40	446	0.130 E-21	0.073	0.730
2793.628	2793.50	446	0.152 E-21	0.073	0.725
2793.840	2793.75	446	0.177 E-21	0.074	0.750
2794.638	} B <sup>†</sup>	2794.60	0.309 E-21	0.075	0.752
2794.702		446	0.548 E-22	0.086	
2795.008	2794.95	446	0.398 E-21	0.075	0.737
2795.431	2795.40	162	0.206 E-24	0.098	0.726
2796.294	2796.25	162	0.525 E-23	0.092	0.186
2796.577	2796.50	162	0.911 E-24	0.065	0.355
2797.472	2797.40	162	0.272 E-23	0.081	0.328
2797.971	2797.90	162	0.271 E-23	0.084	0.322
2798.747	2798.70	162	0.313 E-24	0.095	0.682
2799.189	2799.15	162	0.126 E-25	0.089	0.673
2799.193	2799.15	162	0.873 E-25	0.083	0.673
	2799.45				
2799.787	2799.75	162	0.576 E-24	0.096	0.564

\*161 = H<sub>2</sub>O, 162 = HDO, 211 = CH<sub>4</sub>, 446 = N<sub>2</sub>O.<sup>†</sup>B denotes unresolved blend.

## NRL REPORT 8618

listed in column 1, which is the limiting accuracy of the FTS hardware and plotting software. Improvements in the FTS frequency scale calibration to  $< 0.05 \text{ cm}^{-1}$  are possible by using independent measurements of multiline laser spectra and interpolation procedures, but this was not done for the spectra shown in Figs. 19 to 22 which are sufficiently well calibrated in frequency to provide unambiguous comparisons to the spectral lines listed in column 1 of Table 5.

Derivation of path-integral HDO concentrations was performed by simply measuring the peak absorption (minimum transmission) values of each absorption line at line center and relating this measurement (appropriately corrected for the spectral line base absorption value, i.e., local transmission maximum) to the average numerical density of the HDO molecule along the absorption path. This procedure is less exact than integrating the area under a spectral absorption line and equating that value to the line strength, particularly when the line profile suffers significant modification due to the effects of finite resolution of the measuring instrument. In the present case the full unapodized-base width of the FTS instrument function is  $0.0625 \text{ cm}^{-1}$  which is equivalent to about  $0.05 \text{ cm}^{-1}$  for an apodized spectrum using a conventional spectroscopic definition for resolution (Rayleigh criterion).

This value is 25 to 50% of the full-width at half maximum (FWHM) value for most of the lines listed in Table 5 and accordingly does not contribute significantly to a reduction in peak line intensity. HITRAN calculations have been performed for conditions similar to those corresponding to the measurements shown in Figs. 19 to 22 including convolution with  $(\sin x)/x$  instrument functions. Very minor differences are apparent between infinite resolution calculations and those done with instrument functions up to  $0.08 \text{ cm}^{-1}$  wide, therefore it was determined that the errors introduced by measuring minimum transmission at line center as opposed to integrated line area would be less than 10%. A more important factor contributing to errors in determining path-integral molecular concentrations from the spectra shown in Figs. 19 to 22 for many cases is the blending of many weak unresolved lines with a marginally stronger line being measured. This situation exists for most of the  $\text{H}_2\text{O}$ ,  $\text{CH}_4$ , and  $\text{N}_2\text{O}$  lines present in the  $2680$  to  $2800 \text{ cm}^{-1}$  region. Only a rigorous correction for the contribution of the several weaker lines blending with the line being measured would improve the measurement accuracy for the weaker lines. Such an analysis procedure can only be realistically accomplished using several iterations with a HITRAN calculation in the interpretation of the weaker features appearing in these spectra.

Path-integral molecular concentration values were obtained for several of the spectra listed in Table 3 by using the following procedures. The transmission values shown in Figs. 21 and 22 can be related to absorber concentrations and the path length as follows:

$$T = \exp(-u_L K_L - u_C K_C) \quad (1)$$

where  $T$  is the measured transmission,  $u_L$  and  $u_C$  are the absorber amounts corresponding to line and continuum absorptions respectively, and  $K_L$  and  $K_C$  are the corresponding absorption coefficients. Equation (1) can be written as:

$$\ln T = -u_L K_L - u_C K_C. \quad (2)$$

Away from an absorption line  $K_L = 0$  and the "continuum transmission,"  $T'$  is related to the product  $u_C K_C$  by:

$$-\ln T' = u_C K_C. \quad (3)$$

Equation (1) can then be written as:

$$\ln(T'/T) = u_L K_L. \quad (4)$$

Now

$$u_L = 7.34 \times 10^{21} \frac{P L}{\theta} \quad (5)$$

J. A. DOWLING ET AL.

where  $P$  is the pressure in atmospheres,  $L$  is the path length in centimeters, and  $\theta$  is the temperature in degrees kelvin.

The spectral absorption coefficient for a single Lorentz absorption line (true for atmospheric pressures above 0.1 atm) is given by

$$K_L(\nu) = \frac{S}{\pi} \left[ \frac{\alpha}{(\nu - \nu_0)^2 + \alpha^2} \right] \quad (6)$$

where  $S$  is the line strength in  $\text{cm}^2 \text{ mol}^{-1} \text{ cm}^{-1}$ ,  $\alpha$  is the line half-width in  $\text{cm}^{-1}$ , and  $\nu$  is the wavenumber in  $\text{cm}^{-1}$ . At line center when  $\nu = \nu_0$  then Eq. (6) simplifies to

$$K_L = \frac{S}{\pi\alpha}. \quad (7)$$

For the measurements under consideration here  $L$  in Eq. (5) is  $4.07 \text{ km} = 4.07 \times 10^5 \text{ cm}$ , and an average representative temperature is  $55^\circ\text{F} = 286 \text{ K}$ .

Therefore Eq. (4) can be written as:

$$\ln(T'/T) = 4.272 \times 10^{21} \frac{S}{\alpha} P. \quad (8)$$

with the absorber partial pressure  $P$  in units of torr.

The line strength values for HDO listed in Ref. 11 incorporate the HDO/H<sub>2</sub>O abundance ratio of 0.03%; therefore the partial pressure of H<sub>2</sub>O corresponding to measurements of the HDO absorption line-center transmission values for the spectra shown in Figs. 21 and 22 is given by

$$P(\text{torr}) = \ln(T'/T) \times 2.341 \times 10^{-22} \frac{\alpha}{S}. \quad (9)$$

Equation (9) has been used to derive path-integral values for H<sub>2</sub>O based primarily on measurements of several strong, well-isolated HDO lines in the 2680 to 2800  $\text{cm}^{-1}$  region shown in Figs. 21 and 22.

The results of this analysis are contained in Table 6. For the several HDO lines measured average absolute humidity values are summarized in Table 7 and compared to fixed dew-point sampled measurements obtained using the NRL aerosol van system (NRL Code 6532) and by the NRL-operated meteorological tower mounted system (NRL Code 4320) permanently located at site A. Figure 23 is a plot of these comparisons.

### 3.4 Meteorological Measurements

For the purposes of this report the dew point and the aerosol-particle size distribution are probably the most important meteorological parameters. From the dew point derives the water vapor pressure which determines the major portion of the molecular absorption for the wavelengths involved in this measurement. The aerosol-particle size distribution is required to calculate the aerosol extinction at those wavelengths. For certain types of studies in the marine environment the air temperature, the wind speed, and the wind direction can also be important. This is not so much the case for this measurement on SNI, however, because the air temperature and wind direction showed little variation for the period of the experiment. That is, little can be said about changes in results as a function of these parameters.

## NRL REPORT 8618

Table 6 — Path-Integrated Water Vapor Measurements

			SNI 01DRN Day 121 1731 GMT*			
Line Pos. Cal. (cm <sup>-1</sup> )	Species	α/s (cm <sup>2</sup> /mol)	T	T'	ln $\left(\frac{T'}{T}\right)$	ppH <sub>2</sub> O (torr)
2689.785	162	.200 E23	.095	.828	2.165	10.14
2695.208	162	.188 E23	.092	.828	2.197	09.67
2708.179	162	.237 E23	.160	.828	1.644	09.12
2726.161	162	.183 E23	.083	.820	2.291	09.81
2730.928	162	.370 E23	.266	.818	1.123	09.73
2747.412	162	.105 E24	.570	.805	.345	08.50
2768.634	162	.249 E23	.168	.780	1.535	08.95
2797.472	162	.298 E23	.202	.780	1.351	09.43
2797.971	162	.310 E23	.223	.780	1.252	09.09
						09.38 ± .510

\*time of laser calibration measurement

Table 6 — Path-Integrated Water Vapor Measurements (Continued)

			SNI 06DRN Day 122 1546 GMT*				SNI 09DRN Day 122 2204 GMT*			
Line Pos. Cal. (cm <sup>-1</sup> )	Species	α/s (cm <sup>2</sup> /mol)	T	T'	ln $\frac{T'}{T}$	ppH <sub>2</sub> O (torr)	T	T'	ln $\frac{T'}{T}$	ppH <sub>2</sub> O (torr)
2689.785	162	.200 E23					.120	.620	1.642	7.69
2708.179	162	.237 E23	.107	.695	1.871	10.38	.152	.600	1.373	7.62
2730.928	162	.370 E23	.210	.704	1.210	10.48	.230	.610	.9624	8.34
2747.412	162	.105 E24	.475	.696	.382	9.40	.442	.616	.332	8.20
2768.634	162	.249 E23	.125	.700	1.723	10.04	.148	.615	1.424	8.30
2797.472	162	.298 E23	.147	.689	1.545	10.78	.172	.604	1.256	8.76
2797.971	162	.310 E23	.165	.689	1.429	10.37	.183	.604	1.194	8.66
						10.24 ± .476				8.22 ± .390

\*time of laser calibration measurement

Table 6 — Path-Integrated Water Vapor Measurements (Continued)

			SNI 04DRN Day 127 0153 GMT*			
Line Pos. Cal. (cm <sup>-1</sup> )	Species	α/s (cm <sup>2</sup> /mol)	T	T'	ln $\left(\frac{T'}{T}\right)$	ppH <sub>2</sub> O (torr)
2708.179	162	.237 E23	.110	.680	1.822	10.11
2730.928	162	.370 E23	.217	.679	1.141	09.88
2747.412	162	.105 E24	.468	.670	.359	08.80
2768.634	162	.249 E23	.137	.677	1.598	09.31
2797.472	162	.298 E23	.173	.633	1.343	09.37
2797.971	162	.310 E23	.188	.663	1.260	09.15
						09.44 ± .481

\*time of laser calibration measurement

Table 6 — Path-Integrated Water Vapor Measurements (Continued)

			SNI 10DRN Day 123 0126 GMT*				SNI 11DRN Day 123 1528 GMT*			
Line Pos. Cal. (cm <sup>-1</sup> )	Species	α/s (cm <sup>2</sup> /mol)	T	T'	ln $\frac{T'}{T}$	ppH <sub>2</sub> O (torr)	T	T'	ln $\frac{T'}{T}$	ppH <sub>2</sub> O (torr)
2689.785	162	.200 E23	.080	.617	2.043	09.56	.688	.705	2.081	09.74
2695.208	162	.188 E23	.082	.617	2.018	08.80	.088	.706	2.082	09.16
2708.179	162	.237 E23	.102	.607	1.784	09.90	.155	.709	1.520	08.43
2730.928	162	.370 E23	.182	.597	1.188	10.29	.225	.692	1.123	09.73
2747.412	162	.105 E24	.410	.603	.386	09.50	.486	.692	.353	08.70
2768.634	162	.249 E23	.090	.593	1.885	10.99	.120	.669	1.718	10.01
2797.472	162	.298 E23	.140	.580	1.421	09.91	.162	.647	1.385	09.66
2797.971	162	.310 E23	.133	.580	1.473	10.69	.167	.647	1.354	09.83
						9.96 ± .700				
										9.41 ± .518

\*time of laser calibration measurement

Table 6 — Path-Integrated Water Vapor Measurements (Continued)

			SNI 12DRN Day 124 0133 GMT*				
Line Pos. Cal (cm <sup>-1</sup> )	Species	α/s (cm <sup>2</sup> /mol)	T	T'	ln $\left(\frac{T'}{T}\right)$	ppH <sub>2</sub> O (torr)	
2689.785	162	.200 E23	.130	.910	1.946	9.11	
2695.208	162	.188 E23	.125	.905	1.980	8.71	
2708.179	162	.237 E23	.190	.900	1.555	8.63	
2726.161	162	.183 E23	.115	.900	2.058	8.82	
2730.928	162	.370 E23	.340	.900	.973	8.43	
2747.412	162	.105 E24	.613	.900	.384	9.40	
2768.634	162	.249 E23	.192	.893	1.537	8.96	
2797.472	162	.298 E23	.238	.877	1.304	9.10	
2797.971	162	.310 E23	.263	.877	1.204	8.74	
							8.89 ± .295

\*time of laser calibration measurement

Table 6 — Path-Integrated Water Vapor Measurements (Concluded)

			SNI 14DRN Day 127 2216 GMT*				SNI 16DRN Day 128 0139 GMT*				
Line Pos. Cal. (cm <sup>-1</sup> )	Species	α/s (cm <sup>2</sup> /mol)	T	T'	ln $\frac{T'}{T}$	ppH <sub>2</sub> O (torr)	T	T'	ln $\frac{T'}{T}$	ppH <sub>2</sub> O (torr)	
2689.785	162	.200 E23	.080	.555	1.937	9.07	.096	.603	1.838	8.61	
2695.208	162	.188 E23	.072	.555	2.042	8.99	.090	.600	1.897	8.35	
2708.179	162	.237 E23	.106	.555	1.656	9.19	.130	.600	1.529	8.48	
2726.161	162	.183 E23	.060	.538	2.194	9.40	.072	.595	2.112	9.05	
2830.928	162	.370 E23	.186	.542	1.070	9.27	.215	.590	1.009	8.74	
2742.412	162	.105 E24	.391	.553	.347	8.50	.428	.587	.316	7.80	
2768.634	162	.249 E23	.112	.533	1.560	9.09	.139	.583	1.434	8.36	
2797.472	162	.298 E23	.127	.525	1.419	9.90	.152	.575	1.330	9.28	
2797.971	162	.310 E23	.142	.525	1.308	9.49	.159	.575	1.285	9.33	
							9.29 ± .384	8.67 ± .494			

\*time of laser calibration measurement

Table 7 — Summary of Water Vapor Concentration Measurements

GMT		PDT		Spectrum	CONC H <sub>2</sub> O		
Day	Time*	Day	Time*		FTS (torr)	NRL 6532	NRL 4320
121	1700	5-1	1000	SNI 01DRN	9.38 ± .510	9.0	
122	0153	5-1	1850	SNI 04DRN	9.44 ± .481	8.7	8.2
122	1546	5-2	0846	SNI 06DRN	10.24 ± .476	8.6	8.6 <sup>†</sup>
122	2204	5-2	1504	SNI 09DRN	8.22 ± .390	8.9	9.1
123	0126	5-2	1826	SNI 10DRN	9.96 ± .700	8.8	9.2
123	1528	5-3	0830	SNI 11DRN	9.41 ± .518	8.9	9.2
124	0130	5-3	1830	SNI 12DRN	8.89 ± .295	7.9	8.5
127	2215	5-7	1515	SNI 14DRN	9.21 ± .384	8.8	9.2
128	0130	5-7	1830	SNI 16DRN	8.69 ± .494	8.8	9.3

\*time of laser transmission calibration measurements

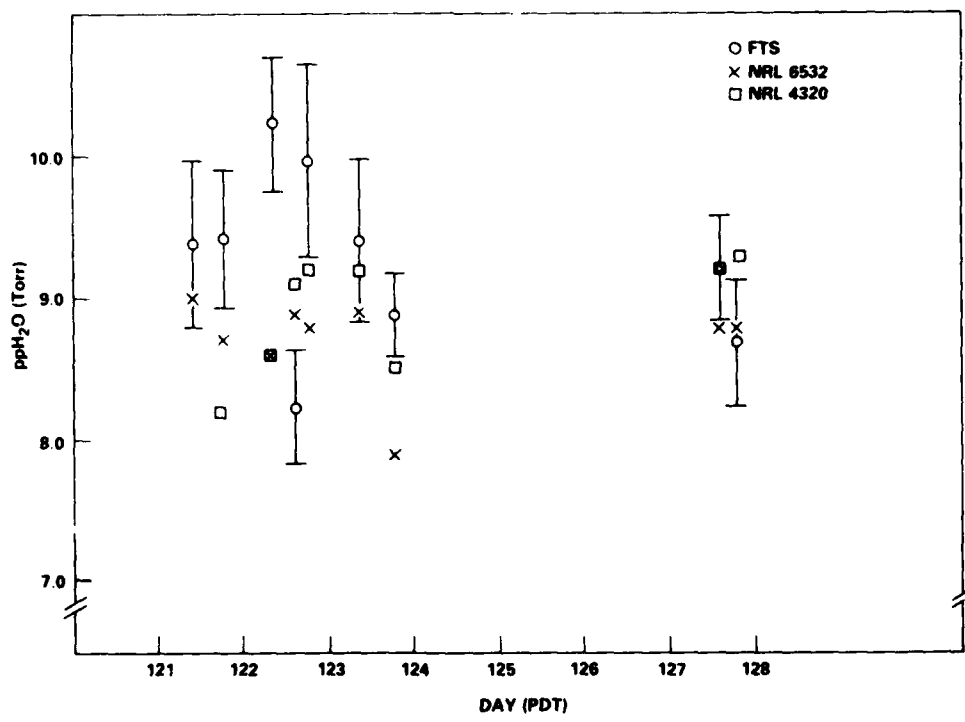
<sup>†</sup>interpolated

Fig. 23 — Comparison of FTS and point measurements of water vapor concentration

In the aerosol van the PMS Data Acquisition System stores the aerosol-particle size counts and the analog meteorological data on 9-track magnetic tape. Simultaneously, the data are directed to a PDP 11/34 computer for real-time processing. For displaying and analyzing our aerosol and meteorological data we have developed a rather elaborate set of software [12]. This software allows postprocessing of the magnetic tape as well as real-time processing. As an example of the postprocessing, and in support of the statement about the small variation in air temperature, Fig. 24 shows the frequency-of-occurrence of the air temperature for the 290 30-minute averages obtained during the experiment.

One reason for measuring meteorological parameters during optical propagation experiments is for aid in validating or developing models. The Wells-Munn/Katz-Ruhnke (WMKR) aerosol model [13,14] has wind speed as one of its input parameters. There was some variation in wind speed as Fig. 25 shows. At beach sites, however, it is important to keep track of wind direction because the surf-generated aerosol can be dominant in the aerosol particle size distribution. Figure 26 gives the distribution of the wind direction. Since the direction is nearly the same for the entire period, that can simply be noted. Unfortunately that direction is directly from the sea, and the surf spray was quite strong at the aerosol sampling site. The problem is exacerbated by the fact that a group of rocks lie just off shore and upwind where more surf action occurs. Thus, to attempt to use the measured wind speeds in an open-sea aerosol model such as the WMRK would be foolish because of the surf influence.

The last one-dimensional meteorological parameter we measured is dew-point temperature. Figure 27 shows the distribution of those measurements. As stated earlier, we use this parameter to determine the water vapor pressure for molecular absorption calculations. Figure 28 shows how the resultant partial pressure varied during the period. For many aerosol studies, the relative humidity is an important value. We derive that from the air temperature and dew point reading. Figure 29 gives the distribution of the relative humidity, showing that the values were usually high. Thus, we can assume that the aerosol particles are made primarily of water and hence spherical.

To calculate extinction due to aerosols we use measured aerosol-particle size distributions. Figure 30 provides a sample aerosol-particle size distribution for each day of the measurement. Note that there is a hump in the curves near  $0.8 \mu\text{m}$ . This is due to a double-valued sensitivity function and is thus an artifact of the measurement process. Therefore, in doing the extinction coefficient calculations we discard the data from the eight largest bins of the active probe and replace them with a straight line.

Because the transmittance measurement equipment takes longer to set up than the meteorological and aerosol equipment, Figs. 24 through 30 include several days of data during which there were no transmittance results. For the sake of completeness, and for other participants who may have use for the data from those other days, Table 8 includes all the 30-minute averages obtained during our stay on SNI.

Table 8 needs little explanation with respect to the meteorological parameters discussed above. One point to note for comparison purposes is that the listed times are the ends of the 30-minute averaging periods. The last four columns are calculated aerosol extinction coefficients in units of inverse kilometers. We obtain those values by doing a Mie-scattering calculation on the measured aerosol-particle size distribution, assuming spherical particles of water (supported by Fig. 29), using the equation

$$\sigma_{\text{ext}}(\lambda, n) = \int_R \frac{dN}{dR} Q(\lambda, n) \pi R^2 dR,$$

where  $dN/dR$  is the particle size distribution in particles  $\text{cm}^{-3} \mu\text{m}^{-1}$  and  $Q$  is the Mie extinction efficiency function. As noted  $Q$  is a function of wavelength and the complex index of refraction of the particle material. In this table, molecular absorption is not included.

J. A. DOWLING ET AL.

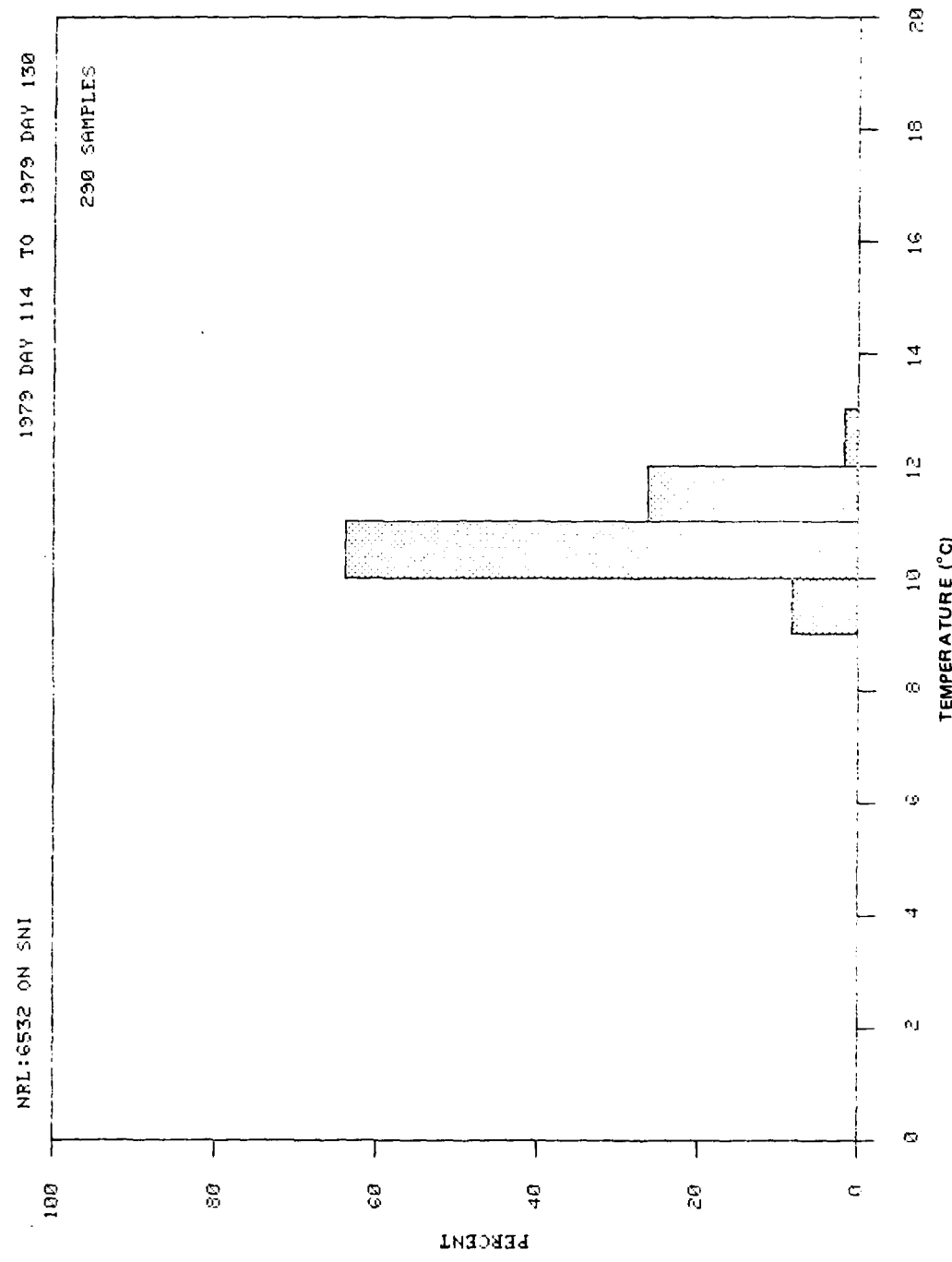


Fig. 24 — Frequency-of-occurrence plot of air temperature

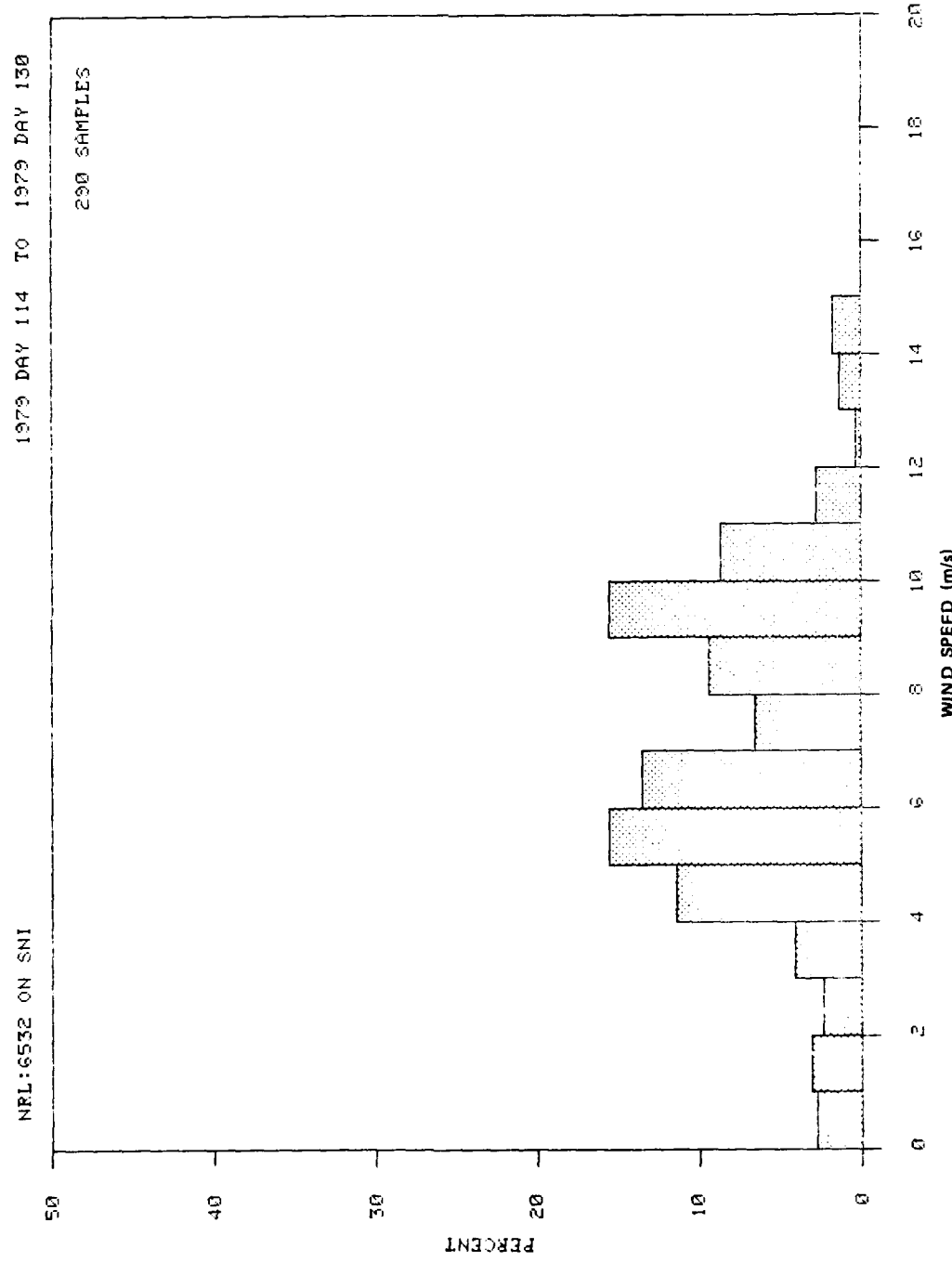


Fig. 25 — Frequency-of-occurrence plot of wind speed

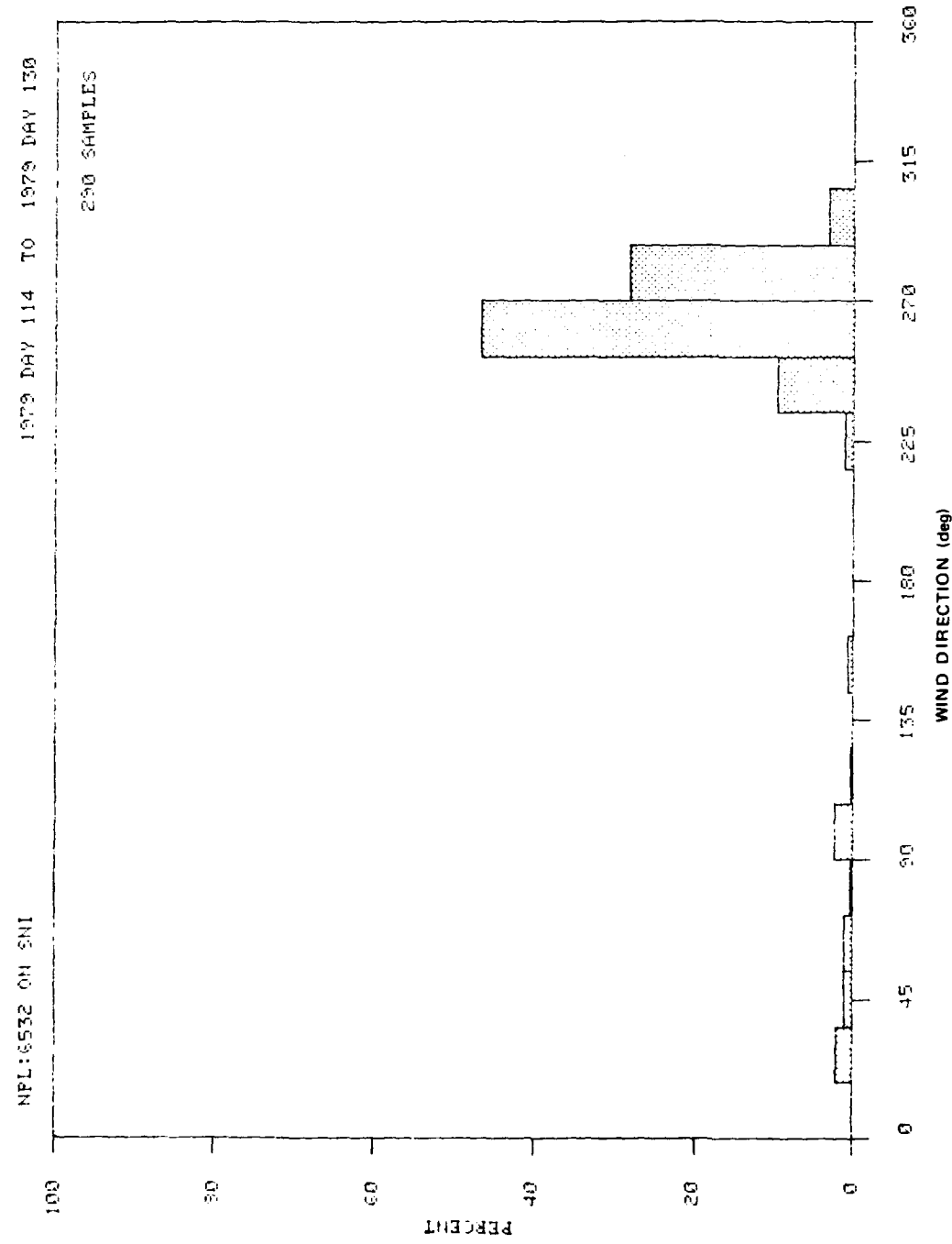


Fig. 26 — Frequency-of-occurrence plot of wind direction

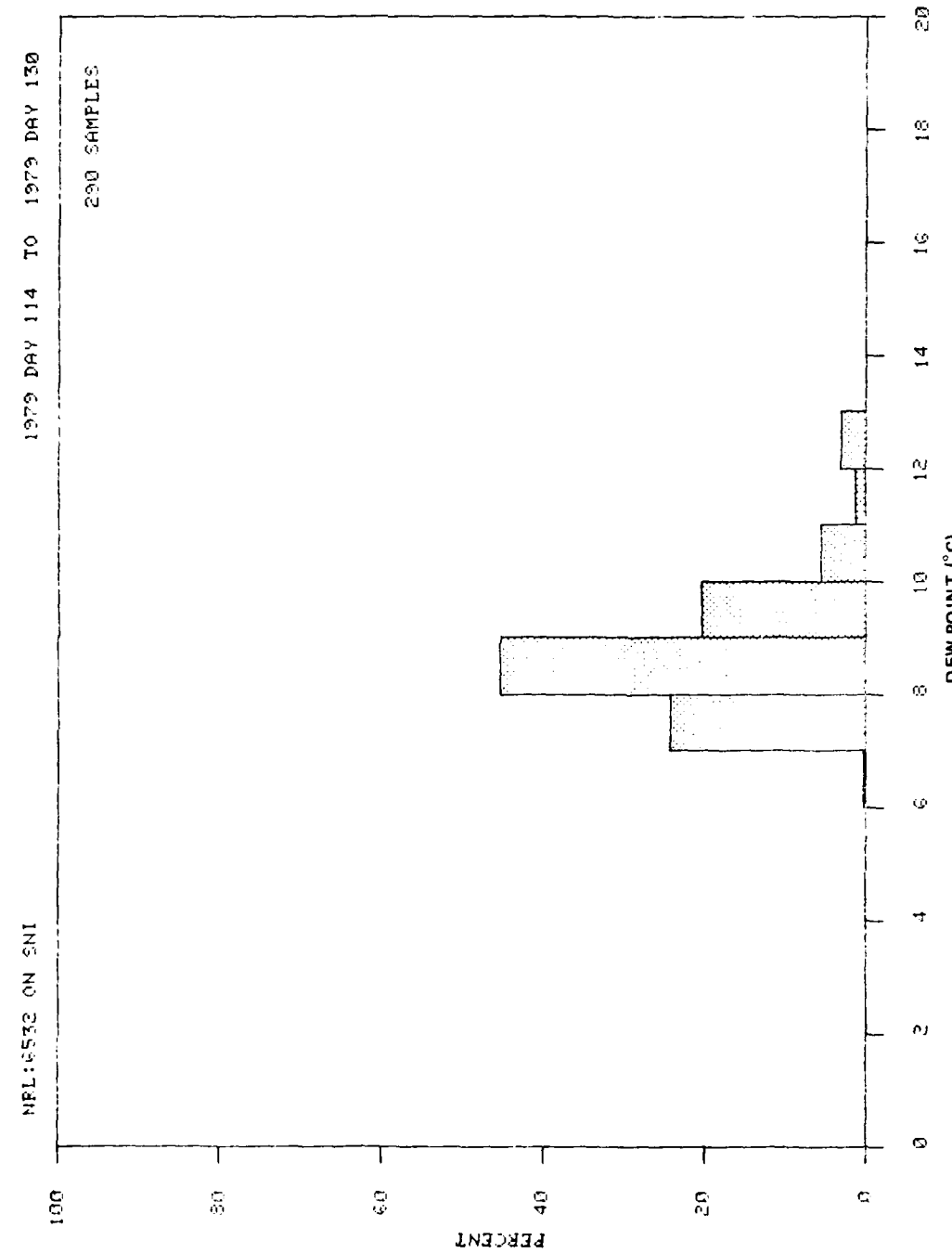


Fig. 27 — Frequency-of-occurrence plot of dew-point temperature

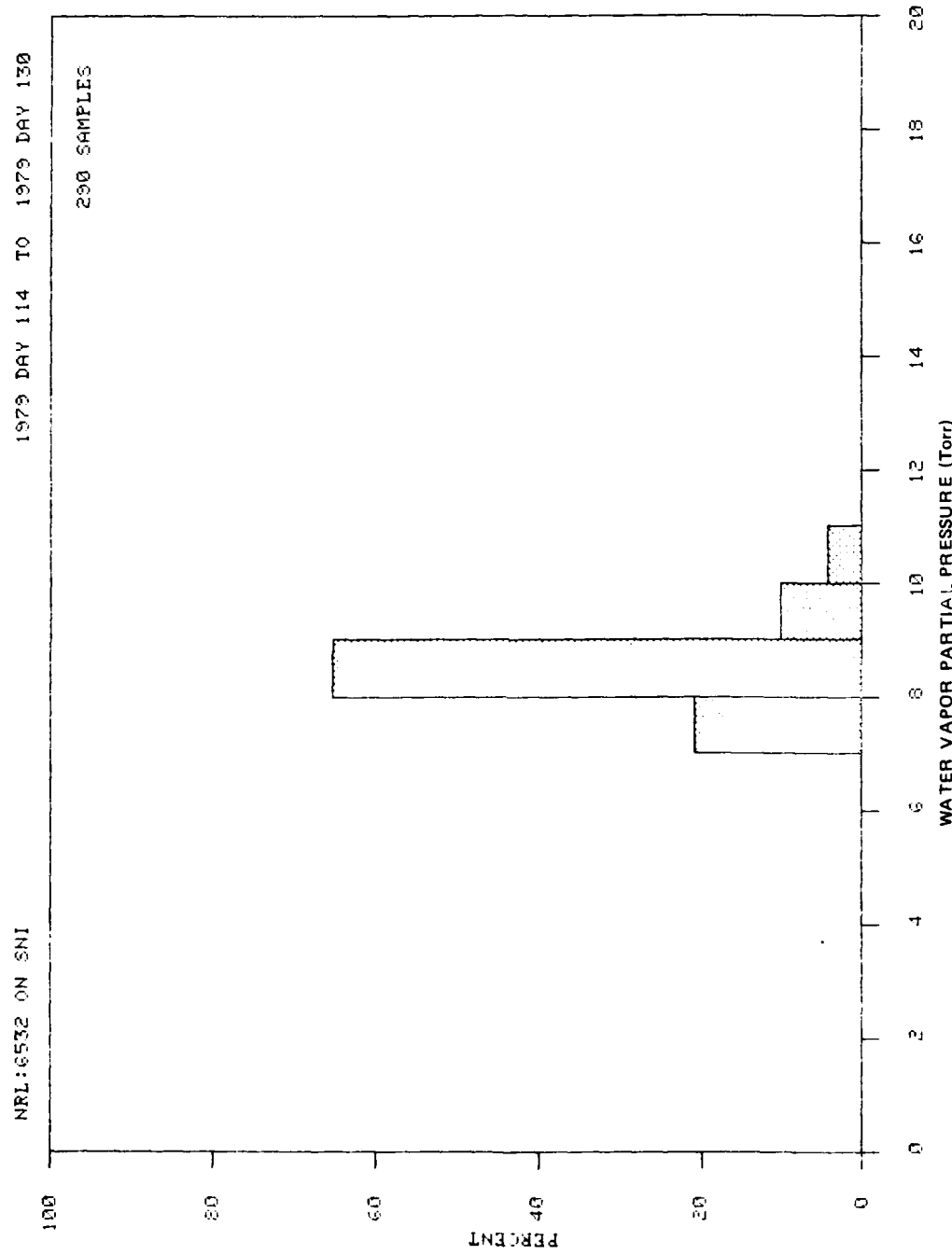


Fig. 28 - Frequency-of-occurrence plot of water vapor partial pressure

NRL REPORT 8618

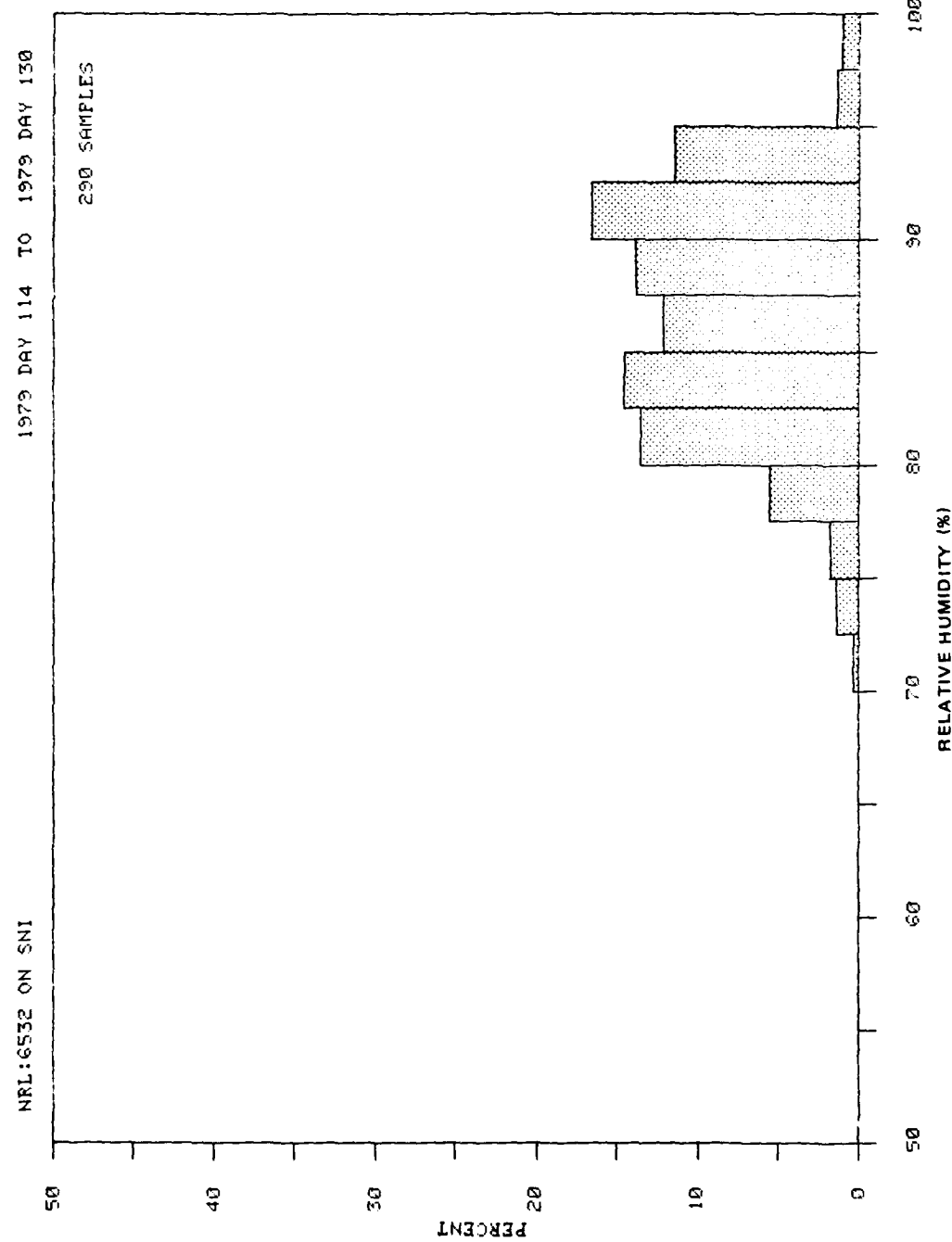


Fig. 29 — Frequency-of-occurrence plot of relative humidity

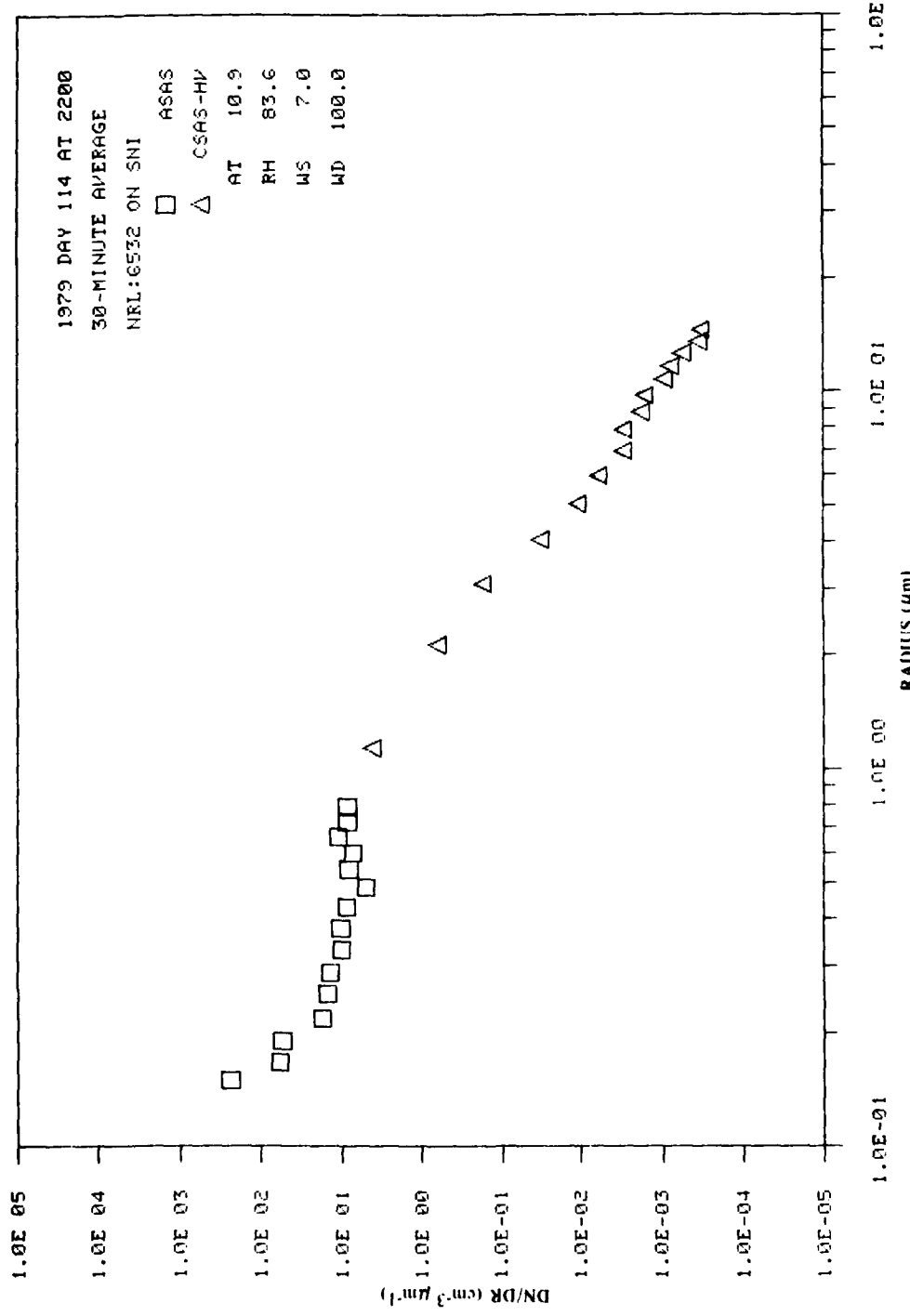


Fig. 30(a) — Measured aerosol-particle size distributions

NRL REPORT 8618

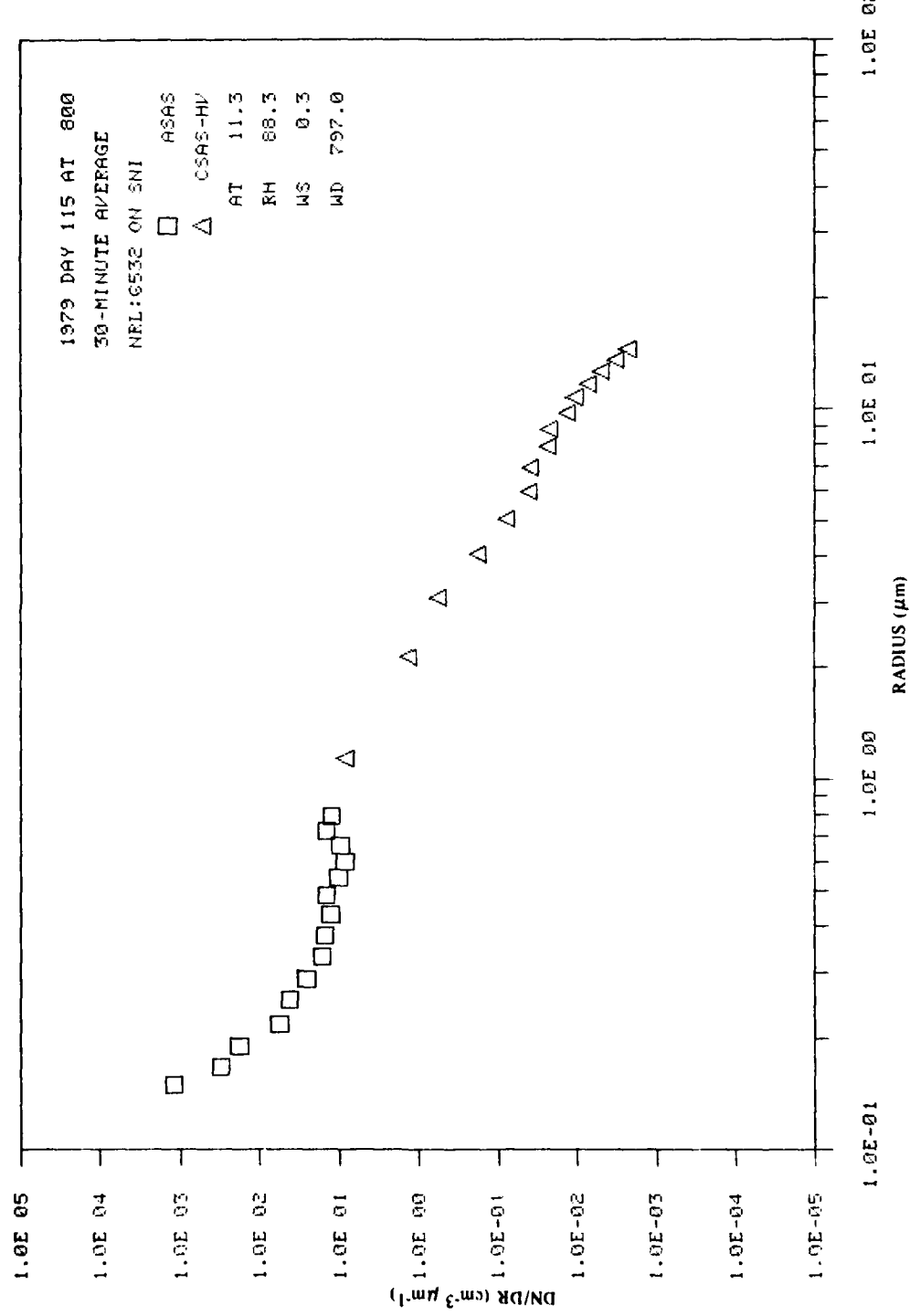


Fig. 30(b) — Measured aerosol-particle size distributions

J. A. DOWLING ET AL.

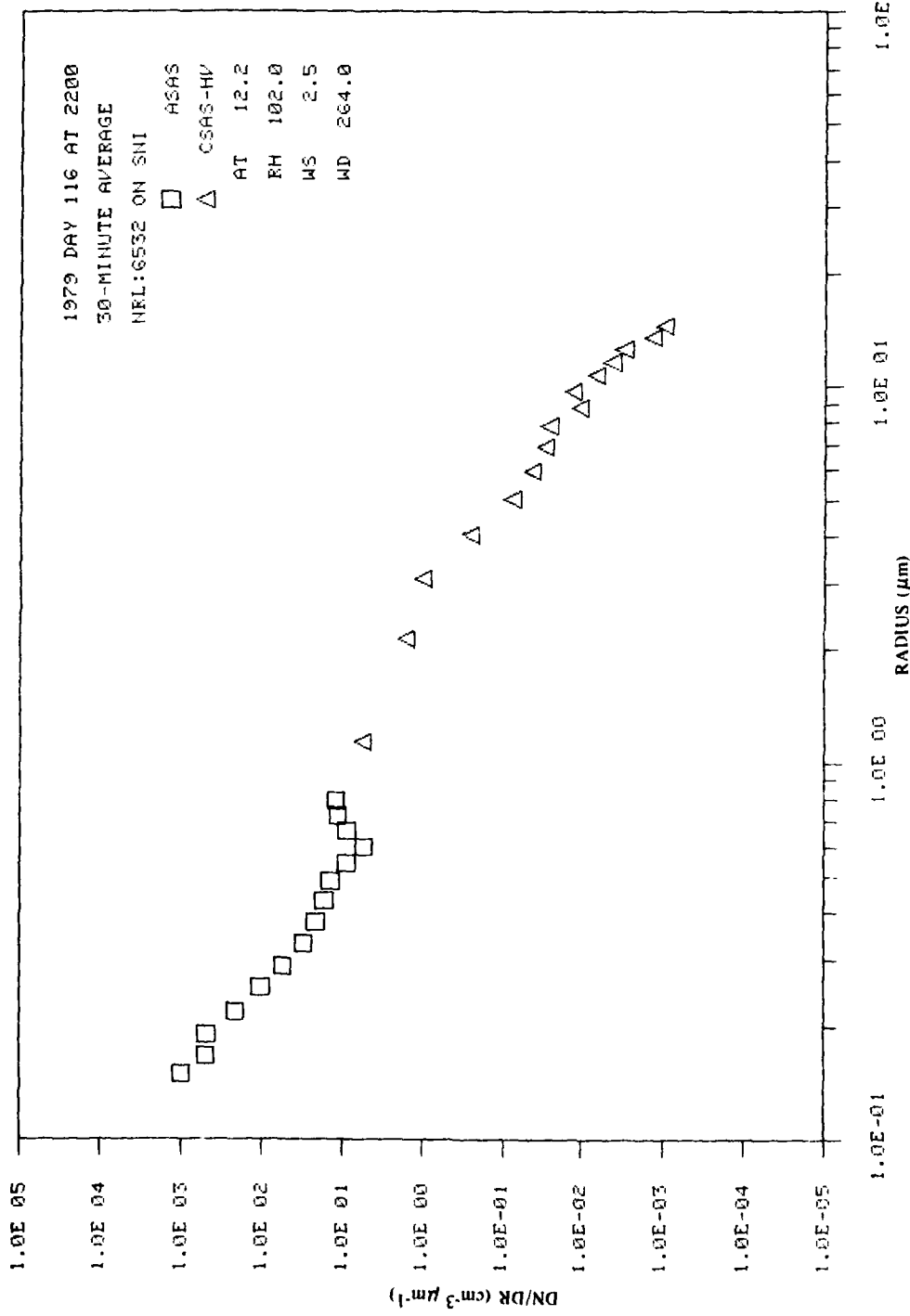


Fig. 30(c) — Measured aerosol-particle size distributions

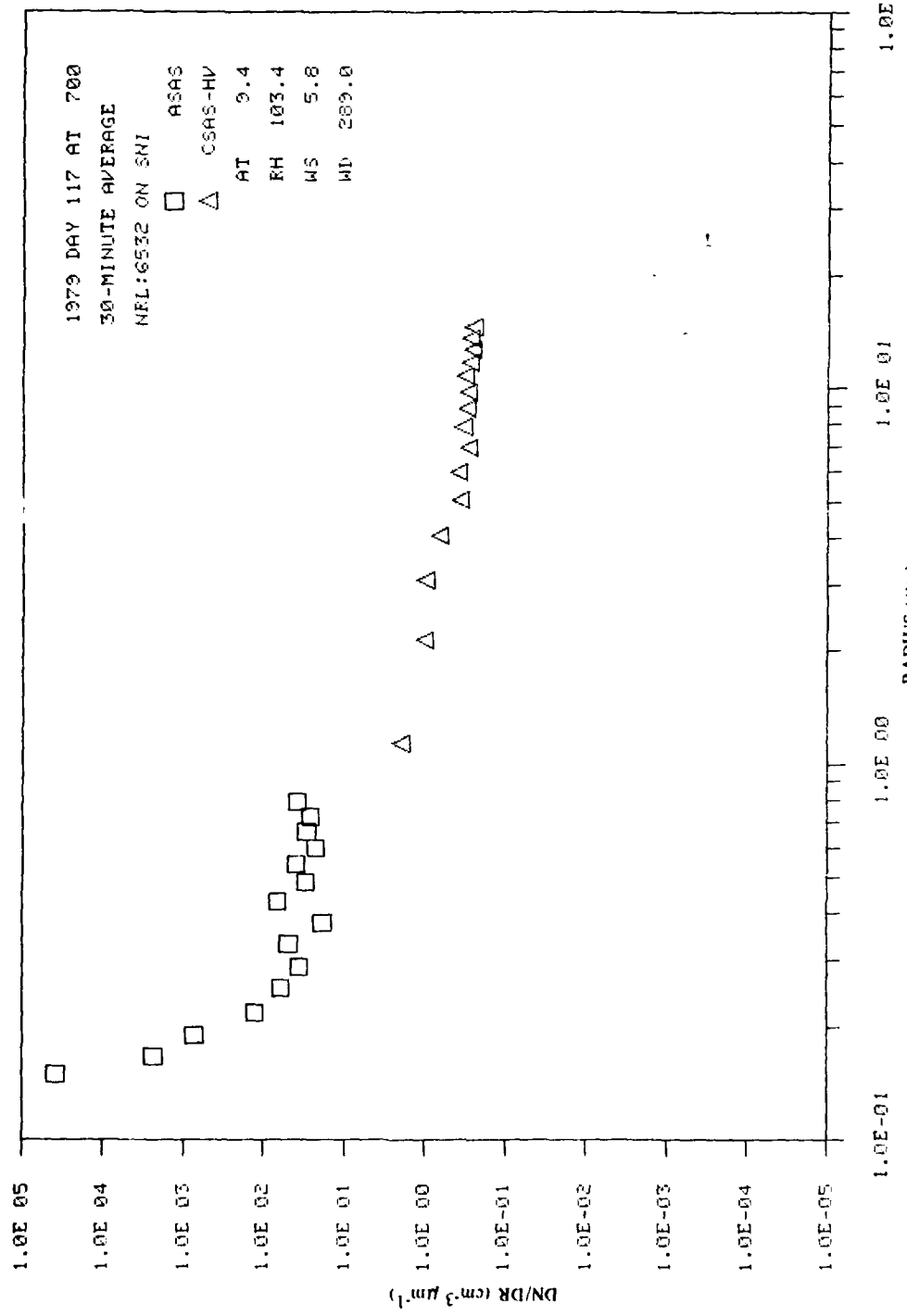


Fig. 30(d) — Measured aerosol-particle size distributions

J. A. DOWLING ET AL.

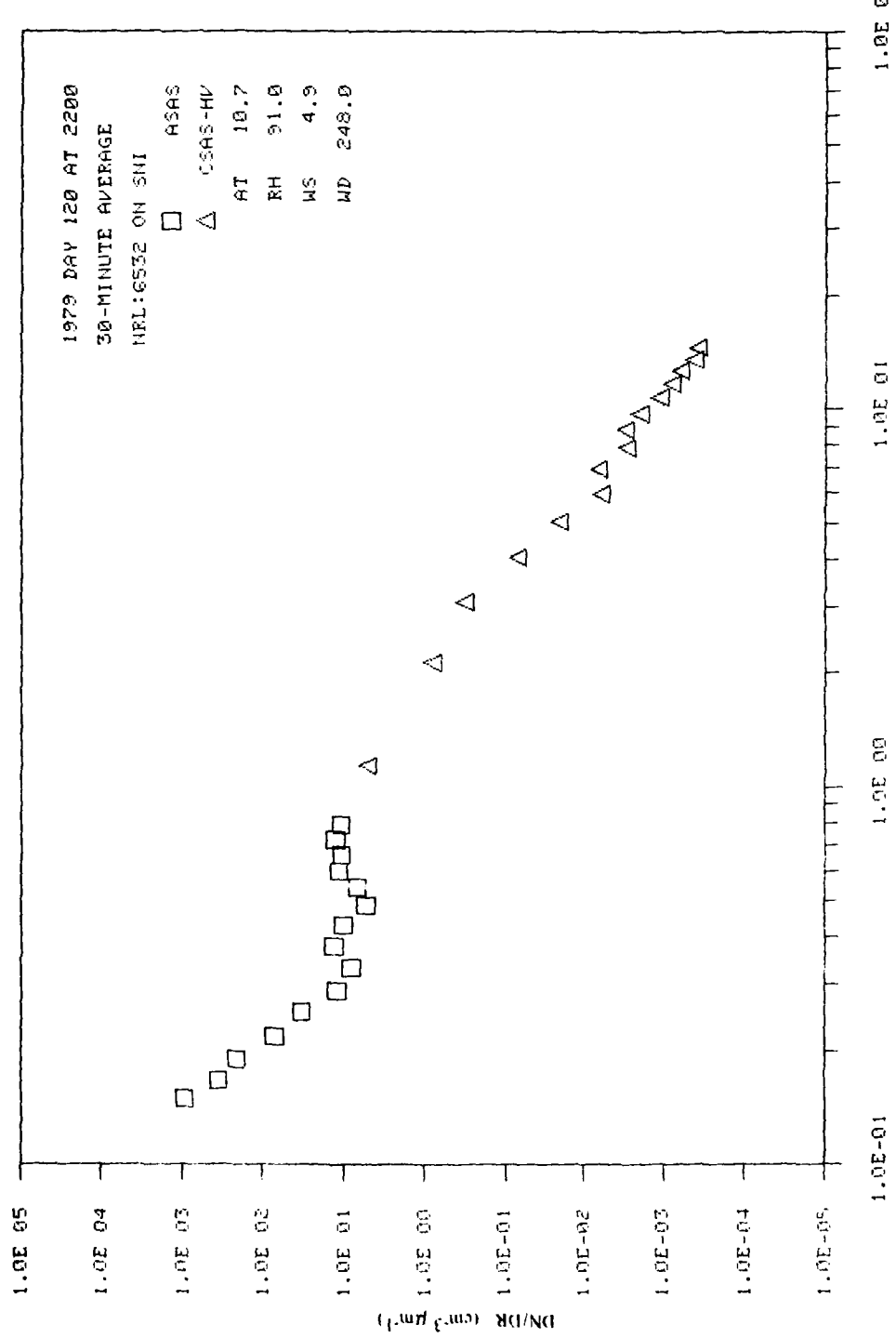


Fig. 30(3) - Measured aerosol-particle size distributions

NRL REPORT 8618

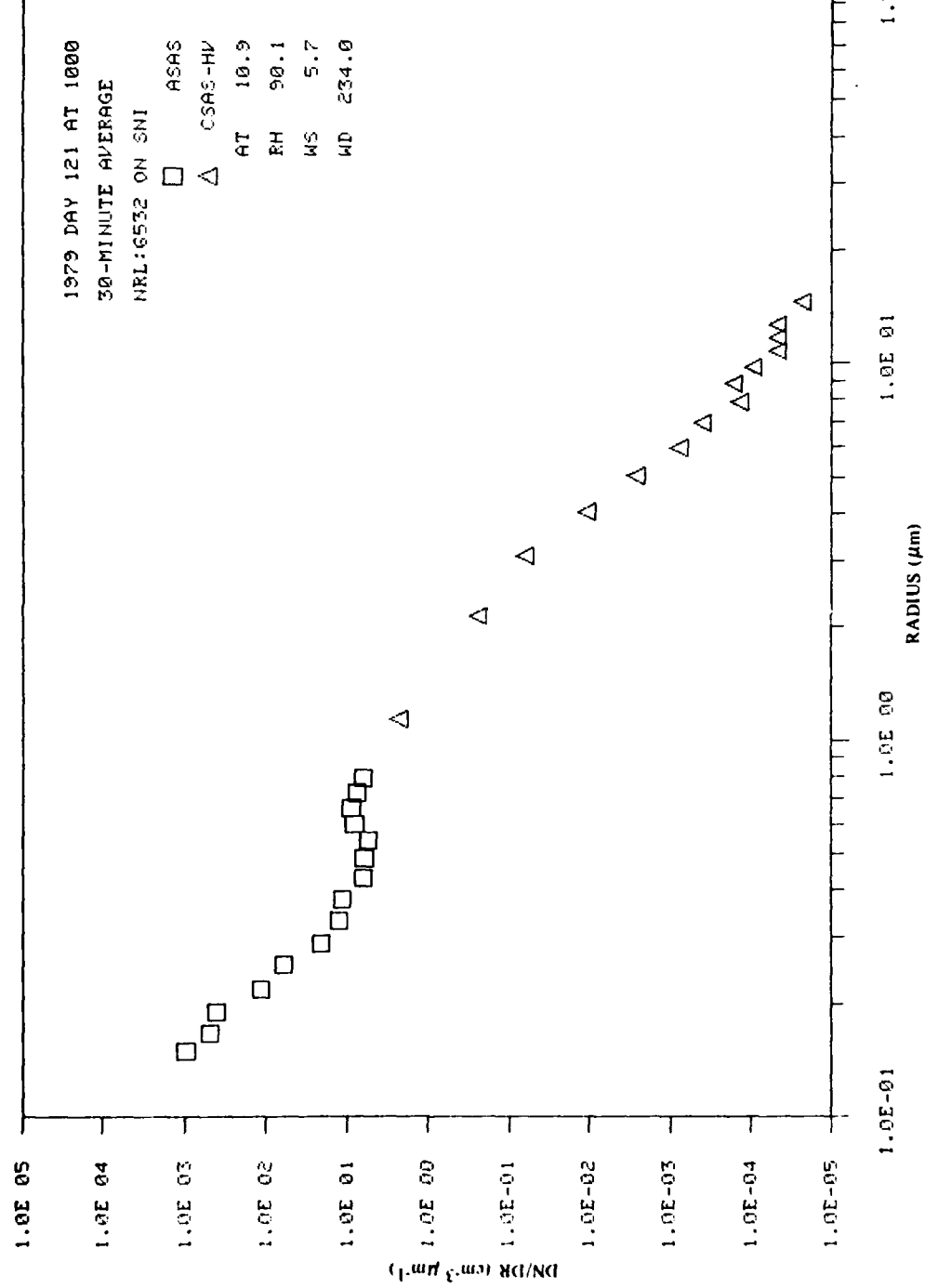


Fig. 30(f) — Measured aerosol:particle size distributions

J. A. DOWLING ET AL.

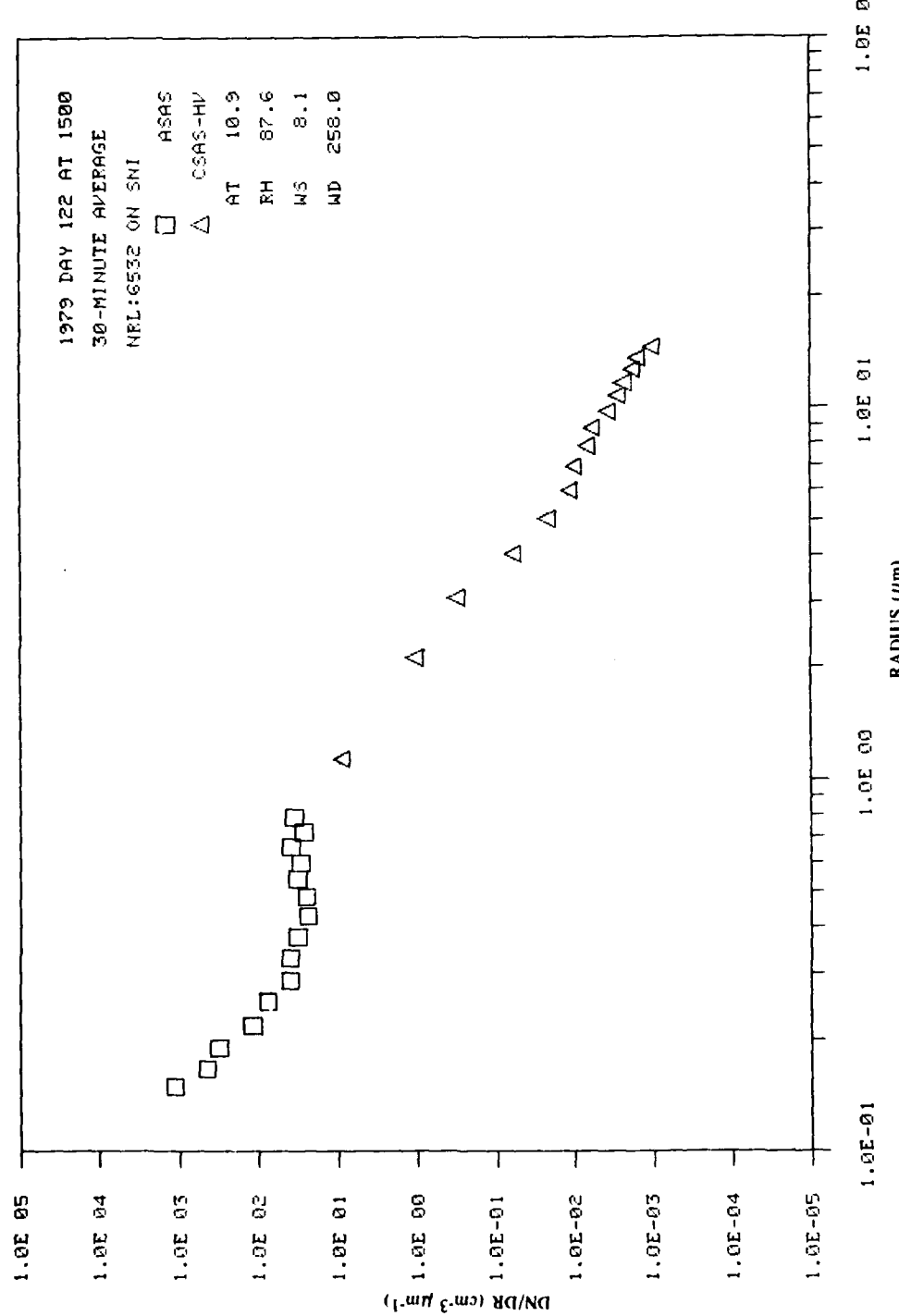


Fig. 30(g) – Measured aerosol-particle size distributions

NRL REPORT 8618

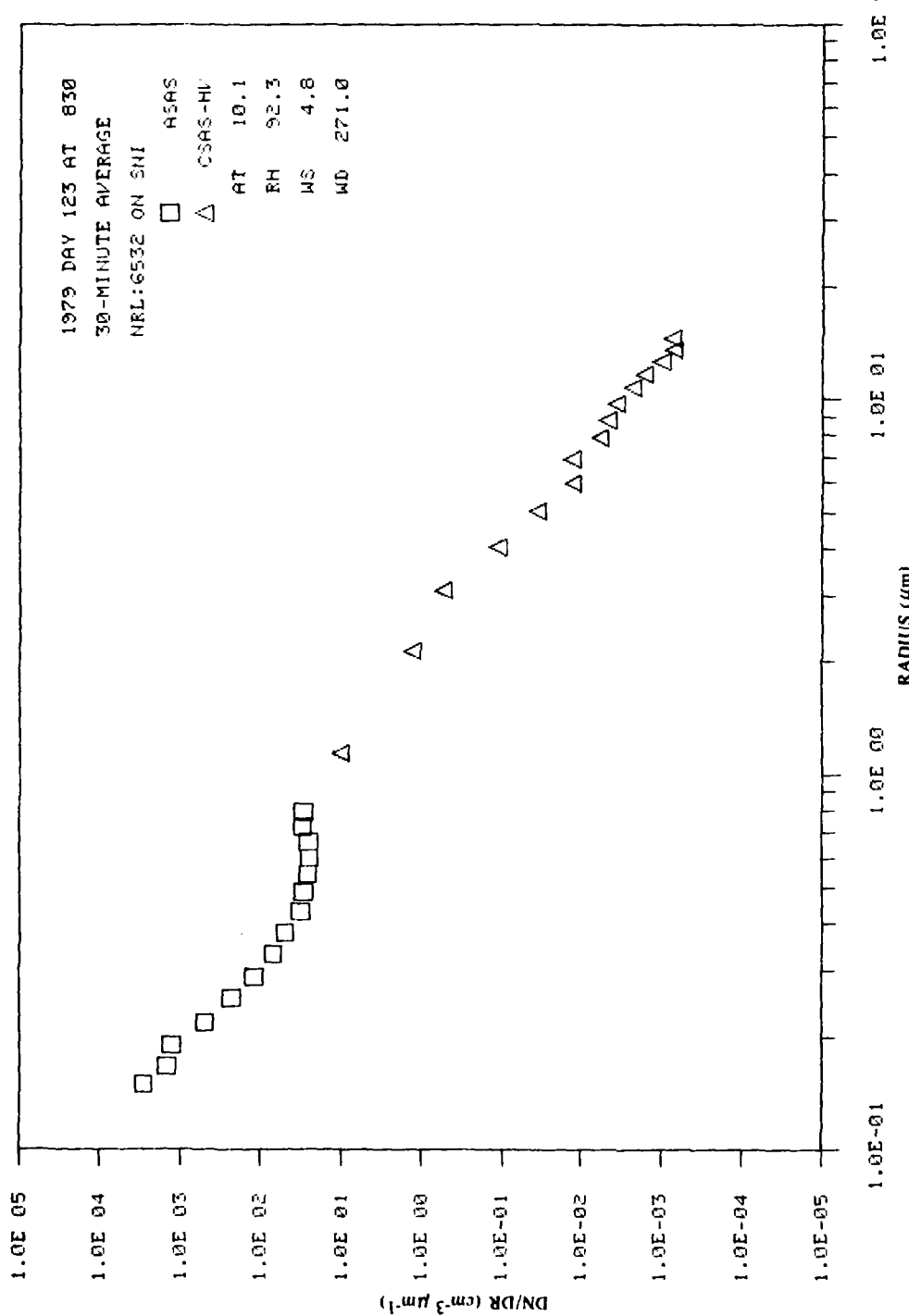


Fig. 30(h) – Measured aerosol-particle size distributions

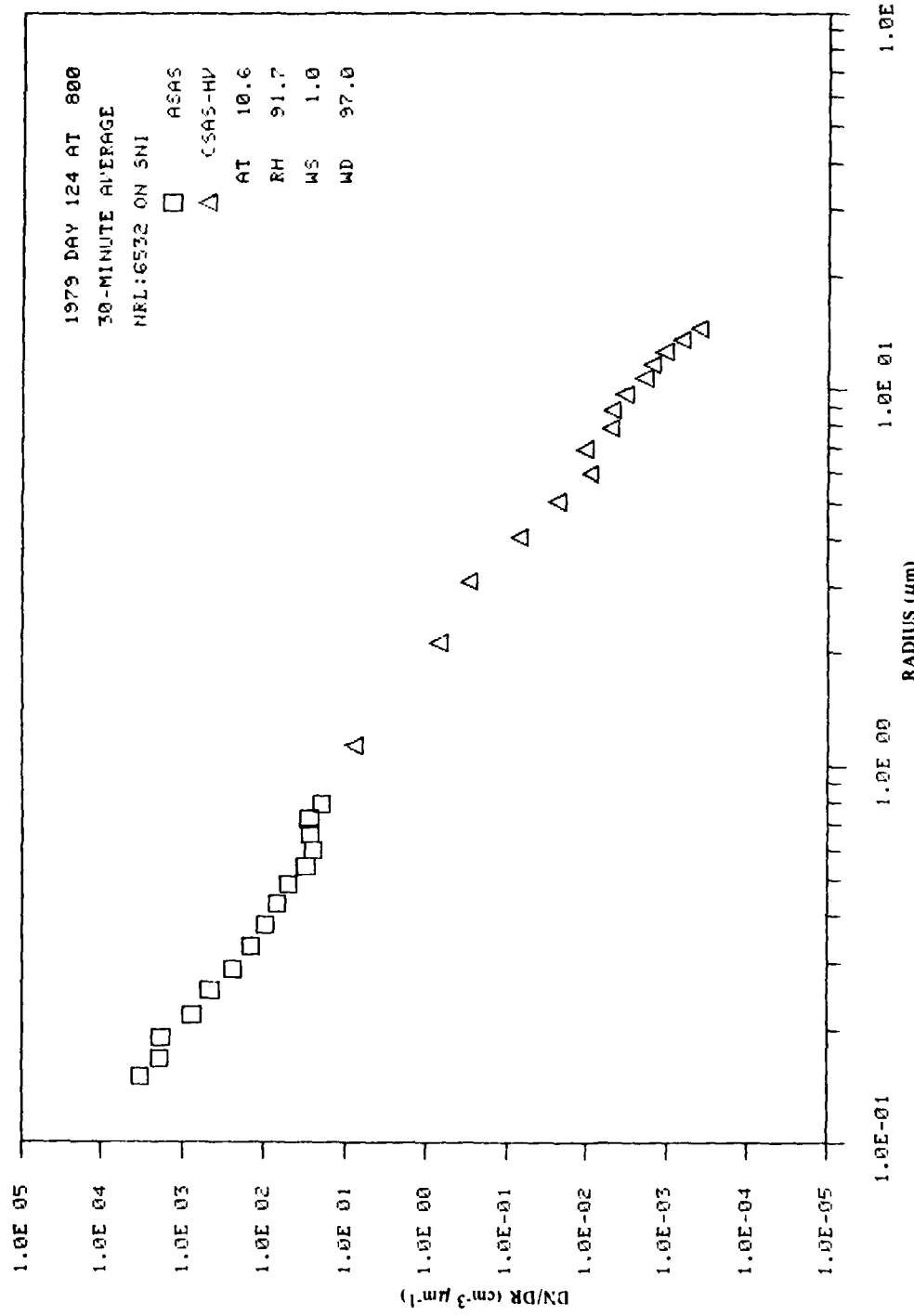


Fig. 30(i) — Measured aerosol-particle size distributions

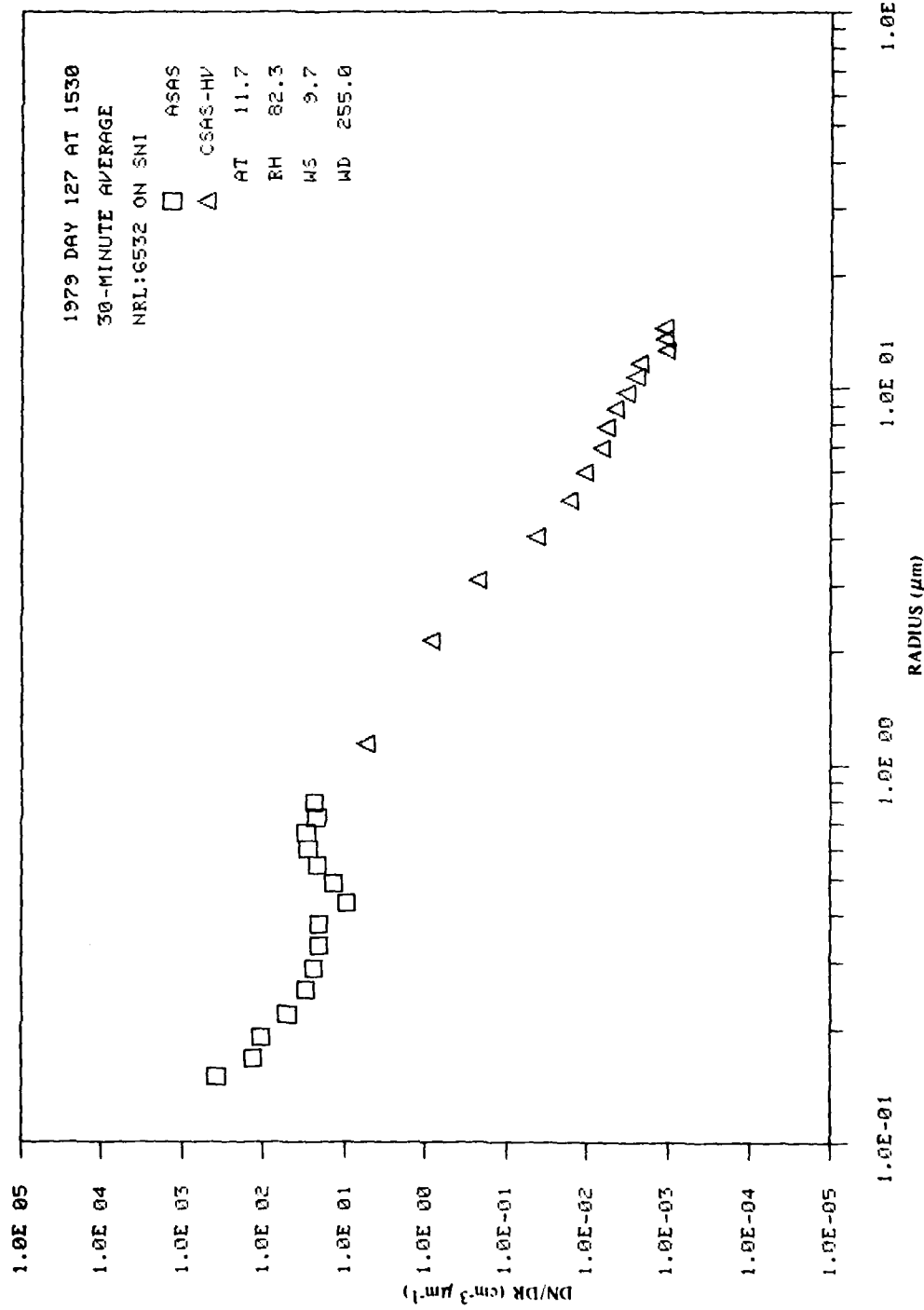


Fig. 30(j) — Measured aerosol-particle size distributions

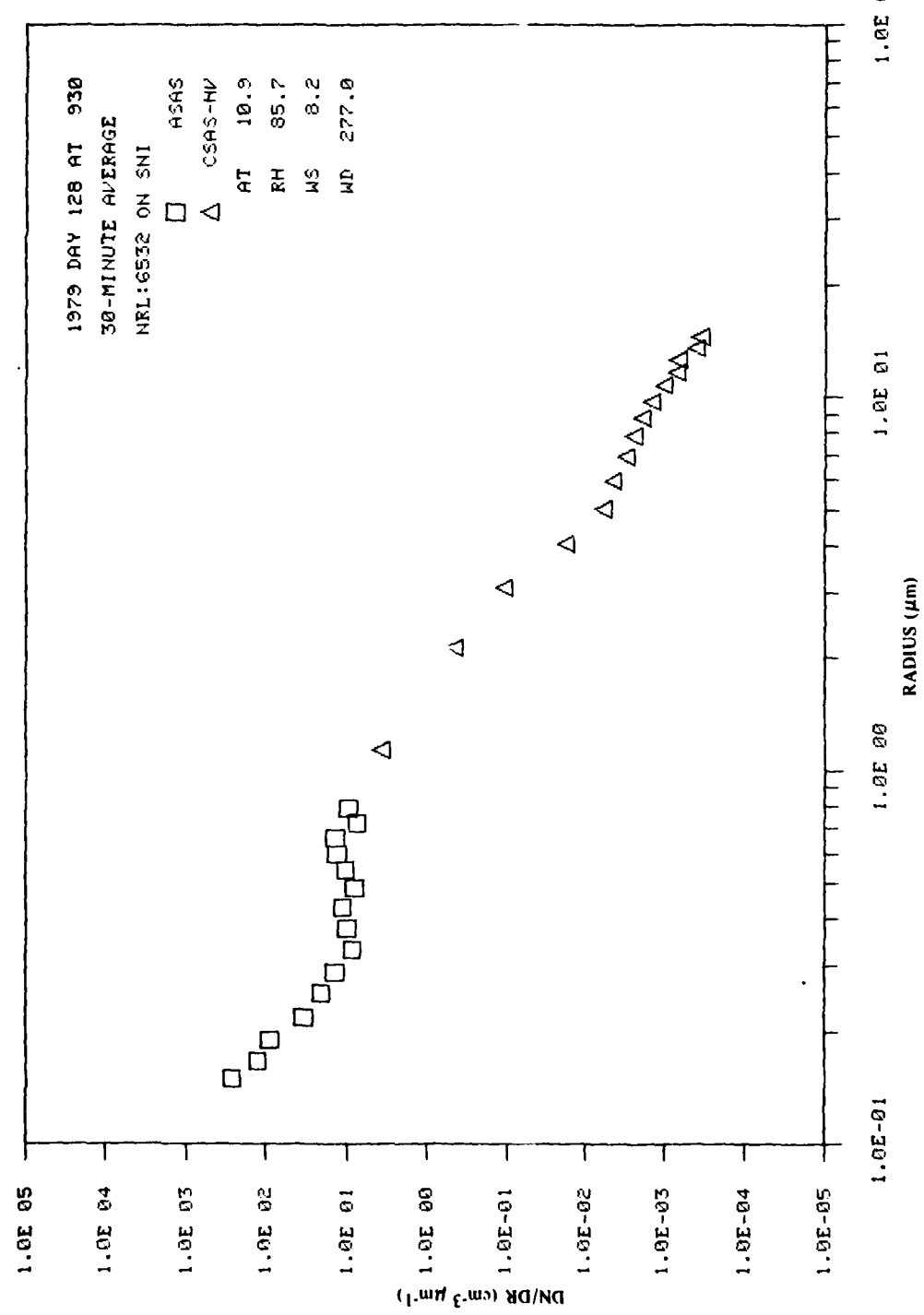
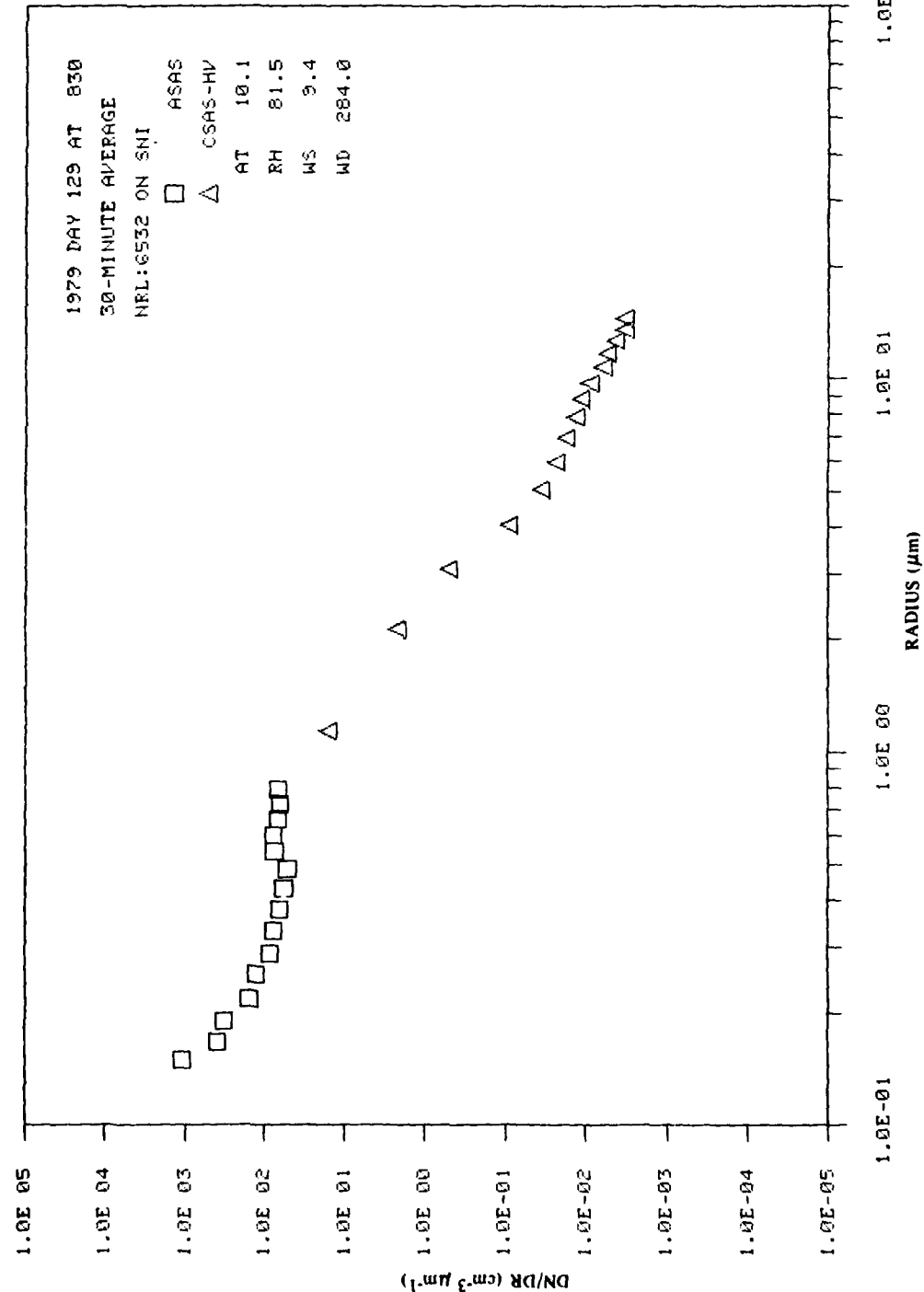


Fig. 30(k) — Measured aerosol-particle size distributions

NRL REPORT 8618



**Fig. 30(1) – Measured aerosol-particle size distributions**

Table 8 — Thirty-Minute Averages of Measured and Calculated Aerosol Parameters  
(PROCESSED ON 08-MAR-82)

PROGRAM A4ENRL : NRL:6532 ON SNI YEAR DAY TIME	AEROSOL/MET DATA TABULATION						EXTINCTION (1/KM)					
	AT	RH	WS (M/S)	WD (DEG)	WMP (TOFP)	NUM (1-CC)	AREA (MM <sup>2</sup> /CC)	VOL (MM <sup>3</sup> /CC)	0.55	1.06	3.80	10.6
79 114 2200 10.9 83.6 83.4 10.9 100 8.2 16.0 43.2 142.1 0.106 0.121 0.0760 0.0176												
100 82.4 11.0 81.5 11.0 102 8.1 16.0 40.5 129.4 0.100 0.113 0.0703 0.0158												
102 81.0 11.0 79.8 11.0 95.0 8.0 15.0 40.3 130.0 0.099 0.113 0.0699 0.0159												
107 79.8 11.0 79.4 11.0 107 7.6 15.0 39.3 134.1 0.096 0.110 0.0686 0.0169												
79 115 0 11.0 78.7 78.4 11.1 107 7.7 14.0 36.7 124.0 0.090 0.103 0.0642 0.0156												
100 79.8 11.0 79.1 11.0 29.1 7.8 15.0 38.1 133.7 0.093 0.106 0.0668 0.0171												
130 79.6 10.9 81.6 10.9 75.0 8.0 14.0 38.0 122.6 0.093 0.107 0.0669 0.0150												
200 19.3 10.9 84.1 19.3 79.4 8.2 17.0 45.2 158.0 0.113 0.128 0.0829 0.0199												
230 19.3 10.9 83.4 19.3 79.1 7.8 19.0 47.8 161.0 0.118 0.131 0.0846 0.0202												
300 19.3 10.9 82.4 19.3 80.1 8.0 19.0 47.4 167.6 0.116 0.131 0.0848 0.0215												
330 10.8 10.8 82.4 10.8 79.4 8.0 18.0 45.9 163.5 0.111 0.127 0.0837 0.0210												
400 10.8 10.8 83.0 10.8 80.0 8.1 20.0 51.3 184.3 0.125 0.141 0.0945 0.0238												
430 10.7 10.7 85.5 10.7 80.4 8.3 22.0 52.8 184.9 0.128 0.146 0.0981 0.0236												
500 10.6 10.6 88.6 10.6 71.6 8.5 25.0 58.3 212.8 0.140 0.160 0.1113 0.0275												
530 10.6 10.7 89.5 10.7 70.0 8.6 25.0 69.2 214.2 0.145 0.166 0.1157 0.0273												
600 10.7 10.7 89.0 10.7 26.2 8.6 24.0 63.6 245.7 0.153 0.175 0.1237 0.0327												
630 10.8 10.8 88.6 10.8 148 8.6 23.0 56.2 262.1 0.140 0.162 0.1100 0.0256												
700 10.9 10.9 89.3 10.9 153 8.7 25.0 69.1 268.3 0.166 0.189 0.1326 0.0358												
730 11.3 11.3 88.3 11.3 71.3 8.9 65.0 176.7 290.5 0.411 0.449 0.3689 0.1506												
800 11.3 11.3 88.3 11.3 79.7 8.9 50.0 132.2 718.3 0.308 0.340 0.2752 0.1082												
79 116 2200 12.2 102.0 104.9 11.7 264 10.9 67.0 137.1 667.8 0.321 0.330 0.3188 0.0970												
2230 12.0 104.0 104.0 274 10.9 126.5 40.6 943 262.3 8.749 8.851 10.4825 0.0956												
2300 11.9 104.0 104.0 276 10.9 1506.0 4151.0 46968.4 8.613 8.916 10.1564 7.6846												
2330 11.7 104.0 104.0 281 10.7 1307.0 4922.0 464959.5 10.284 10.448 11.6174 10.7497												
79 117 0 11.8 104.7 2.7 276 10.9 512.0 235.3 0.27282.1 4.998 5.101 5.7905 4.4952												
20 11.7 104.9 2.7 280 10.7 520.0 275.0 0.35403.2 5.766 5.891 5.5414 5.9274												
100 11.4 103.3 2.7 290 10.4 501.0 4243.0 449256.2 8.942 9.153 10.5017 8.1569												
130 11.6 103.3 2.7 281 10.6 1120.0 5574.0 955659.8 11.912 12.188 14.2771 9.3239												
200 11.6 104.0 2.7 283 10.6 1538.0 1722.0 814810.8 3.781 3.889 4.3594 2.3908												
270 11.5 104.0 2.7 285 10.7 585.0 2704.0 814559.7 5.869 5.908 7.1070 4.0101												
300 11.3 103.3 2.7 286 10.7 103.0 211.0 1452.0 0.491 0.493 0.5133 0.2215												
370 11.0 103.3 2.7 288 10.7 103.0 47.0 121.9 0.121 0.123 0.0466 0.0151												
400 10.9 103.3 2.7 289 10.7 103.0 48.0 58.3 69.2 0.129 0.129 0.1270 0.1146												
430 10.2 103.4 2.7 290 10.7 238.0 311.3 4099.2 0.629 0.639 0.6889 0.6844												
500 9.9 103.6 2.7 295 10.7 285.0 502.9 6711.0 1.017 1.030 1.1219 1.1215												
530 9.6 103.7 2.7 296 10.7 285.0 680.7 4075.0 1.377 1.394 1.5231 1.5166												
560 9.5 104.0 2.7 296 10.7 285.0 651.0 111454.9 1.738 1.756 1.9185 1.9120												
630 9.4 103.8 2.7 297 10.7 285.0 745.0 1042.0 913759.0 2.119 2.132 2.3383 2.299												
700 9.4 103.4 2.7 299 10.7 285.0 658.0 1113.0 914938.0 2.269 2.299 2.5197 2.4916												

NRL REPORT 8618

**Table 8 — Thirty-Minute Averages of Measured and Calculated Aerosol Parameters (Continued)**  
 PROGRAM: A43HPL: AEROSOL/MET DATA TABULATION  
 PROCESSED ON 08-NHR-82

Table 8 - Thirty-Minute Averages of Measured and Calculated Aerosol Parameters (Continued)

PROGRAM A48NRL: AEROSOL-MET DATA TABULATION NRL:6532 ON SNI YEAR DAY TIME										(PROCESSED ON 08-MAR-82)					
	AT	RH	VS (M/S)	WD (DEG)	WMP (TORR)	NUM (1/CC)	AERA (1/CC)	VOL (13/CC)	0.55	EXTINCTION (1/KM)	3.80	10.6			
79 121 1400	10.7	89.5	9.1	257	8.6	133.	65.1	234.2	0.146	0.147	0.0966	0.0325			
1430	85.3	8.4	252	8.2	35.	37.6	138.6	0.090	0.098	0.0600	0.0187				
1500	11.0	82.7	8.2	257	8.1	38.	47.1	168.4	0.113	0.124	0.0765	0.0224			
1530	11.1	81.7	8.2	260	8.1	35.	48.5	191.8	0.115	0.128	0.0807	0.0253			
1600	11.2	81.0	8.1	260	8.1	32.	48.8	205.3	0.117	0.129	0.0820	0.0286			
1630	11.3	79.5	8.2	257	8.0	31.	53.2	214.2	0.129	0.142	0.0885	0.0294			
1700	11.4	78.8	9.1	259	7.9	32.	56.4	224.7	0.137	0.150	0.0940	0.0308			
1730	11.4	79.8	9.2	260	8.1	34.	64.9	261.7	0.159	0.173	0.1096	0.0359			
1800	11.4	80.9	9.1	262	8.2	37.	75.9	310.2	0.182	0.201	0.1287	0.0430			
1830	11.3	82.3	9.1	261	8.3	39.	82.7	343.0	0.202	0.221	0.1426	0.0474			
1900	11.3	82.5	10.1	260	8.3	41.	89.2	352.6	0.214	0.237	0.1531	0.0498			
1930	11.1	82.5	9.7	256	8.2	37.	89.8	314.9	0.198	0.219	0.1377	0.0425			
2000	11.0	83.3	10.3	256	8.2	42.	85.8	329.8	0.213	0.235	0.1463	0.0441			
2030	11.1	83.5	10.1	260	8.2	44.	97.5	387.3	0.239	0.262	0.1670	0.0528			
2100	11.1	83.0	10.4	265	8.2	44.	103.4	450.5	0.251	0.277	0.1812	0.0631			
2130	11.0	82.9	10.2	263	8.1	48.	100.4	418.2	0.244	0.269	0.1722	0.0579			
2200	11.0	82.2	9.5	262	8.1	43.	92.7	364.7	0.227	0.250	0.1549	0.0496			
2230	10.8	82.1	10.2	261	8.0	52.	104.9	398.8	0.258	0.283	0.1735	0.0536			
2300	10.9	80.7	9.0	264	7.9	44.	100.5	424.9	0.244	0.271	0.1726	0.0589			
79 122 0	10.8	77.9	9.4	265	7.6	41.	80.4	335.3	0.197	0.197	0.1219	0.0443			
100	10.7	79.9	10.3	259	7.5	46.	102.2	347.3	0.206	0.223	0.1307	0.0467			
120	10.7	81.2	11.7	259	7.8	70.	62.3	424.2	0.249	0.265	0.1347	0.0485			
200	10.6	83.9	10.0	264	8.0	64.	121.3	492.1	0.294	0.322	0.2057	0.0734			
230	10.6	84.1	10.2	259	8.1	75.	122.9	524.8	0.298	0.326	0.2027	0.0677			
300	10.5	83.8	11.0	263	8.0	89.	127.1	533.7	0.307	0.335	0.2104	0.0726			
330	10.4	85.6	10.5	266	8.1	87.	150.8	633.7	0.366	0.398	0.2541	0.0882			
400	10.3	85.8	11.1	267	8.1	94.	157.4	661.7	0.382	0.412	0.2623	0.0924			
430	10.3	83.9	11.9	270	7.9	87.	132.0	547.9	0.320	0.344	0.2148	0.0764			
500	10.3	84.4	11.1	269	7.9	85.	134.9	552.9	0.329	0.354	0.2185	0.0766			
530	10.3	84.7	10.8	269	7.9	82.	128.3	509.3	0.311	0.341	0.2097	0.0682			
600	10.2	86.2	9.8	269	8.0	83.	134.9	525.8	0.327	0.359	0.2240	0.0715			
630	10.2	87.2	9.0	273	8.0	84.	140.9	557.6	0.341	0.379	0.2393	0.0738			
700	10.3	86.5	9.8	267	8.1	84.	149.3	592.0	0.362	0.399	0.2556	0.0807			
730	10.3	87.1	9.6	271	8.1	85.	158.8	643.9	0.384	0.424	0.2724	0.0882			
800	10.3	87.3	9.9	273	8.1	82.	161.2	691.1	0.367	0.403	0.2569	0.0820			
830	10.4	86.4	9.6	266	8.0	83.	137.0	514.2	0.337	0.367	0.2469	0.0689			
930	10.4	86.4	9.8	273	8.0	84.	140.9	557.6	0.341	0.379	0.2393	0.0738			
1000	10.3	86.5	9.8	267	8.1	84.	149.3	592.0	0.362	0.399	0.2556	0.0807			
1030	10.5	86.2	9.2	271	8.1	85.	158.8	643.9	0.384	0.424	0.2724	0.0882			
1100	10.6	86.3	9.2	273	8.1	82.	161.2	691.1	0.367	0.403	0.2569	0.0820			
1130	10.7	87.0	9.3	273	8.1	85.	149.6	592.0	0.341	0.379	0.2393	0.0738			

**Table 8 — Thirty-Minute Averages of Measured and Calculated Aerosol Parameters (Continued)**  
 (PROCESSED ON 08-MAR-82)

PROGRAM: A48NPL:	ON SNI	AEROSOL/MET DATA TABULATION	YEAR DAY TIME	RH	WS (M/S)	WD	WMP (M/S)	NUM (1/CC)	AREA (UM3/CC)	VOL (UM3/CC)	0.55	EXTINCTION (1/KM)	1.06	3.80	10.6
NRL:6532	1200		10.6	87.5	8.1	266	8.4	65.	112.9	441.3	0.273	0.306	0.1877	0.0599	
	1230		10.7	87.3	8.2	263	8.5	66.	113.7	432.1	0.267	0.297	0.1786	0.0563	
	1300		10.8	88.3	8.4	264	8.6	74.	115.1	410.8	0.276	0.309	0.1896	0.0581	
	1330		10.8	88.0	8.4	262	8.6	73.	116.4	498.7	0.289	0.312	0.1853	0.0542	
	1400		10.8	87.7	8.1	259	8.6	67.	103.5	373.6	0.284	0.317	0.1897	0.0534	
	1430		10.9	87.7	8.1	258	8.6	64.	95.3	321.3	0.250	0.282	0.1678	0.0493	
	1500		10.9	87.6	8.1	261	8.6	55.	86.8	304.7	0.232	0.260	0.1509	0.0414	
	1530		10.9	87.6	8.0	259	8.5	64.	85.8	304.7	0.211	0.235	0.1361	0.0400	
	1600		10.8	87.6	7.9	258	8.5	74.	86.9	293.1	0.209	0.234	0.1357	0.0380	
	1630		10.8	88.4	8.1	259	8.6	98.	107.3	350.2	0.258	0.284	0.1668	0.0450	
	1700		10.9	87.5	6.7	259	8.6	94.	104.0	339.9	0.249	0.279	0.1639	0.0434	
	1730		10.9	87.2	7.0	265	8.6	55.	92.	114.3	0.277	0.308	0.1835	0.0476	
	1800		10.8	87.2	7.1	259	8.5	89.	116.7	380.4	0.282	0.316	0.1891	0.0482	
	1830		10.8	87.1	7.5	259	8.5	118.	129.6	419.4	0.311	0.343	0.2061	0.0534	
	1900		10.6	90.0	6.4	268	8.6	149.	144.5	487.4	0.342	0.376	0.2339	0.0632	
	1930		10.5	90.2	7.2	269	8.5	116.	163.0	630.0	0.391	0.424	0.2816	0.0852	
	2000		10.4	90.1	7.2	268	8.5	113.	159.3	593.5	0.383	0.424	0.2735	0.0790	
	2030		10.3	90.4	7.9	269	8.5	167.	166.0	593.5	0.392	0.428	0.2742	0.0787	
	2100		10.2	90.6	7.4	264	8.4	116.	156.4	553.0	0.376	0.418	0.2650	0.0722	
	2130		10.2	90.9	7.2	266	8.5	116.	168.8	650.1	0.405	0.448	0.2932	0.0875	
	2200		10.2	90.2	7.3	275	8.4	120.	159.5	575.0	0.383	0.425	0.2680	0.0759	
	2230		10.1	91.2	6.4	272	8.4	104.	167.5	635.7	0.401	0.449	0.2933	0.0848	
	2300		10.0	91.5	6.6	272	8.4	107.	168.4	604.0	0.407	0.453	0.2925	0.0790	
	2330		10.0	91.8	6.8	264	8.4	173.	173.	648.6	0.450	0.490	0.3179	0.0842	
79	123	0	10.1	92.2	6.2	269.	8.6	138.	221.1	734.0	0.520	0.546	0.3535	0.0959	
	100	30	10.0	92.3	6.1	265	8.6	169.	203.5	727.6	0.467	0.507	0.3799	0.1029	
	130	10.1	93.3	6.3	267	8.6	121.	194.2	705.5	0.456	0.484	0.531	0.0953		
	200	9.8	92.8	6.3	269	8.5	118.	188.0	660.2	0.456	0.493	0.3580	0.0923		
	230	9.8	93.0	6.0	269	8.4	140.	178.9	603.6	0.428	0.474	0.3359	0.0853		
	300	9.9	93.0	6.0	276	8.5	220.	196.9	648.2	0.463	0.499	0.3311	0.0768		
	330	9.9	92.4	6.1	276	8.5	245.	193.7	627.8	0.451	0.483	0.3199	0.0805		
	400	9.9	92.9	5.8	276	8.5	170.	187.1	633.3	0.445	0.485	0.3257	0.0813		
	430	9.8	93.6	5.1	283	8.5	124.	185.2	656.6	0.443	0.491	0.3425	0.0867		
	500	10.1	93.9	4.5	275	8.7	127.	190.0	677.0	0.455	0.503	0.3534	0.0878		
	530	10.1	94.0	4.1	279	8.8	136.	186.5	641.9	0.446	0.494	0.3424	0.0821		
	600	10.1	93.8	4.4	269	8.8	146.	165.6	538.2	0.395	0.434	0.2885	0.0678		
	650	10.1	93.5	3.3	270	8.8	165.	153.3	469.0	0.362	0.395	0.2556	0.0583		
	700	10.1	92.8	4.7	269	8.7	176.	150.4	475.8	0.353	0.381	0.2458	0.0605		
	730	10.2	93.3	5.1	267	8.7	167.	164.9	574.2	0.390	0.417	0.2824	0.0758		
	800	10.1	93.0	4.9	270	8.6	167.	154.7	501.3	0.366	0.390	0.2586	0.0645		
	830	10.1	92.3	4.8	271	8.6	164.	129.7	375.3	0.325	0.306	0.2018	0.0462		

**Table 8 — Thirty-Minute Averages of Measured and Calculated Aerosol Parameters (Continued)**

PROGRAM A48NRL: AEROSOL/MET DATA TABULATION NRL:6532 ON SNI YEAR DAY TIME										(PROCESSED ON 08-HAR-82)					
NRL	SNI	AT	RH	WS	WD	WMP	NUM	AREA	VOL	(WM3/CC)	0.55	EXTINCTION	(1/KM)	10.6	
79	123	900	10.1	92.2	4.2	266	8.5	153.	110.4	300.8	0.260	0.276	0.1633	0.0362	
939	10.1	92.3	4.0	265	8.6	155.	107.5	313.4	0.252	0.266	0.1573	0.0393			
1000	10.2	90.9	3.6	263	8.5	141.	103.9	313.8	0.244	0.259	0.1551	0.0399			
1039	10.2	90.5	3.9	261	8.4	126.	87.4	252.9	0.205	0.219	0.1245	0.0318			
1160	10.3	90.5	3.1	268	8.5	137.	65.9	248.8	0.201	0.210	0.1142	0.0321			
1130	10.3	90.9	4.4	266	8.5	10.	71.2	282.0	0.171	0.208	0.1346	0.0379			
1200	10.3	92.8	5.2	269	8.7	228.	153.6	458.0	0.363	0.363	0.2197	0.0593			
1230	10.2	93.4	5.6	273	8.7	218.	180.4	660.9	0.424	0.433	0.2900	0.0921			
1300	10.1	93.7	5.4	271	8.7	218.	192.7	726.5	0.452	0.464	0.3260	0.1013			
1330	10.2	93.4	5.3	269	8.7	217.	187.2	595.8	0.446	0.457	0.3066	0.0779			
1400	10.2	93.6	5.3	270	8.7	274.	170.7	450.3	0.402	0.402	0.2435	0.0547			
1430	10.3	91.3	4.6	276	8.6	247.	120.5	292.0	0.276	0.274	0.1505	0.0349			
1500	10.4	89.8	4.5	274	8.5	155.	92.7	226.1	0.216	0.226	0.1244	0.0261			
1530	10.4	89.7	4.7	269	8.5	129.	103.6	304.7	0.244	0.252	0.1646	0.0376			
1600	10.5	86.5	5.3	271	8.2	105.	75.9	205.3	0.174	0.191	0.1114	0.0246			
1700	10.5	84.9	4.9	271	8.1	115.	67.6	179.2	0.156	0.166	0.0902	0.0217			
1730	10.6	82.7	4.2	269	7.9	121.	64.5	161.0	0.148	0.156	0.0805	0.0193			
1800	10.4	83.1	5.3	265	7.8	102.	60.9	141.9	0.143	0.150	0.0747	0.0162			
1830	10.5	82.6	5.5	265	7.9	66.	53.4	142.3	0.128	0.141	0.0734	0.0168			
1900	10.5	82.7	5.9	265	7.9	87.	62.5	143.5	0.151	0.162	0.0751	0.0160			
1930	10.4	84.2	6.1	262	8.0	58.	48.3	136.3	0.115	0.127	0.0661	0.0168			
2000	10.4	84.6	6.7	265	8.1	74.	53.8	148.9	0.127	0.137	0.0730	0.0183			
2030	10.5	85.4	6.5	267	8.1	87.	57.4	177.4	0.133	0.142	0.0831	0.0229			
2100	10.4	85.9	6.3	272	8.1	116.	54.2	155.9	0.120	0.124	0.0719	0.0162			
2130	10.4	86.3	6.1	271	8.1	74.	44.7	139.2	0.101	0.110	0.0652	0.0179			
2200	10.3	86.9	5.9	270	8.2	77.	50.8	172.4	0.114	0.123	0.0765	0.0231			
2230	10.2	87.4	6.4	269	8.1	46.	53.7	207.9	0.126	0.141	0.0921	0.0282			
2300	10.1	87.6	6.3	265	8.1	95.	60.1	192.3	0.138	0.145	0.0883	0.0252			
2330	10.1	87.9	6.3	270	8.1	98.	63.6	211.0	0.145	0.155	0.0974	0.0279			
79	124	0	9.9	89.1	8.1	95.	73.9	261.4	0.171	0.184	0.1208	0.0350			
100	9.8	89.3	6.1	266	8.1	129.	95.9	343.4	0.221	0.232	0.1545	0.0464			
130	9.8	89.1	5.8	269	8.0	201.	102.6	309.2	0.232	0.232	0.1416	0.0405			
200	9.9	89.6	5.7	262	8.1	196.	104.3	323.2	0.237	0.237	0.1456	0.0429			
230	9.9	89.9	5.7	263	8.3	195.	100.1	292.3	0.227	0.227	0.1384	0.0378			
300	9.9	91.2	5.7	262	8.3	161.	103.2	297.0	0.236	0.234	0.1429	0.0381			
330	9.9	91.2	5.7	260	8.3	163.	109.8	351.8	0.243	0.243	0.1550	0.0416			
400	9.9	91.9	4.8	259	8.4	149.	105.5	369.6	0.256	0.256	0.1680	0.0462			
430	9.9	92.6	4.7	262	8.5	134.	112.6	415.2	0.261	0.276	0.1762	0.0494			
500	9.9	92.9	4.8	269	8.6	139.	122.3	458.5	0.285	0.285	0.2152	0.0561			
530	9.9	92.8	4.8	269	8.6	127.	115.8	419.9	0.270	0.268	0.2052	0.0562			
600	9.9	92.9	3.7	287	8.6	148.	109.8	342.4	0.258	0.258	0.1718	0.0441			

## NRL REPORT 8-18

**Table 8 — Thirty-Minute Averages of Measured and Calculated Aerosol Parameters (Continued)**

PROGRAM A4GNPL: AEROSOL-MET DATA TABULATION  
(PROCESSED ON 08-MAR-82)

NRL:6532 ON SNI	YEAR DAY	TIME	AT	RH	WS (m/s)	WD	WVF (TDRR)	NUM (1/CC)	AREA (cm <sup>2</sup> /CC)	VOL (cm <sup>3</sup> /CC)	0.55	EXTINCTION (1/km)	3.80	10.6
79 124 630	10.3	91.7	2.5	268	8.6	201.	105.2	248.7	0.249	0.244	0.1283	0.0294		
79 124 630	10.3	91.8	2.1	288	8.7	179.	112.3	303.9	0.266	0.223	0.1522	0.0379		
79 124 630	10.3	90.6	1.7	227	8.7	308.	99.4	213.6	0.233	0.253	0.1069	0.0247		
800 124 630	10.6	91.7	1.9	97	8.8	224.	112.4	274.2	0.263	0.252	0.1290	0.0339		
800 124 630	10.6	91.1	-0.1	29	8.9	215.	111.8	275.9	0.264	0.252	0.1295	0.0342		
900 124 630	10.8	91.4	0.2	48	8.9	212.	94.7	178.9	0.223	0.207	0.0904	0.0197		
900 124 630	10.8	91.4	0.5	29	8.9	250.	106.0	183.8	0.251	0.227	0.0921	0.0195		
79 127 1230	11.6	85.9	9.0	256	8.8	41.	100.0	374.8	0.245	0.273	0.1778	0.0494		
79 127 1300	11.6	84.6	10.3	258	8.6	46.	106.5	408.0	0.261	0.288	0.1871	0.0544		
79 127 1330	11.7	81.9	10.3	169	8.4	49.	92.6	366.7	0.225	0.251	0.1624	0.0435		
1400 127 1430	11.7	83.2	10.0	255	8.6	349.	91.6	340.7	0.225	0.249	0.1608	0.0450		
1430 127 1500	11.7	84.0	10.4	258	8.6	41.	97.1	370.8	0.239	0.262	0.1699	0.0495		
1430 127 1530	11.7	83.8	9.8	257	8.6	34.	83.1	313.5	0.204	0.226	0.1483	0.0415		
1600 127 1630	11.6	82.3	9.7	255	8.5	28.	63.2	242.3	0.154	0.172	0.1099	0.0324		
1630 127 1700	11.7	83.6	9.7	251	8.5	30.	64.2	226.6	0.157	0.176	0.1080	0.0294		
1630 127 1730	11.7	82.3	10.5	249	8.5	35.	68.2	233.0	0.168	0.186	0.1131	0.0298		
1700 127 1730	11.7	80.9	10.1	252	8.3	35.	70.4	258.9	0.172	0.191	0.1191	0.0342		
1730 127 1800	11.7	82.6	9.5	249	8.5	38.	72.0	253.5	0.176	0.196	0.1222	0.0328		
1800 127 1830	11.8	79.4	9.3	251	8.2	35.	64.0	224.0	0.158	0.173	0.1043	0.0291		
1830 127 1900	11.8	82.1	9.7	256	8.5	37.	78.5	295.3	0.192	0.211	0.1362	0.0393		
1900 127 1930	11.6	85.1	8.5	253	8.7	34.	82.9	319.8	0.202	0.225	0.1509	0.0427		
1930 127 2000	11.5	84.6	8.4	255	8.6	29.	69.0	259.5	0.169	0.189	0.1204	0.0344		
2000 127 2000	11.3	82.4	9.1	261	8.3	22.	48.2	192.9	0.117	0.132	0.0815	0.0264		
79 128 300	10.7	85.4	8.2	282	8.4	19.	35.1	108.2	0.086	0.100	0.0542	0.0132		
79 128 330	10.9	85.7	8.2	277	8.2	19.	33.5	113.7	0.087	0.101	0.0565	0.0145		
1000 128 1030	11.1	82.5	9.5	274	8.4	24.	41.2	158.9	0.101	0.111	0.0650	0.0146		
1100 128 1130	11.3	79.4	10.4	277	8.0	26.	43.0	184.1	0.107	0.116	0.0716	0.0257		
1130 128 1200	11.3	80.9	10.5	276	8.1	28.	50.8	219.7	0.123	0.135	0.0863	0.0309		
1200 128 1230	11.4	78.9	11.1	275	8.0	34.	58.3	248.2	0.141	0.154	0.0975	0.0347		
1230 128 1300	11.5	72.7	11.2	279	7.9	49.	69.5	298.3	0.168	0.183	0.1171	0.0419		
1300 128 1330	11.2	76.7	11.1	281	8.0	36.	66.1	238.5	0.162	0.173	0.1169	0.0417		
1330 128 1400	11.3	70.9	10.9	281	8.0	47.	66.1	142.7	0.209	0.221	0.1500	0.0626		
1400 128 1430	11.6	78.9	11.1	275	8.0	34.	58.3	148.7	0.226	0.239	0.1624	0.0689		
1430 128 1500	11.5	72.7	11.2	279	7.9	49.	69.5	298.3	0.168	0.183	0.1171	0.0419		
1500 128 1530	11.3	76.7	11.1	281	8.0	36.	66.1	142.7	0.209	0.221	0.1500	0.0626		
1530 128 1600	11.9	72.9	11.1	281	8.0	47.	66.1	142.7	0.209	0.221	0.1500	0.0626		
1600 128 1630	12.0	72.1	11.1	275	8.0	34.	58.3	148.7	0.226	0.239	0.1624	0.0689		
1630 128 1700	12.1	73.7	11.2	279	7.9	49.	69.5	298.3	0.168	0.183	0.1171	0.0419		
1700 128 1730	12.0	73.7	11.2	279	7.9	49.	69.5	298.3	0.168	0.183	0.1171	0.0419		
1730 128 1760	12.0	75.5	11.2	281	8.0	36.	66.1	142.7	0.209	0.221	0.1500	0.0626		

J. A. DOWLING ET AL.

**Table 8 — Thirty-Minute Averages of Measured and Calculated Aerosol Parameters (Concluded)**

PROGRAM R4SNRL : AEROSOL MET DATA TABULATION NRL:6532 OH SNI YEAR DAY TIME AT RH WS WD UWP (M/S) (MM) (TORR)										PROCESSED ON 08-MAR-82)				
79	123	1800	11.9	77.4	14.2	284	8.1	96.	177.4	965.2	0.424	0.445	0.3109	0.1446
NUM (1/CC)	AREA (UM <sup>2</sup> /CC)	VOL (UM <sup>3</sup> /CC)	EXTINCTION (1/KM) 1.06 3.80											
800	10.1	81.6	10.7	283	7.6	106.	205.1	811.1	0.504	0.550	0.3310	0.1109		
800	10.1	82.3	10.1	281	7.6	100.	199.0	797.7	0.486	0.537	0.3266	0.1091		
800	10.1	81.6	9.6	282	7.6	94.	188.9	725.9	0.465	0.513	0.3048	0.0924		
830	10.1	81.5	9.4	284	7.7	88.	178.7	688.1	0.438	0.483	0.2918	0.0838		
900	10.1	82.6	8.4	282	7.7	85.	172.6	633.4	0.425	0.473	0.2768	0.0839		
930	10.1	83.2	8.1	279	7.7	81.	185.5	701.9	0.456	0.505	0.3023	0.0898		
1000	10.3	81.7	7.8	274	7.7	79.	177.5	672.3	0.436	0.488	0.2938	0.0898		
1030	10.3	81.7	7.7	267	7.7	74.	156.0	554.5	0.395	0.445	0.2698	0.0808		
1100	10.3	81.5	7.7	269	7.7	89.	157.4	566.2	0.386	0.430	0.2532	0.0725		
1130	10.3	82.3	7.6	268	7.7	76.	159.2	574.9	0.391	0.439	0.2545	0.0744		
1200	10.4	82.9	7.6	268	7.8	89.	176.0	629.5	0.434	0.481	0.2861	0.0826		
1230	10.4	83.3	7.6	269	7.9	89.	184.8	680.8	0.455	0.506	0.3042	0.0902		
1300	10.5	83.1	8.7	270	7.9	89.	184.5	678.8	0.453	0.506	0.3046	0.0897		
1330	10.5	81.1	8.2	269	7.8	83.	162.2	594.1	0.400	0.445	0.2612	0.0785		
1400	10.6	81.8	9.4	269	7.8	89.	176.1	657.4	0.434	0.479	0.2843	0.0878		
1430	10.6	83.0	8.8	271	7.9	91.	184.9	703.8	0.454	0.503	0.3027	0.0943		
1500	10.6	83.2	8.3	273	8.0	84.	179.1	697.7	0.438	0.469	0.3019	0.0939		
1530	10.7	83.3	8.7	268	8.0	89.	180.4	683.3	0.444	0.488	0.2987	0.0916		
1600	10.7	83.6	10.3	269	7.9	84.	179.1	716.2	0.438	0.484	0.3034	0.0975		
1630	10.8	82.4	9.8	271	8.0	80.	167.9	659.7	0.413	0.453	0.2808	0.0895		
1700	10.9	89.5	9.4	279	7.9	70.	149.9	573.2	0.366	0.404	0.2469	0.0774		
1730	10.9	79.6	9.6	269	7.8	66.	140.4	530.1	0.345	0.393	0.2307	0.0707		
1800	10.9	81.1	9.6	269	7.9	76.	157.6	587.8	0.390	0.427	0.2572	0.0784		
1830	10.9	81.9	9.3	272	8.0	77.	162.7	615.8	0.400	0.443	0.2704	0.0822		
1900	11.0	89.3	10.1	276	8.0	74.	154.5	586.4	0.379	0.421	0.2544	0.0785		
1930	10.9	81.7	9.3	275	8.0	76.	160.1	596.8	0.394	0.437	0.2659	0.0793		
2000	10.9	82.8	8.6	271	8.0	74.	164.5	605.5	0.404	0.452	0.2758	0.0799		
2030	10.9	83.2	8.3	80.	7.9	74.	161.7	617.1	0.430	0.481	0.2884	0.0802		
79	130	600	10.2	92.3	10.2	132.	331.1	1498.1	0.786	0.890	0.6503	0.2129		
		670	10.2	91.3	10.4	132.	397.7	1659.9	0.942	1.055	0.7809	0.2684		
		740	10.2	90.4	10.3	132.	329.0	1451.2	0.783	0.877	0.6429	0.2031		
		810	10.2	90.1	10.3	132.	327.4	1647.6	0.550	0.550	0.4196	0.1130		
		880	10.1	89.1	10.1	132.	325.5	1547.1	0.377	0.436	0.2684	0.0635		
		950	10.1	89.1	10.1	132.	327.4	1672.5	0.240	0.283	0.1662	0.0307		
		1020	10.1	89.1	10.1	132.	325.5	1684.6	0.246	0.287	0.1728	0.0326		
		1090	10.1	89.1	10.1	132.	323.7	1671.9	0.208	0.246	0.1413	0.0244		
		1160	10.1	89.1	10.1	132.	321.8	1666.2	0.218	0.256	0.1528	0.0280		
		1230	10.1	89.1	10.1	132.	320.9	1666.2	0.221	0.261	0.1584	0.0310		
		1300	10.1	89.1	10.1	132.	320.9	1666.2	0.203	0.240	0.1551	0.0251		

For readers who wish to do their own calculations from the aerosol data, we are including in the appendix all the aerosol spectrometer results. At the beginning of that appendix are the bin locations of the two probes. For the ASAP we include only the counts from the first seven bins since we exclude the last eight bins because of the double-valued sensitivity function that occurs in that size region.

### 3.5 Visibility Measurements

Visibility was determined by the contrast method developed by Koschmieder [15]. Here visibility is defined as the distance from an object which produces a threshold contrast between the object and the background.

The contrast formula is

$$\frac{B_X - B_H}{B_H} = e^{-\alpha X} = T_X \text{ (contrast transmittance)}$$

where  $B_X$  and  $B_H$  are the radiances of the cone of air in front of the target at distance  $X$  and the horizon, respectively. The attenuation coefficient  $\alpha$  in the visible region can generally be attributed to aerosol scattering. However, in high-visibility conditions the molecular component is a significant factor and must be considered in determinations of aerosol effects.

For visibility determination we define  $\gamma$  as the threshold contrast where the target is minimally visible and  $R$  as the range at that contrast. For our work we let  $\gamma = 0.02$  at a wavelength of  $0.55 \mu\text{m}$  so that

$$\frac{B_R - B_H}{B_H} = e^{-\alpha R} = 0.02$$

or visibility =  $3.91/\alpha$ . An optical pyrometer is a convenient instrument to use for the determination of  $B_R$  and  $B_H$ . Using a programmable hand calculator, a visibility observation can be made in about 1 minute. Table 9 summarizes the visibility measurements made during the experiment.

Visibility measurements derived from long-path optical transmission measurements performed by PMTC using a Barnes transmissometer system operating in the spectral band between  $0.50$  and  $0.61 \mu\text{m}$  were recorded also during the experimental period. These measurements are tabulated as well in Table 9. In cases where differing values were obtained from the NRL-optical pyrometer and PMTC-transmissometer measurements an average value for  $\sigma_{0.55}$  for the two measurements was used for the data listed in Table 1 and Figs. 6 through 10.

## 4. COMPARISON OF MEASURED AND CALCULATED TRANSMISSION VALUES

### 4.1 Laser Extinction Measurements

Table 1 and Figs. 6 through 10 show comparisons of measured extinction coefficients to calculated molecular absorption values for the DF laser lines studied in this experiment. It was observed in Section 3.1 that the consistently negative slope of the plots of  $\alpha$ -CMA shown in Figs. 6 through 10 is probably due to an overestimation of the molecular absorption coefficient by the  $\text{H}_2\text{O}$  continuum model of Watkins and White [7] at the high-wavenumber end of the interval shown in the figures.

If it is assumed that the Watkins and White  $\text{H}_2\text{O}$  continuum absorption model predicts approximately the correct absorption coefficient magnitude near the center of the interval shown in Figs. 6 through 10, i.e.,  $\sim 2650 \text{ cm}^{-1}$  but that the wavenumber dependence of the model is too strong, then the values of  $\alpha$ -CMA from the curves shown in Figs. 6 through 10 at  $2650 \text{ cm}^{-1}$  can be used as measures of the aerosol extinction occurring during the measurement time. These values for  $\sigma$  are seen to vary from a maximum of  $0.250 \text{ km}^{-1}$  occurring on 10 May 1979 at 0826 PDT to a minimum value of

Table 9 — Visibility Measurements

Date	Time (PDT)	PMTC		NRL	
		$\sigma_{.5-.61}$ (km $^{-1}$ )	VIS (km)	$\sigma_{.55}$ (km $^{-1}$ )	VIS (km)
5-1-79	0909	.085	45.8		
	0920			.085	45.9
	1120			.072	54.8
	1135	.076	51.5		
	1239	.088	44.6		
	1250			.076	51.3
	1300			.100	39.3
	1309	.093	42.0		
	1400			.129	30.3
	1417	.091	43.2		
	1800			.159	24.6
	1808	.119	32.9		
5-2-79	1157	.146	26.7		
	1200			.165	23.7
	1330			.158	24.8
	1336	.145	27.0		
	1450	.135	29.0		
	1500			.190	20.6
	1521	.129	30.3		
	1530			.151	25.9
	1536	.122	32.1		
	1600			.153	25.6
	1606	.152	25.7		
	1621	.157	24.9		
5-3-79	1800			.159	24.6
	1025	.159	24.5		
	1030			.133	29.5
	1040	.162	24.1		
	1055	.162	24.2		
	1100			.133	29.5
	1255	.240	16.3		
	1300			.202	19.4
	1310	.235	16.6		
	1355	.229	17.1		
	1400			.231	17.0
	1524	.171	22.9		
	1525			.194	20.2
	1933	.102	38.4		
	1935			.117	33.4
	1948	.123	31.9		

## NRL REPORT 8618

Table 9 — Visibility Measurements (Concluded)

Date	Time (PDT)	PMTC		NRL	
		$\sigma_{.5-.61}$ (km $^{-1}$ )	VIS (km)	$\sigma_{.55}$ (km $^{-1}$ )	VIS (km)
5-4-79	0738	.224	17.5		
	0745			.260	15.1
	0754	.260	15.0		
	0854	.309	12.7		
	0900			.314	12.5
	1000			.296	13.2
	1009	.421	9.3		
	1030			.329	11.9
	1039	.442	8.8		
	1054	.348	11.3		
	1304	.126	31.1		
	1330			.165	23.8
5-7-79	1359	.147	26.6		
	1400			.162	24.2
	1420			.164	23.9
	1429	.127	30.8		
	1558	.108	36.2		
	1600			.164	23.9
	1758	.105	37.0		
	1800			.158	24.9
	1925			.096	41.0
	1933	.093	42.2		
	1945			.107	36.5
	1948	.082	47.7		
5-8-79	0845			.080	48.8
	0848	.097	40.3		
	0918	.077	50.6		
	0920			.083	47.4
	0941	.083	47.4		
	0945			.061	64.5
	0951	.076	51.5		
	1100			.068	57.4
	1106	.087	44.9		
	0900	.226	17.3	.234	16.7
	1000			.205	19.2
	1004	.209	18.7		
5-9-79	1105			.199	19.7
	1119	.204	19.2		
	1249	.227	17.2		
	1250			.188	20.8
	1800			.237	16.6
	1802	.197	19.8		
	1926	.188	20.8		
	1930			.158	24.8
	1941	.198	19.8		

about  $0.005 \text{ km}^{-1}$  on 1 May 1979 at 1004 PDT and again on 3 May 1979 at 1833 PDT. In the latter two cases the measured visibilities were among the higher range of values recorded during the experiment and were 48 km and 35 km respectively.

Attempts to establish correlations of the  $\sigma$  values obtained from the long-path DF laser extinction measurements with windspeed (WS) and/or relative humidity (RH) have not been successful as no trends can be determined from the data for the ranges of  $\sigma$ , WS, and RH observed in the experiment.

Recently the long-path DF laser extinction data collected at SNI have been reviewed as part of a maritime environment characterization [16]. During this review the values of  $\sigma_{\text{DF}}$  obtained from the curves, shown in Figs. 6 through 10 and values for aerosol extinction at visible wavelengths derived from visibility measurements were used to form ratios of  $\sigma_{\text{DF}}/\sigma_{\text{VIS}}$ . These ratios were then compared with  $\sigma_{\text{IR}}/\sigma_{\text{VIS}}$  predictions obtained using the Katz/Ruhnke (K/R) [14] and LOWTRAN 5 [17] aerosol models for the measurements where visibility and DF laser extinction data were both available.

Table 10 contains a summary of values for  $\sigma_{\text{DF}}$  and  $\sigma_{\text{DF}}/\sigma_{\text{VIS}}$  thus obtained for several measurements at SNI. Comparison values obtained from aerosol spectrometer data presented in Section 3.4 are shown also. Predicted values of  $\sigma_{\text{DF}}/\sigma_{\text{VIS}}$  based on the K/R and LOWTRAN 5 models are shown as well.

Table 10 — Comparison of Values for  $\sigma_{\text{DF}}$  and  $\sigma_{\text{DF}}/\sigma_{\text{VIS}}$  Obtained from Long-Path Optical Transmission and Aerosol Spectrometer Measurements with Predictions Based on the K/R and LOWTRAN 5 Aerosol Models

Date	Time (PDT)	VIS (km)	PPH <sub>2</sub> O (torr)	AT (°C)	WS (m/s)	RH %	$\sigma_{\text{VIS}}$	$\sigma_{\text{VIS}}$	$\sigma_{\text{DF}}/\sigma_{\text{VIS}}$	K/R	LOWTRAN 5	Aerosol Spectrometer		
							$\sigma_{\text{DF}}$	$\sigma_{\text{VIS}}$	$\sigma_{\text{DF}}/\sigma_{\text{VIS}}$			$\sigma_{\text{DF}}$	$\sigma_{\text{VIS}}$	$\sigma_{\text{DF}}/\sigma_{\text{VIS}}$
5-1-79	1004	48	9.9	11.9	8	94	.010	.081	.123	.34	.72	.028	.054	.52
5-1-79	1344	42	9.9	12.3	14	93	.030	.093	.323	.63	.72	.051	.092	.55
5-1-79	1853	33	8.2	13.3	7.4	73	.090	.118	.763	.33	.55	.153	.214	.71
5-2-79	1504	29	9.1	13.1	10.4	81	.080	.135	.593	.43	.58	.151	.232	.65
5-2-79	1826	24	9.2	12.8	7.7	83	.090	.163	.552	.38	.58	.206	.311	.66
5-3-79	0828	24	9.2	12.2	6.6	87	.053	.163	.325	.25	.67	.202	.306	.66
5-3-79	1833	35	8.5	12.5	7.7	79	.010	.112	.090	.29	.58	.073	.128	.57
5-7-79	1516	36	9.2	13.8	12	79	.115	.109	1.05	.54	.110	.154	.71	
5-7-79	1831	20	9.3	13.1	13	83	.095	.196	.485	.58	.59	.136	.192	.71
5-8-79	0938	47	7.8	12.4	11.3	72	.010	.083	.121	.44	.50	.057	.087	.66
5-9-79	0823	17	8.4	12.0	10.4	80	.073	.230	.317	.42	.58	.277	.425	.65
5-9-79	1331	18	8.5	12.5	11.5	78	.110	.217	.507	.46	.56	.261	.400	.65
5-9-79	1914	21	8.7	12.7	11.7	80	.105	.186	.565	.48	.58	.254	.379	.67

Before making comparisons concerning the aerosol spectrometer results a few words are in order about the value of those measurements at the SNI location. Earlier we noted that a rock pile in the surf upwind from the aerosol spectrometers made comparisons with models less than desirable, especially if those models are based on open-sea parameters. The K/R model has such a base, as does LOWTRAN 5. Thus we do not expect to find much agreement with those models, and we do not. As for the transmittance data, because the transmittance measurement path is neither all downwind from the rocks nor from the surf in general, it is unlikely that the comparisons with those data will be very enlightening, either. Again, we are not disappointed in our prediction.

## NRL REPORT 8618

With respect to the transmittance measurements we would expect, since the aerosol spectrometers are sitting in the surf spray, that the aerosol-predicted extinction coefficients would be higher than the values from the long-path IMORL measurement. This is usually the case. Also, since the aerosol particles near the surf are likely to have a larger mean diameter than over the open water, the extinction should be relatively higher at longer wavelengths, i.e., the values for  $\sigma_{DF}/\sigma_{VIS}$  should be larger in the surf. Again, this is usually, but not always, the case.

We should point out that the aerosol sensors are not literally sitting on the beach in the surf spray. We did place them at the same level as the transmittance path, about 15 m above the water surface. Nevertheless the increased number of larger particles typical of surf conditions was quite evident. A detailed description of the aerosol probe location and comparisons of the results from several aerosol probes at that location is found in Ref. 18.

The conclusion is, then, that the conditions of wind direction combined with aerosol spectrometer and transmittance path location do not lend themselves to reasonable comparisons.

#### 4.2 Fourier Transform Spectrometer and Broadband Transmissometer Values

FTS spectra such as shown in Figs. 11-22 can be averaged or convolved with a broadband filter response function for comparison to a transmissometer measurement performed at the same time as the FTS spectra are recorded. Simultaneous measurements using the NRL laser-calibrated FTS system and the PMTC Barnes transmissometer system were performed at SNI. The FTS spectra were then convolved with measured responses for each of the transmissometer filters for several sets of measurements. The results of the two simultaneous and independent transmission measurements were compared (Table 11).

Figures 31 through 42 show comparisons for a series of eight filter bands each identified by a different symbol and code number. The half-power bandwidths of the filters are given in the inset in Fig. 30. As shown in the figures, there is generally good agreement between the two measurement systems within the combined measurement accuracy of the two techniques, the possible exception being with respect to the filter identified by the code 2154.\* Figure 43 shows an overall comparison for all the data collected during the simultaneous experiments. The overall agreement between the two measurement techniques is good on the average; however, appreciable scatter about the unity slope line is evident in the figure. The scatter shown in Fig. 43 is due in part to changing atmospheric conditions occurring during some of the measurement periods. Measurements with both laser and broadband transmissometer systems during this experiment showed variations as large as  $\pm 30\%$  in transmission for several repetitions of the same measurement within a 30-minute time span. Such an example is shown in Fig. 36. The scatter evident in Fig. 43 is probably the minimum that one can expect to obtain in comparing two long-path transmission measurements in a dynamic, coastal environment where surf-generated aerosols and open-sea conditions can give rise to rapidly fluctuating transmission conditions.

\*It was established after the reduction of the data shown in Figs. 31-42 that numerical errors in the convolved and band averaged spectra corresponding to PMTC filter number 2154 had occurred which render the comparisons of FTS and PMTC data for this filter band unreliable.

J. A. DOWLING ET AL.

Table 11 — FTS — Barnes Comparison

Filter	SNI 02 Day 121 1702 GMT	Barnes Value	Barnes Time	SNI 04 Day 122 0152 GMT	Barnes Value	Barnes Time	SNI 06 Day 122 2204 GMT	Barnes Value	Barnes Time
F2013	0.716	0.697	1709	0.505	0.522	0138	0.579	0.553	1544
F2026	0.702	0.568	1709	0.472	0.427	0139	0.548	0.450	1544
F2038	0.574	0.637	1710	0.411	0.479	0140	0.466	0.508	1545
F2051	0.635	0.605	1711	0.450	0.448	0140	0.515	0.466	1546
F2077	0.705	0.654	1712	0.493	0.493	0141	0.566	0.540	1547
F2128	0.476	0.435	1714	0.358	0.342	0144	0.400	0.372	1549
F2154	0.089	0.222	1716	0.084	0.172	0145	0.087	0.191	1551
F2179	0.069	0.127	1718	0.092	0.109	0147	0.091	0.123	1553

Filter	SNI 09 Day 122 2204 GMT	Barnes Value	Barnes Time	Barnes Value	Barnes Time	SNI 12 Day 124 0135 GMT	Barnes Value	Barnes Time
F2013	0.526	0.502	2221	0.550	2150	0.757	0.607	0132
F2026	0.484	0.444	2222	0.463	2150	0.686	0.533	0133
F2038	0.440	0.489	2222	0.516	2151	0.637	0.555	0134
F2051	0.472	0.449	2223	0.478	2151	0.680	0.527	0134
F2077	0.511	0.556	2224	0.551	2153	0.733	0.599	0136
F2128	0.381	0.373	2227	0.363	2155	0.558	0.395	0139
F2154	0.091	0.154	2229	0.188	2157	0.161	0.209	0140
F2179	0.118	0.116	2230	0.113	2159	0.203	0.136	0142

Filter	SNI 13 Day 124 1528 GMT	Barnes Value	Barnes Time	SNI 14 Day 127 2215 GMT	Barnes Value	Barnes Time	SNI 16 Day 128 0123 GMT	Barnes Value	Barnes Time
F2013	0.617	0.569	1524	0.475	0.586	2213	0.517	0.551	0113
F2026	0.532	0.492	1524	0.418	0.508	2214	0.496	0.491	0114
F2038	0.532	0.484	1525	0.407	0.545	2214	0.436	0.515	0114
F2051	0.559	0.467	1526	0.429	0.504	2215	0.465	0.481	0115
F2077	0.592	0.518	1527	0.457	0.577	2216	0.498	0.550	0116
F2128	0.477	0.272	1530	0.358	0.397	2219	0.387	0.366	0119
F2154	0.129	0.189	1531	0.097	0.202	2221	0.107	0.186	0121
F2179	0.161	0.115	1533	0.119	0.124	2223	0.135	0.115	0122

Filter	SNI 17 Day 128 1602 GMT	Barnes Value	Barnes Time	SNI 23 Day 129 2030 GMT	Barnes Value	Barnes Time	SNI 24 Day 130 0211 GMT	Barnes Value	Barnes Time
F2013	0.737	0.628	1636	0.491	0.481	2025	0.479	0.441	0214
F2026	0.684	0.561	1641	0.419	0.414	2026	0.437	0.371	0214
F2038	0.615	0.576	1641		0.433	2026	0.402	0.407	0215
F2051	0.664	0.546	1642	0.447	0.411	2027	0.432	0.384	0216
F2077	0.717	0.625	1643	0.470	0.467	2028	0.465	0.434	0217
F2128	0.541	0.421	1646	0.390	0.316	2031	0.355	0.299	0205
F2154	0.155	0.223	1648	0.114	0.172	2033	0.980	0.159	0206
F2179	0.215	0.162	1649	0.164	0.113	2034	0.128	0.105	0208
F3000				0.368	0.452	2030	0.390	0.423	0231
F3013				0.414	0.523	2025	0.442	0.484	0211
F3026				0.403	0.484	2026	0.432	0.467	0228
F3038				0.377	0.449	2027	0.408	0.421	0228

## NRL REPORT 8618

Table 11 — FTS — Barnes Comparison (Concluded)

Filter	SNI 25 Day 130 1718 GMT	SNI 26 Day 130 1718 GMT	Average SNI 25 & SNI 26	Barnes Value	Barnes Time
F2013	0.457	0.452	0.455	0.477	1717
F2026	0.399	0.403	0.401	0.393	1717
F2038	0.392	0.384	0.391	0.445	1718
F2051	0.414	0.408	0.411	0.405	1718
F2077	0.440	0.437	0.438	0.460	1720
F2128	0.351	0.339	0.345	0.326	1722
F2154	0.097	0.087	0.092	0.170	1723
F2179	0.116	0.104	0.110	0.098	1725
F3000		0.253		0.392	1707
F3013		0.283		0.444	1717
F3026		0.284		0.458	1718
F3038		0.269		0.388	1719

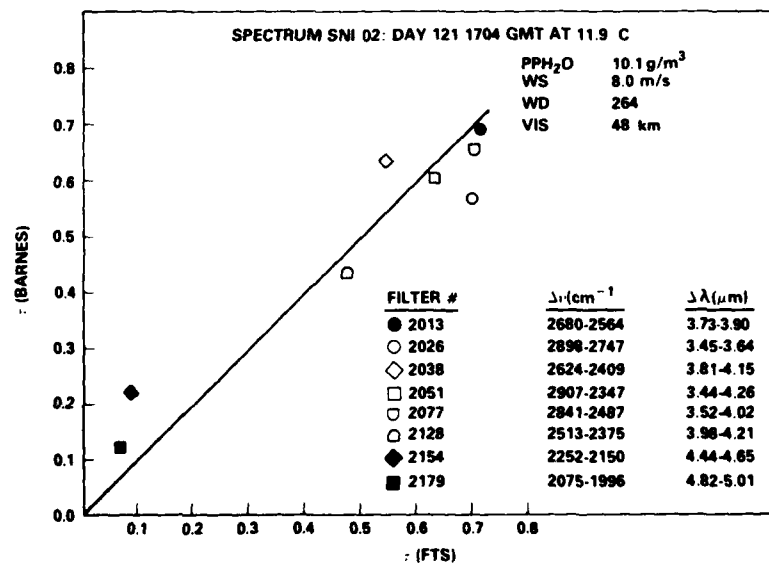


Fig. 31 — Comparison of FTS and Barnes transmissometer data for  
Day 121 at 1704 GMT

J. A. DOWLING ET AL.

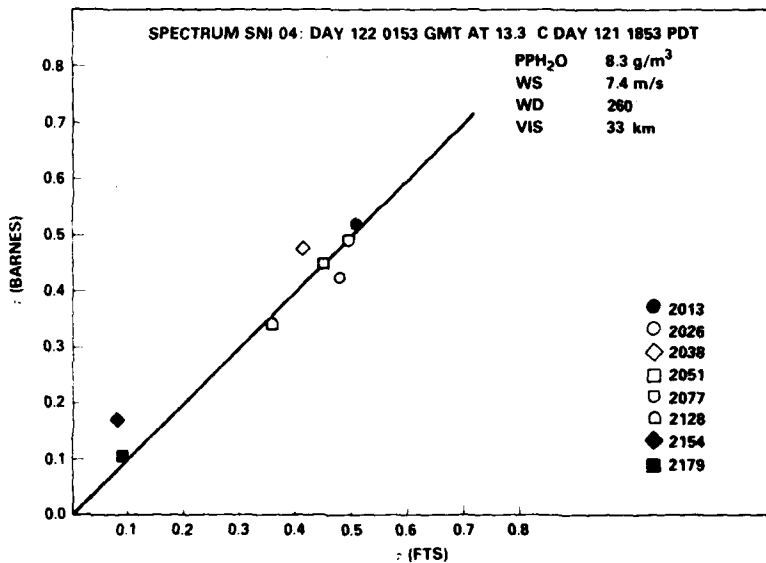


Fig. 32 — Comparison of ETS and Barnes transmissometer data for Day 122 at 0153 GMT

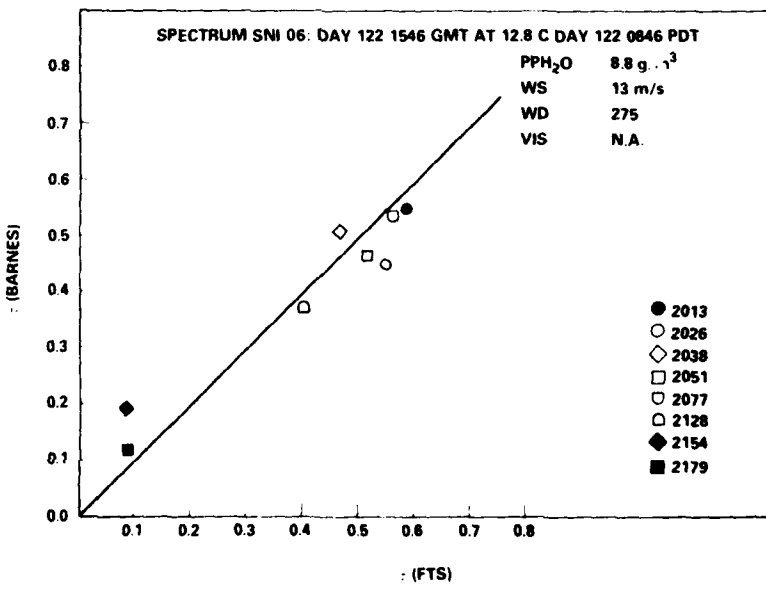


Fig. 33 — Comparison of ETS and Barnes transmissometer data for Day 122 at 1546 GMT

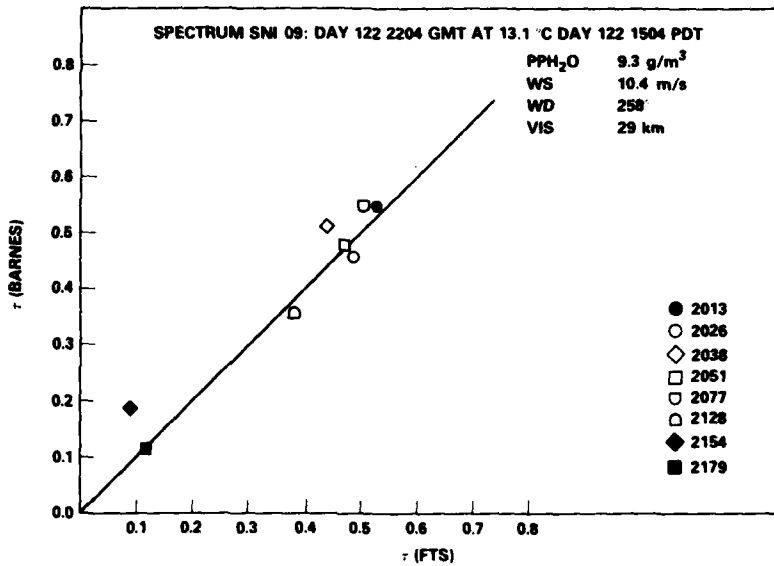


Fig. 34 — Comparison of FTS and Barnes transmissometer data for Day 122 at 2204 GMT

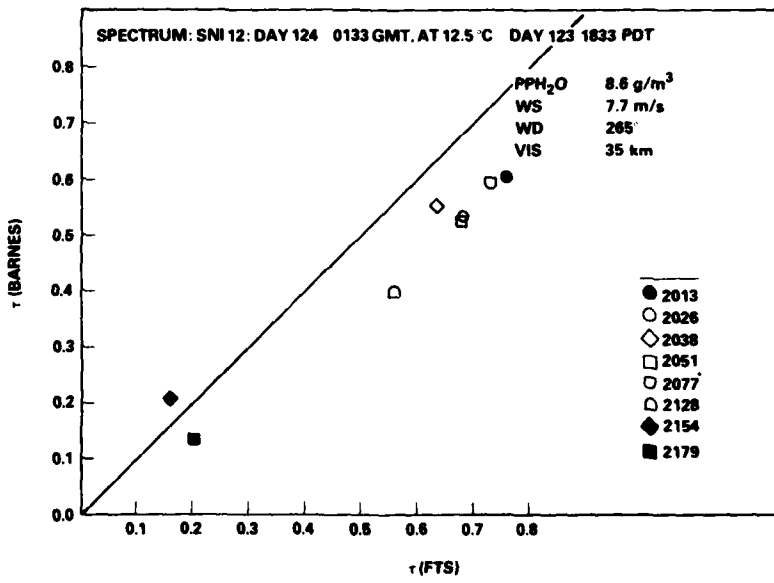


Fig. 35 — Comparison of FTS and Barnes transmissometer data for Day 124 at 0133 GMT

J. A. DOWLING ET AL.

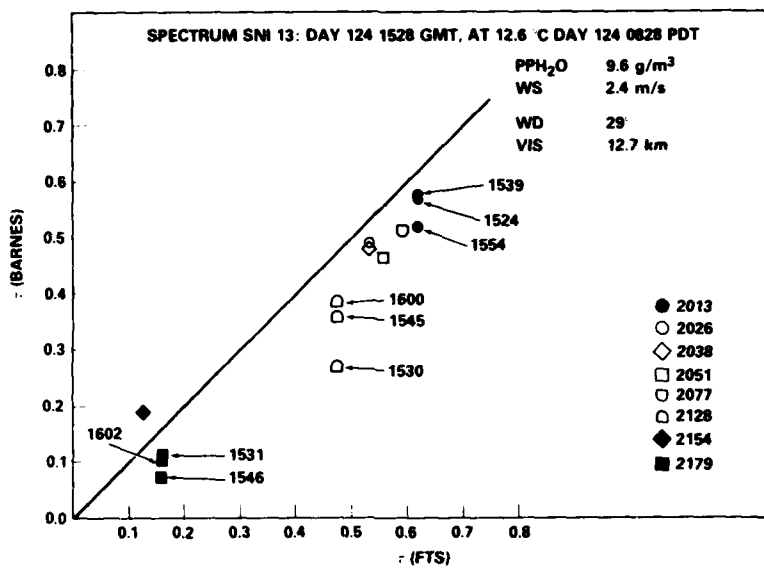


Fig. 36 — Comparison of FTS and Barnes transmissometer data for Day 124 at 1548 GMT

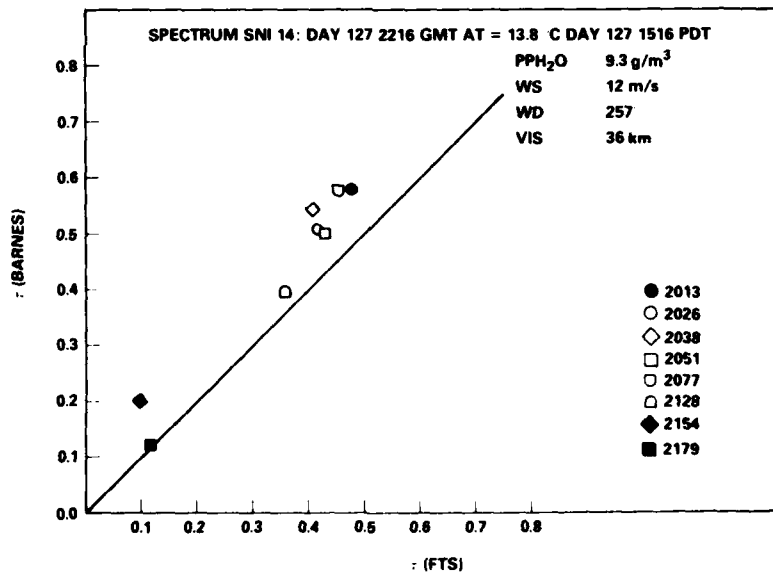


Fig. 37 — Comparison of FTS and Barnes transmissometer data for Day 127 at 2216 GMT

## NRL REPORT 8618

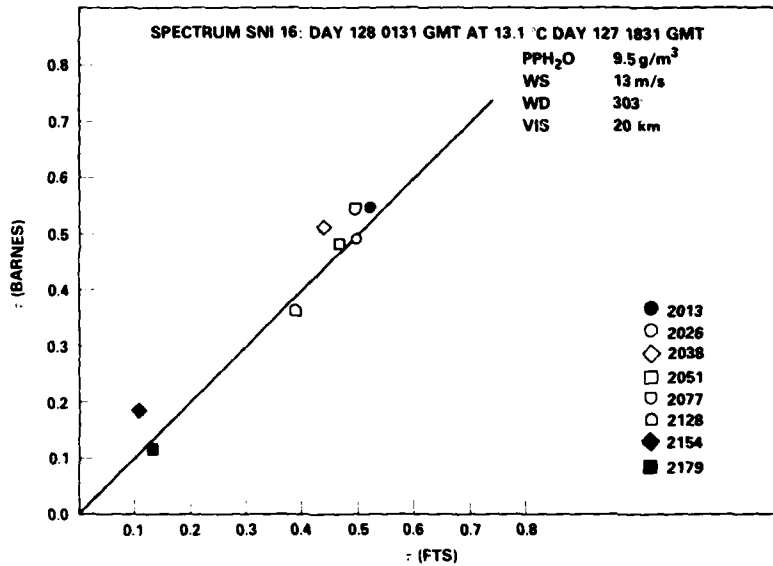


Fig. 38 — Comparison of FTS and Barnes transmissometer data for Day 128 at 0131 GMT

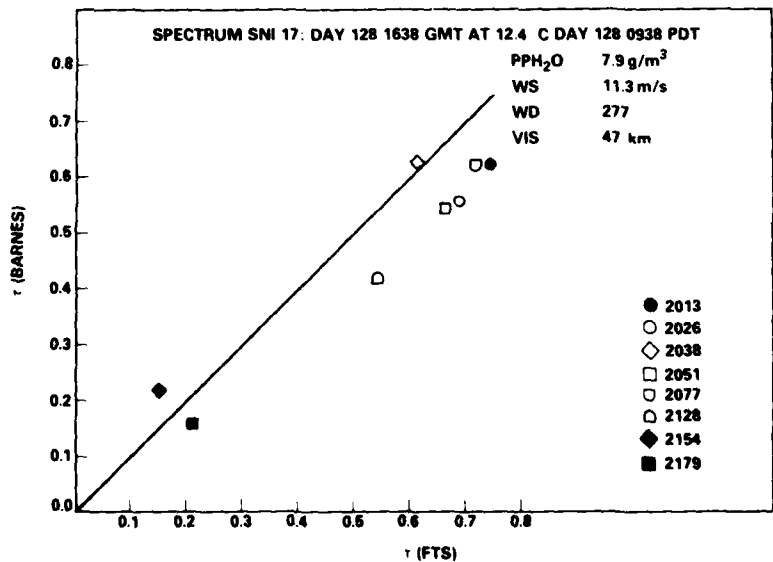


Fig. 39 — Comparison of FTS and Barnes transmissometer data for Day 128 at 1638 GMT

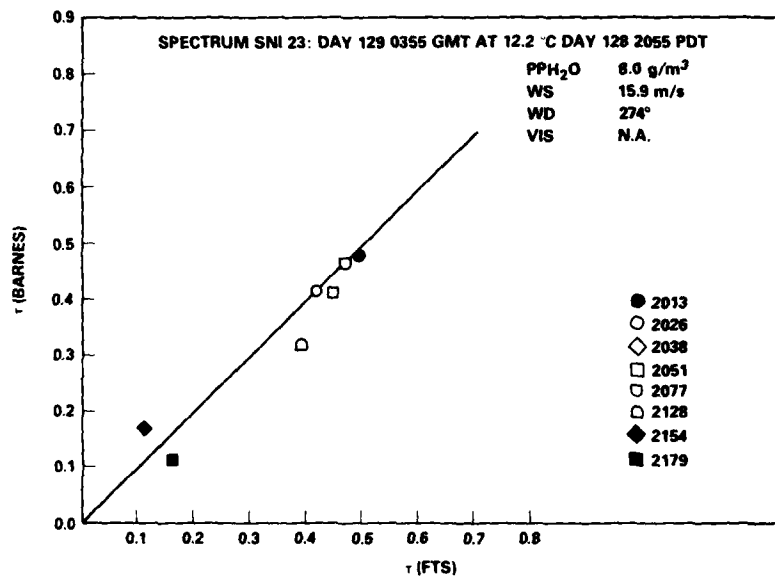


Fig. 40 — Comparison of FTS and Barnes transmissometer data for Day 129 at 0355 GMT

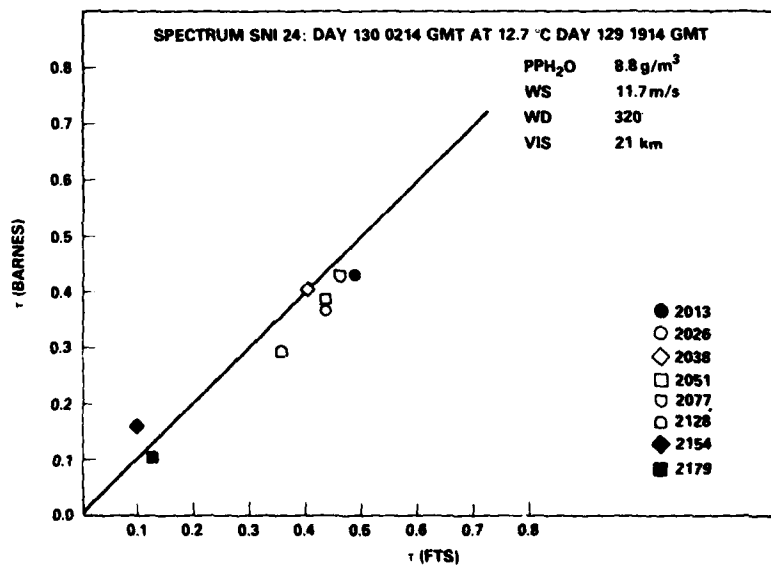


Fig. 41 — Comparison of FTS and Barnes transmissometer data for Day 130 at 0214 GMT

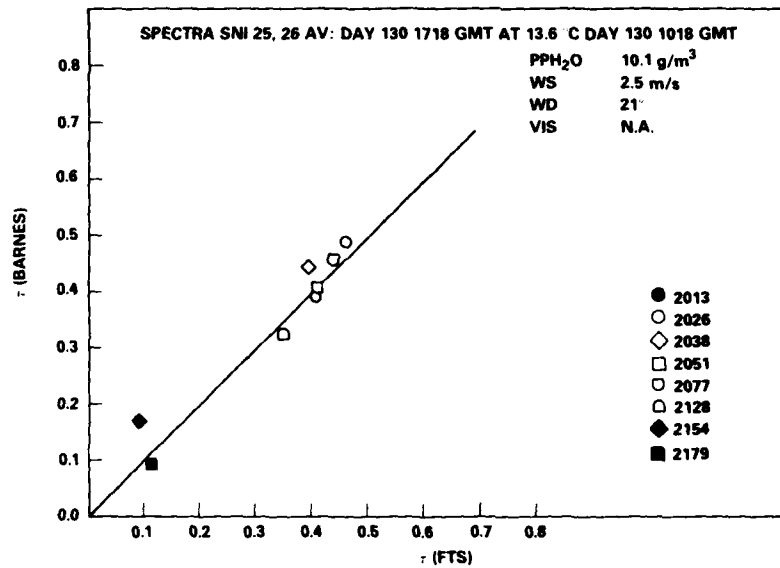


Fig. 42 — Comparison of FTS and Barnes transmissometer data for Day 130 at 1718 GMT

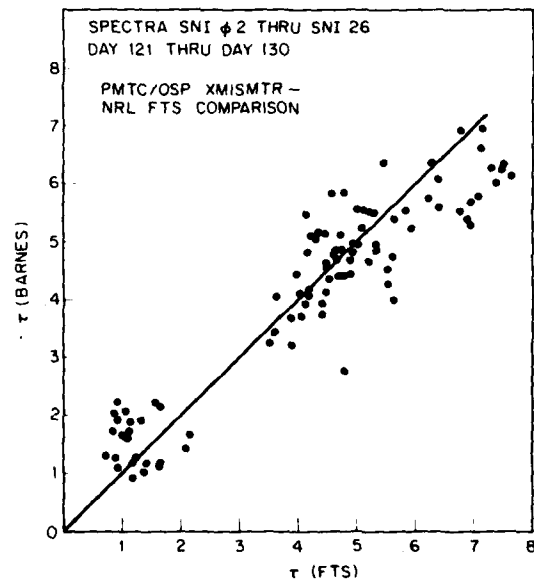


Fig. 43 — Comparison of FTS and Barnes transmissometer data for all days of the experiment

## 5. CONCLUSIONS AND RECOMMENDATIONS

Several conclusions can be reached as a result of analysis and evaluation of the measurements described in this report. The most important findings can be summarized as follows:

- The DF laser extinction measurement data presented in Figs. 6 through 10 consistently show that the differences between measured extinction coefficients and calculated molecular absorption coefficients systematically decrease with increasing wavenumber, leading to a conclusion that the water vapor continuum absorption model (Watkins and White) used in the data reduction predicts too strong an increase of absorption at wavenumbers  $\gtrsim 2650 \text{ cm}^{-1}$ .
- The average aerosol extinction coefficient values,  $\sigma_{DF}$ , derived from the long-path DF laser extinction measurements, show a wide range of values between  $0.005 \text{ km}^{-1}$  and  $0.250 \text{ km}^{-1}$  (see Figs. 6 through 10). The magnitude of  $\sigma_{DF}$  thus determined does not show a significant correlation with measured visibility, windspeed, or relative humidity.
- Several accurately calibrated high-resolution transmission spectra of the 4.07 km overwater path between sites A and C at SNI were obtained. The data contained in Table 4 show that absolute transmission normalizations of these spectra are consistently within a range of  $\pm 2\%$ , occasionally showing a larger variation but still within a range of  $\pm 5\%$ .
- Path integrated water vapor density measurements compare favorably to within  $\pm 15\%$  with point measurements obtained with dew point measurement systems located on shore near site A. Figure 23 shows an example of these comparisons. Some difference in the overwater path-integrated readings compared to the fixed-site shore measurements can be expected due to inhomogeneities along the 4.07 km path. The data shown in Fig. 23 indicate that these differences are within  $\pm 20\%$  for the several comparisons considered. These differences are about twice the magnitude of the differences seen between the two sets of dew point readings shown in Fig. 23.
- Meteorological conditions observed during the comparison portion of the experimental period remained fairly constant. Air temperature varied between  $11.9^\circ$  and  $13.8^\circ\text{C}$ , absolute humidity ranged between 7.8 and 9.9 torr partial pressure of  $\text{H}_2\text{O}$ , and windspeed values varied between 8 and 14 m/s.
- Visibilities measured during the experiment varied between a high value of 64.5 km on 8 May 1979 at 0945 PDT and a low value of 8.8 km on 4 May 1979 at 1039 PDT. A comparison of visibility measurements performed by PMTC and NRL shows that for most of the data where the visibility or meteorological range,  $R_V$ , was less than 35 km, the NRL data were consistently lower than PMTC values by typically 10 to 15% and occasionally by as much as 25%. For data acquired on 8 May 1979 when  $R_V > 45 \text{ km}$ , NRL data were higher than the PMTC data by about 25%. On 7 May 1979 when  $R_V \gtrsim 17$  to 20 km, the NRL readings were 5 to 25% higher than the PMTC values.
- Excursions of as much as  $\pm 30\%$  in transmission were observed during 30-minute intervals in the PMTC measurements. Comparisons of average transmission values in spectral bands corresponding to the PMTC transmissometer bandpasses showed comparable scatter when compared to the transmissometer readings. The large scatter is indicative of the fact that instantaneous values can show that much variation with respect to 30- to 60-minute average values in the dynamic, surf-influenced SNI environment.

Certain recommendations are appropriate upon evaluation of the observations discussed above; principal among these are the following:

- (1) The data described in this report and shown in Figs. 6 through 10 should be used together with other field-measured long-path laser extinction and laser-extinction-calibrated FTS data in a systematic validation of the 3 to 5  $\mu\text{m}$  water vapor continuum absorption model.
- (2) Further attempts should be made using overwater infrared transmission data to quantify infrared aerosol extinction, to relate the observed values to meteorological observables such as windspeed and relative humidity, and to improve the modeling prediction of infrared aerosol extinction in the marine environment. The use of aerosol spectrometer measurement locations for comparison purposes which are not affected by artificial surf-generated aerosols should be emphasized. Airborne or shipborne aerosol counter measurement platforms, and possibly off-shore tower sites should be considered in planning future experiments.
- (3) Although shore-based and path-integrated water vapor density measurements have shown good agreement in this experiment, some differences have been noted, most probably due to moderate inhomogeneities along the several-kilometer optical path. Consideration should be given to the use of path-integrated water vapor measurements obtained from high-resolution transmission spectra such as described in this report in future transmission model validation exercises. Development of a single-ended LIDAR type system for both aerosol and water-vapor profile measurements should be considered. An advantage offered by a system of this type compared to the measurements described herein is that slant-path measurements could be performed.
- (4) Comparable measurement averaging times should be used in any future comparisons of transmissometer-band-averaged FTS measurements since it has been observed in this experiment that fluctuations in transmission values as large as  $\pm 30\%$  were observed within a 30-minute period. Hence it seems reasonable that if a 30- to 45-minute measurement interval is required to obtain the laser-calibrated FTS transmission band values, that a comparable averaging time should be used in obtaining comparison values with a banded transmissometer system such as the one used by PMTC in this experiment.

## 6. ACKNOWLEDGMENTS

The authors express their thanks to Dr. Juergen Richter, manager of the Navy Electro-Optical Meteorology Program, for support of the measurements described herein. The help in logistics and equipment transportation provided by Chuck Elliott, PMTC is greatly appreciated. The assistance of Gary Matthews, PMTC in making the PMTC transmissometer filter wheel assemblies available to NRL personnel for filter response measurements and the use of a MIDAC Corp. owned FTS system identical to the NRL system provided by Gerald Auth of the MIDAC Corporation were both essential to the comparison measurements described in this report, and as such are greatly appreciated. The assistance of Stephen J. Dowling in completing data reduction was most helpful. The authors also thank Claude Acton for his assistance in preparing many of the figures. The painstaking typing, especially of the numerous and lengthy tables in this report, by Mrs. Nell Grimely is especially appreciated.

## 7. REFERENCES

- I. J.A. Dowling, R.F. Horton, G.L. Trusty, T.H. Cosden, K.M. Haught, J.A. Curcio, C.O. Gott, S.T. Hanley, P.B. Ulrich, and W.L. Agambar, "Atmospheric Transmission Measurement and Field Test Plan," NRL Report 8059, November 1977.

2. R.W. Harris, "Electronic Instrumentation for a High-Accuracy Atmospheric Extinction Experiment," Abstract, J. Opt. Soc. Am. **65**, 1201 (1975).
3. J.A. Dowling, K.M. Haught, R.F. Horton, G.L. Trusty, J.A. Curcio, T.H. Cosden, S.T. Hanley, C.O. Gott, and W.L. Agambar, "Atmospheric Extinction Measurements at Nd-YAG and DF Laser Wavelengths Performed in Conjunction with JAN Propagation Tests, June-September 1975," NRL Report 8058, February 1978.
4. T.V. Blanc, "Micrometeorological Data Report for the November 1978 Electro-Optics Meteorology (EOMET) Experiment at San Nicolas Island, California," NRL Memorandum Report 4056, August 1979.
5. G.L. Trusty and T.H. Cosden, "Optical Extinction Predictions from Measurements on the Open Sea," NRL Report 8260, Jan. 1979.
6. J.A. Dowling, R.F. Horton, S.T. Hanley, and K.M. Haught, "High Resolution Measurement of Atmospheric Transmission," SPIE Proceedings **142**, 25 (1978).
7. W.R. Watkins and K.O. White, Opt. Ltrs. **1**, 31 (1977).
8. D.E. Burch, D.A. Gryvnak, and J.D. Pembrook, "Investigation of the Absorption of Infrared Radiation by Atmospheric Gases: Water, Nitrogen, Nitrous Oxide," Philco-Ford Aeronutronic Division Report U-4784 (AFCRL-71-0124), January 1974.
9. J.A. Dowling, S.T. Hanley, J.A. Curcio, C.O. Gott, and M.A. Woytko, "Laser Extinction and High Resolution Atmospheric Transmission Measurements Conducted at White Sands Missile Range, New Mexico, March 1979," NRL Report 8446, October 1980.
10. R.A. McClatchey, W.S. Benedict, S.A. Clough, D.E. Burch, R.F. Calfee, K. Fox, L.S. Rothman, and J.S. Garing, "AFCRL Atmospheric Line Parameters Compilation," Report AFCRL-TR-73-0096 (Air Force Cambridge Research Laboratories, Hanscom AFB, Mass.), 1973.
11. L.S. Rothman, "Update of the AFGL Atmospheric Absorption Line Parameters Compilation," Appl. Opt. **17**, 3517 (1978).
12. G.L. Trusty and K.M. Haught, "An Aerosol Data Base Format," NRL Memorandum Report 4605, September 1981.
13. W.C. Wells, G. Gal, and M.W. Munn, "Aerosol Distributions in Maritime Air and Predicted Scattering Coefficients in the Infrared," Appl. Opt. **16**, 654 (1977).
14. V.R. Noonkester, "Offshore Aerosol Spectra and Humidity Relations Near Southern California," Am. Meteor. Soc. **113** (1980).
15. W.E.K. Middleton, *Vision Through the Atmosphere*, University of Toronto Press, 1952, pp. 61-64.
16. J.A. Dowling and T.J. Rogne, "Shipboard Visibility Measurement System Definition Study," OptiMetrics, Inc. Report OMI-82-003, January 1982.
17. F.Y. Kneizys et al., "Atmospheric Transmittance/Radiance: Computer Code LOWTRAN 5," Air Force Geophysics Laboratory Report AFGL-TR-80-0067, 1980.
18. D. Jensen, R. Jeck, G. Trusty, and G. Schacher, "Intercomparison of PMS Particle Site Spectrometers," Naval Ocean Systems Center Technical Report 555, June 1980.

**Appendix**  
**AEROSOL SPECTROMETER DATA**

Table A1 — Bin-Edge Locations  
for Probes in Table A2

Particle Radius ( $\mu\text{m}$ )	
ASAP Probe 1	CSASP Probe 2
.142	0.75
.157	1.7
.176	2.65
.202	3.6
.235	4.55
.270	5.5
.310	6.45
.355	7.4
.405	8.35
.457	9.3
.510	10.25
.570	11.2
.630	12.15
.690	13.1
.755	14.05
.820	15.0

**Table A2 – Thirty Minute Averages of  $dN/dR$  ( $\text{cm}^{-3} \mu\text{m}^{-1}$ ) vs Radius ( $\mu\text{m}$ )**  
**DISTRIBUTION TABULATION** (PROCESSED ON 08-MAR-82)

**Table A2 (Continued)**

**Table A2 (Continued)**  
(PROCESSED ON 08-14R-82)

PROGRAM A49HRL:		AEROSOL DISTRIBUTION TABULATION										
NRL:6532 ON SNI		TRIBUTATION										
RADIUS	---	0.15	0.17	0.19	0.22	0.25	0.29	0.33	0.37	0.40		
79	121	1.400	2.71E 93	1.39E 93	1.21E 93	3.55E 02	5.73E 01	3.40E 01	4.19E 00	6.23E -01	4.68E -02	
1430	7.32E 02	3.14E 02	1.96E 02	1.76E 02	6.37E 01	2.05E 01	1.89E 01	1.47E 00	4.19E -01	2.47E -02		
1500	1.14E 01	3.05E 02	1.93E 02	1.73E 02	6.27E 01	1.97E 01	1.65E 01	1.43E 00	5.69E -01	3.17E -02		
1530	1.14E 01	3.05E 02	1.93E 02	1.73E 02	6.27E 01	1.97E 01	1.65E 01	1.43E 00	5.69E -01	3.17E -02		
1600	5.93E 02	1.51E 02	1.81E 02	1.71E 02	6.23E 01	1.76E 01	1.74E 01	1.47E 00	5.76E -01	3.18E -02		
1630	5.61E 02	1.52E 02	1.82E 02	1.72E 02	6.20E 01	1.75E 01	1.75E 01	1.49E 00	5.76E -01	3.18E -02		
1700	5.61E 02	2.01E 02	1.35E 02	1.35E 02	5.93E 01	1.66E 01	1.67E 01	2.37E 01	4.57E 00	6.49E 00	3.38E -02	
1730	4.93E 02	2.01E 02	1.36E 02	1.36E 02	5.83E 01	1.67E 01	1.68E 01	2.37E 01	4.58E 00	6.49E 00	3.55E -02	
1800	5.79E 02	1.34E 02	1.82E 02	1.53E 02	6.01E 01	1.51E 01	1.51E 01	2.77E 01	5.71E 00	9.49E -01	4.94E -02	
1830	5.80E 02	1.34E 02	1.82E 02	1.53E 02	6.01E 01	1.51E 01	1.51E 01	2.77E 01	5.71E 00	9.49E -01	4.94E -02	
1900	6.60E 02	2.02E 02	1.56E 02	1.56E 02	6.01E 01	1.67E 01	1.67E 01	2.73E 01	5.54E 00	1.16E 00	6.03E -02	
1930	5.31E 02	1.76E 02	1.39E 02	1.39E 02	6.68E 01	1.46E 01	1.46E 01	2.98E 01	7.09E 00	1.04E 00	5.30E -02	
2000	5.78E 02	2.08E 02	1.56E 02	1.57E 02	6.17E 01	1.35E 01	1.35E 01	3.35E 01	7.69E 00	1.17E 00	5.41E -02	
2030	6.05E 02	2.02E 02	1.53E 02	1.53E 02	6.17E 01	1.35E 01	1.35E 01	3.35E 01	7.69E 00	1.17E 00	5.41E -02	
2100	6.29E 02	1.91E 02	1.62E 02	1.62E 02	6.09E 01	1.55E 01	1.55E 01	4.01E 01	8.29E 00	1.28E 00	6.42E -02	
2130	7.44E 02	2.40E 02	1.69E 02	1.69E 02	6.75E 01	1.78E 01	1.78E 01	3.22E 01	3.52E 00	1.32E 00	6.70E -02	
2160	5.63E 02	1.91E 02	1.45E 02	1.45E 02	6.67E 01	1.52E 01	1.52E 01	3.51E 01	3.96E 00	1.28E 00	6.66E -02	
2200	5.53E 02	2.50E 02	1.45E 02	1.45E 02	6.52E 01	1.43E 01	1.43E 01	4.02E 01	8.08E 00	1.17E 00	5.84E -02	
2300	6.12E 02	1.97E 02	1.70E 02	1.70E 02	6.24E 01	1.49E 01	1.49E 01	4.88E 01	9.18E 00	1.11E 00	6.08E -02	
2330	5.93E 02	1.97E 02	1.70E 02	1.70E 02	6.24E 01	1.49E 01	1.49E 01	4.88E 01	9.18E 00	1.11E 00	6.33E -02	
79	122	9	5.93E 02	1.34E 02	1.34E 02	5.91E 01	3.67E 01	2.95E 01	6.35E 00	8.79E -01	1.94E -01	4.21E -02
100	6.12E 02	2.16E 02	1.57E 02	1.57E 02	6.13E 01	4.11E 01	3.83E 01	6.35E 00	9.56E -01	2.07E -01	4.55E -02	
130	1.06E 03	4.32E 02	3.69E 02	3.69E 02	6.35E 01	4.42E 01	5.01E 01	7.00E 00	9.97E -01	2.09E -01	4.65E -02	
200	9.90E 02	1.33E 02	1.33E 02	1.33E 02	6.39E 01	5.81E 01	6.01E 01	8.13E 00	1.47E 00	3.45E -01	5.37E -02	
230	1.34E 03	4.98E 02	3.54E 02	3.54E 02	6.13E 01	5.14E 01	5.34E 01	8.39E 00	1.49E 00	3.56E -01	7.33E -02	
300	1.42E 03	5.26E 02	3.95E 02	3.95E 02	6.08E 01	5.42E 01	5.69E 01	8.59E 00	1.54E 00	3.54E -01	7.12E -02	
330	1.48E 03	5.09E 02	3.94E 02	3.94E 02	6.12E 01	5.48E 01	5.74E 01	8.64E 00	1.54E 00	3.54E -01	6.94E -02	
400	1.52E 03	5.87E 02	4.40E 02	4.40E 02	6.26E 01	6.45E 01	7.69E 01	1.23E 01	1.92E 00	4.47E -01	8.97E -02	
430	1.43E 03	5.11E 02	4.29E 02	4.29E 02	6.23E 01	6.38E 01	6.59E 01	1.26E 01	1.98E 00	4.54E -01	9.07E -02	
500	1.41E 03	5.21E 02	3.79E 02	3.79E 02	6.17E 01	6.15E 01	7.11E 01	1.11E 01	1.65E 00	7.08E -01	7.12E -02	
530	1.50E 02	5.66E 02	3.77E 02	3.77E 02	6.11E 01	5.47E 01	6.01E 01	7.17E 01	1.11E 01	1.67E 00	3.60E -01	
600	1.44E 03	5.78E 02	4.19E 02	4.19E 02	6.14E 01	5.74E 01	5.74E 01	7.15E 01	1.15E 01	1.64E 00	3.55E -01	
700	1.47E 03	5.76E 02	4.16E 02	4.16E 02	6.10E 01	5.65E 01	5.65E 01	7.12E 01	1.14E 01	1.7AE 00	4.29E -01	
730	1.51E 03	6.01E 02	4.60E 02	4.60E 02	6.17E 01	5.91E 01	6.17E 01	7.32E 01	1.23E 01	1.7AE 00	4.39E -01	
800	1.55E 03	6.51E 02	4.97E 02	4.97E 02	6.19E 01	6.41E 01	6.41E 01	7.39E 01	1.28E 01	1.7AE 00	4.49E -01	
830	1.55E 03	6.51E 02	4.97E 02	4.97E 02	6.19E 01	6.41E 01	6.41E 01	7.39E 01	1.28E 01	1.7AE 00	4.49E -01	
900	9.40	1.62E 03	6.75E 02	6.75E 02	6.23E 01	6.75E 01	6.75E 01	7.45E 01	1.31E 01	1.7AE 00	4.59E -01	
1000	1.25E 03	6.75E 02	6.75E 02	6.75E 02	6.23E 01	6.75E 01	6.75E 01	7.45E 01	1.31E 01	1.7AE 00	4.59E -01	
1030	1.23E 03	6.75E 02	6.75E 02	6.75E 02	6.23E 01	6.75E 01	6.75E 01	7.45E 01	1.31E 01	1.7AE 00	4.59E -01	
1100	1.04E 03	4.16E 02	4.16E 02	4.16E 02	5.31E 01	5.31E 01	5.31E 01					
1130	1.04E 03	4.16E 02	4.16E 02	4.16E 02	5.31E 01	5.31E 01	5.31E 01					

**Table A2** (Continued)  
 (PROCESSED ON MAR-19-82)

Table A2 (Continued)  
(PROCESSED ON 08-MAR-82)

PROGRAM A49NPL:		AEROSOL DISTRIBUTION TABULATION												
NPL	ON SHI RADIUS	0.15	0.17	0.19	0.21	0.22	0.25	0.29	0.33	1.23	2.18	3.12	4.08	
79	123	900	2.76E 03	1.46E 01	1.18E 03	4.04E 02	2.25E 02	1.15E 02	6.79E 01	9.18E 00	1.05E 00	4.43E -01	9.40E -01	
100	100	2.76E 03	1.46E 03	1.18E 03	4.04E 03	2.25E 02	1.15E 02	6.79E 01	9.18E 00	1.05E 00	4.43E -01	9.40E -01	9.67E -02	
1010	2.51E 03	1.39E 03	1.08E 03	3.65E 03	1.08E 03	3.65E 02	1.18E 02	1.05E 02	5.72E 01	8.44E 00	3.97E -01	8.45E -01	8.45E -02	
1030	2.31E 03	1.18E 03	1.04E 03	3.25E 02	1.04E 03	3.25E 02	1.75E 02	7.56E 01	5.30E 01	7.45E 00	7.78E -01	3.04E -01	6.04E -01	
1110	2.51E 03	1.32E 03	1.12E 03	3.81E 02	1.12E 03	3.81E 02	1.75E 02	7.56E 01	5.63E 01	7.45E 00	6.73E -01	2.59E -01	4.99E -02	
11150	0.100E -01	0.00E -01	0.00E -01	0.00E -01	0.00E -01	0.00E -01	0.00E -01	0.00E -01	0.00E -01	0.00E -01	0.00E -01	0.00E -01	6.33E -02	
1190	3.54E 03	1.89E 03	1.89E 03	1.93E 03	1.93E 03	1.76E 02	4.42E 02	2.14E 02	1.41E 02	1.41E 02	1.37E 00	5.49E -01	1.19E -01	
1230	3.34E 03	1.85E 03	1.72E 03	6.89E 02	4.03E 02	1.82E 02	1.29E 02	1.29E 02	1.19E 02	1.19E 02	1.16E 00	6.86E -01	1.67E -01	
1300	3.62E 03	1.87E 03	1.67E 03	6.43E 02	3.83E 02	1.98E 02	1.23E 02	1.23E 02	1.23E 02	1.23E 02	1.73E 00	8.06E -01	2.20E -01	
1330	3.38E 03	1.68E 03	1.67E 03	6.15E 02	3.72E 02	1.62E 02	1.84E 02	1.37E 02	1.37E 02	1.37E 02	1.29E 01	1.86E 00	8.33E -01	
1400	4.25E 03	2.54E 03	2.54E 03	2.30E 03	8.17E 02	4.68E 02	2.16E 02	1.53E 02	1.22E 02	1.22E 02	1.22E 01	1.58E 00	6.84E -01	
1450	4.80E 03	2.54E 03	2.19E 03	7.82E 02	3.85E 02	1.71E 02	1.09E 02	1.09E 02	8.96E 00	8.96E 00	8.95E 00	9.83E 01	3.89E -01	
1500	2.88E 03	1.56E 03	1.25E 03	4.05E 02	2.05E 02	1.30E 02	6.21E 00	5.88E -01	7.61E -02					
1530	2.73E 03	1.51E 03	9.35E 02	6.03E 02	1.20E 02	1.05E 02	7.01E 01	4.94E 01	8.41E 00	8.41E 00	8.41E 00	4.34E -01	8.89E -02	
1600	2.40E 03	1.15E 03	6.04E 02	1.93E 02	1.93E 02	1.37E 01	4.93E 01	2.68E 01	6.70E 00	6.70E 00	6.70E 00	8.51E 01	4.95E -02	
1700	2.31E 03	1.21E 03	9.43E 02	9.82E 02	3.13E 02	1.30E 02	5.88E 01	3.98E 01	5.76E 00	5.76E 00	5.76E 00	6.84E -01	6.95E -02	
1730	2.39E 03	1.32E 03	9.82E 02	8.13E 02	1.31E 02	6.41E 01	4.32E 01	5.51E 00	5.51E 00	5.51E 00	5.51E 00	5.84E -01	3.30E -02	
1800	2.09E 03	1.08E 03	7.14E 02	2.34E 02	1.16E 02	1.19E 01	4.69E 01	5.70E 00	5.70E 00	5.70E 00	5.70E 00	5.96E -01	2.82E -02	
1830	1.45E 03	5.44E 02	5.44E 02	5.83E 02	2.17E 02	1.75E 01	9.15E 01	5.70E 01	5.70E 01	5.70E 01	5.70E 01	5.17E 00	1.55E -01	
1900	1.60E 03	7.40E 02	5.83E 02	5.83E 02	2.17E 02	1.75E 01	5.28E 01	5.28E 01	6.97E 00	6.97E 00	6.97E 00	5.44E -01	1.49E -01	
1930	1.11E 03	5.25E 02	3.90E 02	1.93E 02	1.93E 02	1.37E 01	4.93E 01	2.68E 01	6.70E 00	6.70E 00	6.70E 00	5.44E -01	1.49E -02	
2000	1.45E 03	6.90E 02	5.36E 02	9.43E 02	3.82E 02	1.30E 02	5.48E 01	3.98E 01	5.76E 00	5.76E 00	5.76E 00	6.06E -01	2.66E -02	
2030	1.80E 03	8.90E 02	7.00E 02	2.03E 02	1.30E 02	6.41E 01	4.91E 01	5.15E 00	3.89E -02					
2100	2.45E 03	1.25E 03	1.01E 03	2.94E 02	2.94E 02	1.37E 02	5.68E 01	2.91E 01	4.10E 00	4.10E 00	4.10E 00	4.63E -01	1.53E -01	
2130	1.64E 03	8.01E 02	5.44E 02	4.42E 02	2.13E 02	1.75E 01	3.91E 01	1.60E 01	3.72E 00	3.72E 00	3.72E 00	4.32E -01	1.48E -01	
2200	1.99E 03	8.85E 02	5.12E 02	1.22E 02	1.22E 02	1.34E 01	7.14E 01	5.28E 01	3.98E 00	3.98E 00	3.98E 00	4.74E -01	1.71E -01	
2230	1.02E 03	4.34E 02	2.13E 02	8.62E 01	4.23E 01	2.00E 01	1.38E 01	1.38E 01	4.51E 00	4.51E 00	4.51E 00	5.84E -01	4.70E -02	
2300	1.90E 03	9.51E 02	8.21E 02	8.28E 02	2.13E 02	9.55E 01	4.91E 01	2.45E 01	4.96E 00	4.96E 00	4.96E 00	5.74E -01	4.48E -02	
2330	2.05E 03	1.08E 03	1.08E 03	8.28E 02	2.13E 02	9.55E 01	4.91E 01	2.45E 01	4.96E 00	4.96E 00	4.96E 00	5.28E -01	4.89E -02	
79	124	9	2.26E 03	9.77E 02	6.67E 02	1.81E 02	8.28E 01	4.73E 01	2.50E 01	5.77E 00	5.77E 00	5.77E 00	7.72E -01	2.94E -01
79	123	900	1.46E 03	1.46E 03	1.46E 03	1.46E 02	1.46E 02	1.46E 02	7.11E 01	4.45E 01	4.45E 01	3.74E 01	8.49E -01	
109	3.45E 03	2.05E 03	1.80E 03	1.80E 03	1.80E 02	1.44E 02	1.44E 02	1.44E 02	7.82E 01	6.12E 01	6.12E 01	9.33E 01	7.16E -02	
130	3.51E 03	1.96E 03	1.72E 03	1.72E 03	1.72E 02	1.47E 02	1.47E 02	1.47E 02	8.19E 01	6.87E 01	6.87E 01	9.19E 01	8.05E -02	
2000	2.16E 03	1.99E 03	1.72E 03	1.72E 03	1.72E 02	1.58E 02	1.58E 02	1.58E 02	7.87E 01	6.67E 01	6.67E 01	8.86E 01	7.92E -02	
2300	2.15E 03	1.94E 03	1.68E 03	1.68E 03	1.68E 02	1.53E 02	1.53E 02	1.53E 02	8.04E 01	6.36E 01	6.36E 01	7.94E 01	8.14E -02	
2700	2.64E 03	1.48E 03	1.35E 03	1.35E 03	1.35E 02	1.25E 02	1.25E 02	1.25E 02	7.64E 01	5.38E 01	5.38E 01	9.18E 01	9.18E -02	
4000	2.13E 03	1.45E 03	1.19E 03	1.19E 03	1.19E 02	1.16E 02	1.16E 02	1.16E 02	7.59E 01	5.16E 01	5.16E 01	9.06E 01	1.01E -01	
4300	2.12E 03	1.32E 03	1.32E 03	1.32E 03	1.32E 02	1.16E 02	1.16E 02	1.16E 02	7.58E 01	5.14E 01	5.14E 01	9.06E 01	1.01E -01	
5000	2.12E 03	1.19E 03	1.05E 03	1.05E 03	1.05E 02	1.02E 02	1.02E 02	1.02E 02	7.57E 01	5.05E 01	5.05E 01	9.06E 01	1.01E -01	
5300	2.12E 03	1.19E 03	9.78E 02	9.78E 02	9.78E 02	1.02E 02	1.02E 02	1.02E 02	7.56E 01	5.05E 01	5.05E 01	9.06E 01	1.01E -01	
6000	2.12E 03	1.35E 03	1.17E 03	1.17E 03	1.17E 02	1.33E 02	1.33E 02	1.33E 02	7.55E 01	5.05E 01	5.05E 01	9.06E 01	1.01E -01	

## NRL REPORT 8618

PROGRAM A43NPL : PERSONAL DISTRIBUTION TABULATION  
NFL:1532 ON SNI  
PHENOM --- 0.15 0.17 0.19 0.22 0.25 0.29 0.33 1.23 2.18 3.12 4.08

79	124	730	2.35E-03	1.78E-03	1.71E-03	1.66E-02	3.19E-02	2.72E-02	1.12E-02	7.85E-09	7.53E-01	3.33E-01	7.50E-02
	700	2.59E-03	1.55E-03	1.42E-03	6.00E-02	3.63E-02	1.88E-02	1.11E-02	8.26E-09	8.58E-01	4.00E-01	8.16E-02	
730	3.93E-03	1.86E-03	1.74E-03	6.72E-02	4.06E-02	2.21E-02	1.74E-02	7.38E-09	6.98E-01	2.65E-01	5.79E-02		
800	3.66E-03	1.90E-03	1.84E-03	7.72E-02	4.62E-02	2.45E-02	1.41E-02	8.00E-09	7.15E-01	3.01E-01	7.10E-02		
830	3.16E-03	1.68E-03	1.79E-03	7.39E-02	4.45E-02	2.43E-02	1.53E-02	7.92E-09	7.19E-01	2.95E-01	7.36E-02		
900	2.90E-03	1.71E-03	1.82E-03	7.55E-02	4.71E-02	2.53E-02	1.65E-02	6.90E-09	5.72E-01	1.95E-01	4.08E-02		
930	3.32E-03	1.93E-03	1.94E-03	2.09E-03	9.06E-02	6.00E-02	2.02E-02	7.54E-09	5.65E-01	1.97E-01	4.00E-02		
79	127	1230	5.14E-02	1.66E-02	1.33E-02	6.72E-01	4.67E-01	2.92E-01	3.22E-01	8.76E-01	1.34E-00	4.10E-01	7.73E-02
	1300	6.16E-02	2.08E-02	1.50E-02	7.09E-01	4.91E-01	3.95E-01	4.95E-01	9.16E-01	1.45E-00	4.02E-01	7.45E-02	
1330	5.73E-02	1.69E-02	1.58E-02	7.09E-01	5.26E-01	3.13E-01	2.55E-01	8.12E-01	1.28E-00	3.22E-01	6.10E-01	6.10E-02	
1400	4.95E-02	1.70E-02	1.45E-02	6.06E-01	5.30E-01	3.75E-01	3.05E-01	6.03E-01	1.27E-00	3.48E-01	6.56E-01		
1450	4.10E-02	1.94E-02	1.42E-02	8.13E-01	4.78E-01	3.23E-01	3.52E-01	8.35E-01	8.13E-00	3.33E-01	6.55E-01		
1500	4.35E-02	1.51E-02	1.19E-02	5.51E-01	3.71E-01	2.35E-01	2.53E-01	7.23E-01	7.23E-00	1.15E-01	3.15E-02		
1550	3.89E-02	1.35E-02	1.05E-02	5.13E-01	3.65E-01	2.42E-01	2.08E-01	5.55E-01	5.55E-00	8.49E-01	2.45E-01	4.31E-02	
1600	4.46E-02	1.41E-02	1.41E-02	2.38E-01	5.09E-01	2.38E-01	2.22E-01	8.45E-01	8.65E-01	5.85E-01	1.21E-01	4.18E-02	
1630	4.83E-02	2.05E-02	1.31E-02	6.84E-01	4.72E-01	3.88E-01	3.88E-01	1.60E-01	6.25E-01	9.65E-01	2.23E-01	4.04E-02	
1700	5.44E-02	1.88E-02	1.61E-02	6.06E-01	4.51E-01	4.40E-01	2.14E-01	6.30E-01	9.78E-01	2.33E-01	4.32E-02		
1730	6.45E-02	2.12E-02	1.66E-02	6.67E-01	4.39E-01	2.67E-01	2.45E-01	6.45E-01	9.78E-01	2.44E-01	4.34E-02		
1800	5.44E-02	2.08E-02	1.32E-02	6.84E-01	3.31E-01	2.50E-01	3.11E-01	5.71E-01	8.74E-01	1.98E-01	3.75E-02		
1830	5.45E-02	2.09E-02	1.43E-02	5.93E-01	4.38E-01	1.97E-01	3.00E-01	6.10E-01	8.72E-01	2.85E-01	5.46E-02		
1900	5.09E-02	1.51E-02	1.52E-02	6.24E-01	4.34E-01	2.35E-01	2.35E-01	7.04E-01	8.70E-01	3.10E-01	6.82E-02		
1930	3.87E-02	1.25E-02	9.54E-02	5.87E-01	3.57E-01	2.27E-01	2.24E-01	6.17E-01	8.78E-01	2.67E-01	5.15E-02		
2000	3.52E-02	1.05E-02	8.46E-02	4.30E-01	1.94E-01	1.35E-01	1.64E-01	4.75E-01	5.61E-01	1.57E-01	3.15E-02		
79	128	930	2.79E-02	1.16E-02	9.99E-02	3.82E-01	2.05E-01	1.45E-01	1.03E-01	3.76E-01	4.52E-01	1.04E-01	1.5KE-02
	1000	2.56E-02	1.28E-02	1.03E-02	9.38E-01	4.42E-01	2.06E-01	1.29E-01	3.70E-01	4.05E-01	1.09E-01	1.75E-02	
1030	3.64E-02	1.34E-02	1.09E-02	4.60E-01	1.09E-01	1.93E-01	2.02E-01	3.62E-01	5.37E-01	5.05E-01	1.05E-01		
1100	4.04E-02	1.59E-02	1.23E-02	4.60E-01	3.48E-01	2.35E-01	2.44E-01	3.69E-01	5.36E-01	5.36E-01	1.12E-01		
1130	4.37E-02	1.49E-02	1.49E-02	5.74E-01	3.98E-01	2.42E-01	1.84E-01	4.20E-01	7.20E-01	7.40E-01	1.42E-01		
1200	5.09E-02	1.95E-02	1.91E-02	6.84E-01	4.91E-01	2.62E-01	2.65E-01	4.82E-01	7.42E-01	7.42E-01	1.42E-01		
1230	6.37E-02	1.42E-02	1.83E-02	8.13E-01	5.18E-01	3.88E-01	2.71E-01	5.19E-01	7.47E-01	7.47E-01	1.42E-01		
1260	6.17E-02	2.08E-02	1.81E-02	7.75E-01	5.25E-01	3.11E-01	4.34E-01	5.19E-01	7.49E-01	7.49E-01	1.42E-01		
1270	5.21E-02	2.16E-02	2.09E-02	6.59E-01	6.59E-01	2.09E-01	2.09E-01	6.10E-01	6.10E-01	6.10E-01	6.10E-01		
1300	1.74E-02	3.49E-02	3.69E-02	8.74E-01	5.74E-01	4.74E-01	4.74E-01	6.43E-01	6.43E-01	6.43E-01	6.43E-01		
1330	1.81E-02	3.11E-02	3.11E-02	6.11E-01	6.11E-01	3.11E-01	3.11E-01	6.11E-01	6.11E-01	6.11E-01	6.11E-01		
1360	1.04E-02	1.92E-02	1.92E-02	6.81E-01	6.81E-01	1.92E-01	1.92E-01	6.81E-01	6.81E-01	6.81E-01	6.81E-01		
1390	1.15E-02	2.14E-02	2.14E-02	7.13E-01	7.13E-01	2.14E-01	2.14E-01	7.13E-01	7.13E-01	7.13E-01	7.13E-01		
1400	1.15E-02	1.74E-02	1.74E-02	7.04E-01	7.04E-01	1.74E-01	1.74E-01	7.04E-01	7.04E-01	7.04E-01	7.04E-01		
1430	1.14E-02	4.23E-02	4.23E-02	5.95E-01	5.95E-01	1.45E-01	1.45E-01	5.95E-01	5.95E-01	5.95E-01	5.95E-01		
1460	1.14E-02	4.14E-02	4.14E-02	5.96E-01	5.96E-01	1.46E-01	1.46E-01	5.96E-01	5.96E-01	5.96E-01	5.96E-01		
1490	1.14E-02	4.14E-02	4.14E-02	5.96E-01	5.96E-01	1.46E-01	1.46E-01	5.96E-01	5.96E-01	5.96E-01	5.96E-01		
1520	1.14E-02	4.14E-02	4.14E-02	5.96E-01	5.96E-01	1.46E-01	1.46E-01	5.96E-01	5.96E-01	5.96E-01	5.96E-01		
1550	1.14E-02	4.14E-02	4.14E-02	5.96E-01	5.96E-01	1.46E-01	1.46E-01	5.96E-01	5.96E-01	5.96E-01	5.96E-01		
1580	1.14E-02	4.14E-02	4.14E-02	5.96E-01	5.96E-01	1.46E-01	1.46E-01	5.96E-01	5.96E-01	5.96E-01	5.96E-01		
1610	1.14E-02	4.14E-02	4.14E-02	5.96E-01	5.96E-01	1.46E-01	1.46E-01	5.96E-01	5.96E-01	5.96E-01	5.96E-01		
1640	1.14E-02	4.14E-02	4.14E-02	5.96E-01	5.96E-01	1.46E-01	1.46E-01	5.96E-01	5.96E-01	5.96E-01	5.96E-01		
1670	1.14E-02	4.14E-02	4.14E-02	5.96E-01	5.96E-01	1.46E-01	1.46E-01	5.96E-01	5.96E-01	5.96E-01	5.96E-01		
1700	1.14E-02	4.14E-02	4.14E-02	5.96E-01	5.96E-01	1.46E-01	1.46E-01	5.96E-01	5.96E-01	5.96E-01	5.96E-01		
1730	1.14E-02	4.14E-02	4.14E-02	5.96E-01	5.96E-01	1.46E-01	1.46E-01	5.96E-01	5.96E-01	5.96E-01	5.96E-01		
1760	1.14E-02	4.14E-02	4.14E-02	5.96E-01	5.96E-01	1.46E-01	1.46E-01	5.96E-01	5.96E-01	5.96E-01	5.96E-01		
1790	1.14E-02	4.14E-02	4.14E-02	5.96E-01	5.96E-01	1.46E-01	1.46E-01	5.96E-01	5.96E-01	5.96E-01	5.96E-01		
1820	1.14E-02	4.14E-02	4.14E-02	5.96E-01	5.96E-01	1.46E-01	1.46E-01	5.96E-01	5.96E-01	5.96E-01	5.96E-01		
1850	1.14E-02	4.14E-02	4.14E-02	5.96E-01	5.96E-01	1.46E-01	1.46E-01	5.96E-01	5.96E-01	5.96E-01	5.96E-01		
1880	1.14E-02	4.14E-02	4.14E-02	5.96E-01	5.96E-01	1.46E-01	1.46E-01	5.96E-01	5.96E-01	5.96E-01	5.96E-01		
1910	1.14E-02	4.14E-02	4.14E-02	5.96E-01	5.96E-01	1.46E-01	1.46E-01	5.96E-01	5.96E-01	5.96E-01	5.96E-01		
1940	1.14E-02	4.14E-02	4.14E-02	5.96E-01	5.96E-01	1.46E-01	1.46E-01	5.96E-01	5.96E-01	5.96E-01	5.96E-01		
1970	1.14E-02	4.14E-02	4.14E-02	5.96E-01	5.96E-01	1.46E-01	1.46E-01	5.96E-01	5.96E-01	5.96E-01	5.96E-01		
2000	1.14E-02	4.14E-02	4.14E-02	5.96E-01	5.96E-01	1.46E-01	1.46E-01	5.96E-01	5.96E-01	5.96E-01	5.96E-01		
2030	1.14E-02	4.14E-02	4.14E-02	5.96E-01	5.96E-01	1.46E-01	1.46E-01	5.96E-01	5.96E-01	5.96E-01	5.96E-01		
2060	1.14E-02	4.14E-02	4.14E-02	5.96E-01	5.96E-01	1.46E-01	1.46E-01	5.96E-01	5.96E-01	5.96E-01	5.96E-01		
2090	1.14E-02	4.14E-02	4.14E-02	5.96E-01	5.96E-01	1.46E-01	1.46E-01	5.96E-01	5.96E-01	5.96E-01	5.96E-01		
2120	1.14E-02	4.14E-02	4.14E-02	5.96E-01	5.96E-01	1.46E-01	1.46E-01	5.96E-01	5.96E-01	5.96E-01	5.96E-01		
2150	1.14E-02	4.14E-02	4.14E-02	5.96E-01	5.96E-01	1.46E-01	1.46E-01	5.96E-01	5.96E-01	5.96E-01	5.96E-01		
2180	1.14E-02	4.14E-02	4.14E-02	5.96E-01	5.96E-01	1.46E-01	1.46E-01	5.96E-01	5.96E-01	5.96E-01	5.96E-01		
2210	1.14E-02	4.14E-02	4.14E-02	5.96E-01	5.96E-01	1.46E-01	1.46E-01	5.96E-01	5.96E-01	5.96E-01	5.96E-01		
2240	1.14E-02	4.14E-02	4.14E-02	5.96E-01	5.96E-01	1.46E-01	1.46E-01	5.96E-01	5.96E-01	5.96E-01	5.96E-01		
2270	1.14E-02												

Table A2 (Continued)  
 PROGRAM H49NL: AEROSOL DISTRIBUTION TABULATION  
 (PROCESSED ON 08-MAR-82)

NPL:5532 DN SHI Radius	0.15	0.17	0.19	0.22	0.25	0.29	0.33	1.23	2.18	3.12	4.08
79 128 1800	1.44E 03	4.58E 02	4.48E 02	2.15E 02	1.56E 02	1.06E 02	9.06E 01	1.16E 01	2.05E 00	4.22E 01	1.04E-01
79 129 630	1.45E 03	4.85E 02	3.95E 02	2.05E 02	1.39E 02	1.05E 02	1.05E 02	1.78E 01	2.61E 00	5.41E-01	1.02E-01
79 129 1000	1.42E 03	4.74E 02	4.17E 02	1.96E 02	1.30E 02	9.19E 01	8.26E 01	1.76E 01	2.34E 00	5.52E-01	1.04E-01
79 129 1700	1.20E 03	4.47E 02	3.42E 02	1.72E 02	1.26E 02	8.32E 01	9.11E 01	1.70E 01	2.36E 00	9.61E-02	1.91E-02
79 129 2800	1.14E 03	4.14E 02	3.67E 02	1.66E 02	1.10E 02	8.29E 01	7.15E 01	1.64E 01	2.24E 00	5.27E-01	9.51E-02
79 129 4800	1.04E 03	3.91E 02	3.28E 02	1.55E 02	1.26E 02	8.37E 01	7.66E 01	1.61E 01	2.16E 00	5.07E-01	8.96E-02
79 129 8600	1.16E 03	4.21E 02	3.77E 02	1.42E 02	1.14E 02	1.45E 02	1.40E 02	7.77E 01	1.70E 01	2.30E 00	5.68E-01
79 129 9300	1.11E 03	3.39E 02	5.08E 02	1.08E 02	6.20E 02	6.20E 02	6.20E 02	7.17E 01	1.64E 01	2.13E 00	5.89E-01
79 129 10400	9.01E 02	3.18E 02	2.43E 02	1.18E 02	9.16E 01	5.29E 01	5.56E 01	5.51E 01	1.38E 00	5.51E 01	9.60E-02
79 129 10300	8.93E 02	3.39E 02	2.52E 02	9.73E 01	5.80E 01	5.80E 01	5.80E 01	7.12E 01	1.46E 01	2.12E 00	5.12E-01
79 129 11000	1.96E 03	3.33E 02	3.01E 02	1.41E 02	1.22E 02	7.94E 01	7.19E 01	1.45E 01	1.98E 00	4.97E-01	8.80E-02
79 129 11100	1.19E 03	3.66E 02	2.89E 02	1.21E 02	1.02E 02	6.50E 01	5.83E 01	1.50E 01	1.88E 00	5.36E-01	9.37E-02
79 129 12000	1.17E 03	3.38E 02	3.43E 02	1.60E 02	1.43E 02	8.34E 01	7.43E 01	1.62E 01	2.22E 00	5.68E-01	1.01E-01
79 129 12500	1.26E 03	4.17E 02	2.95E 02	1.54E 02	1.13E 02	8.34E 01	7.75E 01	1.75E 01	2.29E 00	6.07E-01	1.05E-01
79 129 13000	1.27E 03	4.34E 02	3.25E 02	1.34E 02	1.18E 02	8.39E 01	7.15E 01	1.71E 01	2.12E 00	6.03E-01	1.05E-01
79 129 13300	1.15E 03	4.02E 02	3.12E 02	1.19E 02	1.02E 02	6.95E 01	7.91E 01	1.52E 01	2.02E 00	4.86E-01	8.72E-02
79 129 14000	1.14E 03	4.22E 02	3.40E 02	1.56E 02	1.12E 02	8.64E 01	8.44E 01	1.60E 01	2.17E 00	5.31E 01	9.29E-02
79 129 14300	1.25E 03	4.78E 02	3.46E 02	1.65E 02	1.27E 02	8.67E 01	7.75E 01	1.68E 01	2.15E 00	5.57E 01	9.99E-02
79 129 15000	1.22E 03	4.51E 02	3.95E 02	1.57E 02	1.08E 02	7.64E 01	6.48E 01	1.62E 01	2.24E 00	5.97E-01	1.06E-01
79 129 15300	1.23E 03	4.43E 02	3.99E 02	1.47E 02	1.08E 02	7.27E 01	6.51E 01	1.59E 01	2.26E 00	5.87E-01	1.05E-01
79 129 16000	1.24E 03	3.88E 02	3.44E 02	1.35E 02	1.06E 02	7.35E 01	6.33E 01	1.56E 01	2.19E 00	5.76E-01	1.05E-01
79 129 16300	1.16E 03	4.02E 02	3.12E 02	1.19E 02	1.01E 02	7.16E 01	6.62E 01	1.46E 01	2.10E 00	5.38E-01	1.02E-01
79 129 17000	1.14E 03	4.22E 02	3.40E 02	1.56E 02	1.12E 02	8.64E 01	8.44E 01	1.60E 01	2.17E 00	5.31E 01	9.83E-02
79 129 17300	1.25E 03	4.78E 02	3.46E 02	1.65E 02	1.27E 02	8.67E 01	7.75E 01	1.68E 01	2.15E 00	5.57E 01	9.99E-02
79 129 18000	1.22E 03	4.51E 02	3.95E 02	1.57E 02	1.08E 02	7.64E 01	6.48E 01	1.62E 01	2.24E 00	5.97E-01	1.06E-01
79 129 18300	1.01E 03	3.45E 02	2.60E 02	1.47E 02	1.08E 02	7.41E 01	6.50E 01	1.47E 01	2.26E 00	5.87E-01	1.05E-01
79 129 18600	9.27E 02	3.21E 02	2.91E 02	1.50E 02	1.12E 02	7.94E 01	6.22E 01	1.40E 01	2.00E 00	4.73E-01	8.53E-02
79 129 19300	9.49E 02	3.39E 02	2.60E 02	1.31E 02	1.05E 02	8.35E 01	6.54E 01	1.45E 01	2.03E 00	3.31E-01	9.45E-02
79 129 20000	1.04E 03	3.19E 02	2.41E 02	1.16E 02	9.54E 01	6.94E 01	6.08E 01	1.52E 01	2.09E 00	5.73E-01	9.97E-02
79 129 20300	1.02E 03	3.48E 02	2.80E 02	1.44E 02	1.03E 02	7.76E 01	6.77E 01	1.64E 01	2.4E 00	6.01E-01	1.02E-01
79 130 500	3.23E 03	6.46E 02	3.92E 02	2.05E 02	1.11E 02	7.64E 01	6.15E 01	2.60E 01	3.28E 00	1.60E 00	4.27E-01
79 130 670	3.45F 03	6.47E 02	3.93E 02	2.06E 02	1.12E 02	7.30E 01	6.27E 01	2.61E 01	3.60E 00	1.81E 00	5.23E-01
79 130 1000	1.14E 03	4.14E 02	3.12E 02	1.32E 02	1.04E 02	7.13E 01	6.11E 01	2.53E 01	3.51E 00	1.79E 00	4.74E-01
79 130 1400	1.14E 03	4.14E 02	3.12E 02	1.32E 02	1.04E 02	7.13E 01	6.11E 01	2.53E 01	3.51E 00	1.79E 00	4.74E-01
79 130 1500	1.14E 03	4.14E 02	3.12E 02	1.32E 02	1.04E 02	7.13E 01	6.11E 01	2.53E 01	3.51E 00	1.79E 00	4.74E-01
79 130 1700	1.14E 03	4.14E 02	3.12E 02	1.32E 02	1.04E 02	7.13E 01	6.11E 01	2.53E 01	3.51E 00	1.79E 00	4.74E-01
79 130 1800	1.14E 03	4.14E 02	3.12E 02	1.32E 02	1.04E 02	7.13E 01	6.11E 01	2.53E 01	3.51E 00	1.79E 00	4.74E-01
79 130 1900	1.14E 03	4.14E 02	3.12E 02	1.32E 02	1.04E 02	7.13E 01	6.11E 01	2.53E 01	3.51E 00	1.79E 00	4.74E-01
79 130 2000	1.14E 03	4.14E 02	3.12E 02	1.32E 02	1.04E 02	7.13E 01	6.11E 01	2.53E 01	3.51E 00	1.79E 00	4.74E-01
79 130 20300	1.14E 03	4.14E 02	3.12E 02	1.32E 02	1.04E 02	7.13E 01	6.11E 01	2.53E 01	3.51E 00	1.79E 00	4.74E-01
79 130 20400	1.14E 03	4.14E 02	3.12E 02	1.32E 02	1.04E 02	7.13E 01	6.11E 01	2.53E 01	3.51E 00	1.79E 00	4.74E-01
79 130 20500	1.14E 03	4.14E 02	3.12E 02	1.32E 02	1.04E 02	7.13E 01	6.11E 01	2.53E 01	3.51E 00	1.79E 00	4.74E-01
79 130 20600	1.14E 03	4.14E 02	3.12E 02	1.32E 02	1.04E 02	7.13E 01	6.11E 01	2.53E 01	3.51E 00	1.79E 00	4.74E-01
79 130 20700	1.14E 03	4.14E 02	3.12E 02	1.32E 02	1.04E 02	7.13E 01	6.11E 01	2.53E 01	3.51E 00	1.79E 00	4.74E-01
79 130 20800	1.14E 03	4.14E 02	3.12E 02	1.32E 02	1.04E 02	7.13E 01	6.11E 01	2.53E 01	3.51E 00	1.79E 00	4.74E-01
79 130 20900	1.14E 03	4.14E 02	3.12E 02	1.32E 02	1.04E 02	7.13E 01	6.11E 01	2.53E 01	3.51E 00	1.79E 00	4.74E-01
79 130 21000	1.14E 03	4.14E 02	3.12E 02	1.32E 02	1.04E 02	7.13E 01	6.11E 01	2.53E 01	3.51E 00	1.79E 00	4.74E-01
79 130 21100	1.14E 03	4.14E 02	3.12E 02	1.32E 02	1.04E 02	7.13E 01	6.11E 01	2.53E 01	3.51E 00	1.79E 00	4.74E-01
79 130 21200	1.14E 03	4.14E 02	3.12E 02	1.32E 02	1.04E 02	7.13E 01	6.11E 01	2.53E 01	3.51E 00	1.79E 00	4.74E-01
79 130 21300	1.14E 03	4.14E 02	3.12E 02	1.32E 02	1.04E 02	7.13E 01	6.11E 01	2.53E 01	3.51E 00	1.79E 00	4.74E-01
79 130 21400	1.14E 03	4.14E 02	3.12E 02	1.32E 02	1.04E 02	7.13E 01	6.11E 01	2.53E 01	3.51E 00	1.79E 00	4.74E-01
79 130 21500	1.14E 03	4.14E 02	3.12E 02	1.32E 02	1.04E 02	7.13E 01	6.11E 01	2.53E 01	3.51E 00	1.79E 00	4.74E-01
79 130 21600	1.14E 03	4.14E 02	3.12E 02	1.32E 02	1.04E 02	7.13E 01	6.11E 01	2.53E 01	3.51E 00	1.79E 00	4.74E-01
79 130 21700	1.14E 03	4.14E 02	3.12E 02	1.32E 02	1.04E 02	7.13E 01	6.11E 01	2.53E 01	3.51E 00	1.79E 00	4.74E-01
79 130 21800	1.14E 03	4.14E 02	3.12E 02	1.32E 02	1.04E 02	7.13E 01	6.11E 01	2.53E 01	3.51E 00	1.79E 00	4.74E-01
79 130 21900	1.14E 03	4.14E 02	3.12E 02	1.32E 02	1.04E 02	7.13E 01	6.11E 01	2.53E 01	3.51E 00	1.79E 00	4.74E-01
79 130 22000	1.14E 03	4.14E 02	3.12E 02	1.32E 02	1.04E 02	7.13E 01	6.11E 01	2.53E 01	3.51E 00	1.79E 00	4.74E-01
79 130 22100	1.14E 03	4.14E 02	3.12E 02	1.32E 02	1.04E 02	7.13E 01	6.11E 01	2.53E 01	3.51E 00	1.79E 00	4.74E-01
79 130 22200	1.14E 03	4.14E 02	3.12E 02	1.32E 02	1.04E 02	7.13E 01	6.11E 01	2.53E 01	3.51E 00	1.79E 00	4.74E-01
79 130 22300	1.14E 03	4.14E 02	3.12E 02	1.32E 02	1.04E 02	7.13E 01	6.11E 01	2.53E 01	3.51E 00	1.79E 00	4.74E-01
79 130 22400	1.14E 03	4.14E 02	3.12E 02	1.32E 02	1.04E 02	7.13E 01	6.11E 01	2.53E 01	3.51E 00	1.79E 00	4.74E-01
79 130 22500	1.14E 03	4.14E 02	3.12E 02	1.32E 02	1.04E 02	7.13E 01	6.11E 01	2.53E 01	3.51E 00	1.79E 00	4.74E-01
79 130 22600	1.14E 03	4.14E 02	3.12E 02	1.32E 02	1.04E 02	7.13E 01	6.11E 01	2.53E 01	3.51E 00	1.79E 00	4.74E-01
79 130 22700	1.14E 03	4.14E 02	3.12E 02	1.32E 02	1.04E 02	7.13E 01	6.11E 01	2.53E 01	3.51E 00	1.79E 00	4.74E-01
79 130 22800	1.14E 03	4.14E 02	3.12E 02	1.32E 02	1.04E 02	7.13E 01	6.11E 01	2.53E 01	3.51E 00	1.79E 00	4.74E-01
79 130 22900	1.14E 03										

Table A2 (Continued)  
(PROCESSED ON 08-MAR-82)

PROGRAM A49NPL : AEROSOL DISTRIBUTION TABULATION		NRL:6532 OH SNI RADIUS ---										
		5.93	5.97	6.93	7.88	8.83	9.78	10.73	11.68	12.63	13.58	14.53
79	114	2.20E-02	1.98E-02	5.99E-03	2.98E-03	3.02E-03	1.84E-03	1.62E-03	9.55E-04	5.73E-04	3.58E-04	3.34E-04
	2300	9.19E-03	5.90E-03	2.78E-03	2.65E-03	1.50E-03	1.55E-03	6.68E-04	5.48E-04	6.21E-04	3.18E-04	2.63E-04
	2300	8.43E-03	5.66E-03	2.74E-03	3.01E-03	1.50E-03	1.56E-03	8.35E-04	4.97E-04	3.10E-04	3.82E-04	3.82E-04
	2300	8.93E-03	6.06E-03	2.91E-03	3.02E-03	1.79E-03	1.65E-03	1.22E-03	8.83E-04	4.54E-04	4.54E-04	4.06E-04
79	115	0	8.31E-03	5.54E-03	3.01E-03	3.01E-03	1.74E-03	1.84E-03	1.10E-03	5.25E-04	2.63E-04	4.54E-04
	30	9.00E-03	6.73E-03	2.82E-03	3.70E-03	2.74E-03	1.75E-03	1.74E-03	1.07E-03	4.54E-04	5.73E-04	3.34E-04
	100	9.21E-03	6.39E-03	2.74E-03	3.18E-03	1.62E-03	1.50E-03	9.79E-04	6.68E-04	7.16E-04	5.01E-04	4.06E-04
	130	8.59E-03	5.51E-03	2.39E-03	2.79E-03	1.38E-03	1.36E-03	8.59E-04	6.92E-04	4.30E-04	4.54E-04	7.16E-05
	200	1.23E-02	6.87E-03	4.20E-03	3.28E-03	2.29E-03	2.48E-03	1.56E-03	1.17E-03	8.83E-04	6.44E-04	4.49E-04
	230	1.20E-02	6.74E-03	3.63E-03	3.18E-03	3.98E-03	2.48E-03	1.63E-03	1.43E-03	7.48E-04	7.64E-04	4.79E-04
	300	1.24E-02	7.71E-03	3.94E-03	3.10E-03	2.65E-03	1.58E-03	1.58E-03	1.86E-03	1.07E-03	8.59E-04	5.25E-04
	330	1.28E-02	6.92E-03	4.08E-03	3.96E-03	2.26E-03	1.55E-03	1.48E-03	1.48E-03	9.75E-04	5.97E-04	6.44E-04
	390	1.51E-02	8.66E-03	5.32E-03	4.11E-03	2.55E-03	2.55E-03	2.26E-03	2.67E-03	1.12E-03	7.40E-04	6.66E-04
	430	1.64E-02	9.00E-03	5.13E-03	3.72E-03	3.72E-03	2.82E-03	1.67E-03	1.69E-03	1.15E-03	8.59E-04	4.38E-04
	500	1.80E-02	8.64E-03	6.33E-03	4.66E-03	4.66E-03	4.18E-03	1.74E-03	1.74E-03	1.12E-03	9.20E-04	5.63E-04
	530	1.71E-02	8.43E-03	7.66E-03	3.29E-03	3.84E-03	1.88E-03	1.72E-03	6.92E-03	1.05E-03	1.15E-03	5.45E-04
	600	2.44E-02	1.06E-02	1.00E-02	5.11E-03	5.01E-03	2.82E-03	2.27E-03	2.27E-03	1.50E-03	1.12E-03	3.82E-04
	630	2.05E-02	8.39E-03	6.54E-03	6.39E-03	6.39E-03	6.13E-03	6.13E-03	6.49E-03	1.08E-03	7.49E-04	4.77E-04
	700	2.82E-02	1.38E-02	1.01E-02	4.62E-03	4.62E-03	3.49E-03	3.49E-03	3.49E-03	1.65E-03	1.65E-03	5.49E-04
	730	1.11E-01	6.23E-02	5.26E-02	3.75E-02	3.28E-02	1.99E-02	1.44E-02	1.44E-02	9.52E-03	9.37E-03	5.97E-04
	800	7.73E-02	4.03E-02	3.85E-02	2.33E-02	2.27E-02	1.33E-02	1.07E-02	1.07E-02	7.39E-03	5.49E-03	3.27E-03
79	116	2.20E-02	8.01E-02	4.49E-02	3.10E-02	2.73E-02	1.08E-02	1.36E-02	6.59E-03	4.22E-03	3.08E-03	9.79E-04
	2300	1.81E-00	2.07E-00	1.69E-00	1.15E-00	1.04E-00	8.00E-01	8.91E-01	8.75E-01	7.47E-01	6.49E-01	6.49E-01
	2300	1.71E-00	1.53E-00	1.21E-00	1.21E-00	1.21E-00	1.14E-00	1.19E-00	1.26E-00	1.11E-00	1.23E-00	1.16E-00
79	117	0	1.50E-00	1.20E-00	6.37E-01	6.65E-01	5.17E-01	5.04E-01	5.28E-01	4.39E-01	4.02E-01	4.96E-01
	30	1.32E-00	1.18E-00	8.92E-01	1.01E-00	7.40E-01	7.40E-01	7.83E-01	7.90E-01	6.25E-01	6.75E-01	5.89E-01
	100	3.70E-00	2.97E-00	1.33E-00	1.90E-00	1.90E-00	1.90E-00	1.13E-01	9.26E-01	7.49E-01	7.02E-01	6.72E-01
	130	6.10E-00	4.72E-00	1.90E-00	1.90E-00	1.90E-00	1.13E-00	1.00E-00	1.02E-00	1.00E-00	7.52E-01	5.98E-01
	200	1.29E-00	9.71E-01	5.21E-01	5.66E-01	3.26E-01	2.98E-01	2.79E-01	1.87E-01	1.55E-01	1.60E-01	1.22E-01
	300	2.58E-01	2.08E-01	9.54E-01	1.01E-00	5.60E-01	4.64E-01	4.64E-01	2.44E-01	2.44E-01	1.94E-01	1.94E-01
	330	1.42E-01	9.81E-02	4.31E-02	4.39E-02	2.54E-02	2.12E-02	2.12E-02	1.42E-02	1.30E-02	1.29E-02	1.10E-02
	390	4.80E-02	3.03E-03	2.32E-03	2.65E-03	1.41E-03	1.55E-03	1.18E-03	1.00E-03	7.64E-04	9.07E-04	6.44E-04
	460	1.82E-02	2.05E-02	1.27E-02	1.83E-02	1.34E-02	1.33E-02	1.48E-02	1.16E-02	1.14E-02	1.22E-02	1.12E-02
	490	3.16E-02	1.93E-01	7.58E-02	9.81E-02	8.09E-02	8.11E-02	8.93E-02	7.65E-02	7.30E-02	7.30E-02	6.71E-02
	530	1.57E-01	1.66E-01	1.25E-01	1.66E-01	1.38E-01	1.31E-01	1.47E-01	1.25E-01	1.16E-01	1.23E-01	1.10E-01
	530	2.19E-01	2.31E-01	1.81E-01	2.10E-01	1.92E-01	1.77E-01	1.77E-01	1.70E-01	1.58E-01	1.62E-01	1.49E-01
	600	2.52E-01	2.59E-01	2.18E-01	2.57E-01	2.33E-01	2.24E-01	2.45E-01	2.15E-01	2.05E-01	2.07E-01	1.91E-01
	630	3.54E-01	3.51E-01	2.78E-01	3.17E-01	2.90E-01	2.98E-01	2.98E-01	2.60E-01	2.41E-01	2.44E-01	2.22E-01
	700	3.64E-01	3.74E-01	2.90E-01	3.40E-01	3.17E-01	2.87E-01	2.99E-01	2.73E-01	2.60E-01	2.72E-01	2.53E-01

Table A2 (Continued)

PROGRAM A4532 ON SN1		REPSONL DISTRIBUTION TABULATION										(PROCESSED ON 08-MAR-82)									
NPL:	RADIUS	5.03	5.97	6.93	7.88	8.83	9.78	10.73	11.68	12.63	13.58	14.53									
79	120	1.000	1.01E-02	5.56E-03	5.39E-03	4.73E-03	3.06E-03	2.79E-03	2.12E-03	1.31E-03	1.27E-03	5.97E-04	5.01E-04								
	1730	1.60E-02	8.65E-03	5.17E-03	5.08E-03	5.10E-03	2.10E-03	1.79E-03	1.69E-03	1.60E-03	8.83E-04	7.88E-04	7.88E-04	7.88E-04	7.88E-04	7.88E-04	7.88E-04	7.88E-04	7.88E-04	7.88E-04	7.88E-04
1800	1.75E-02	8.47E-03	5.31E-03	5.29E-03	5.28E-03	3.14E-03	2.05E-03	2.24E-03	1.65E-03	9.31E-04	7.16E-04	7.16E-04	7.16E-04	7.16E-04	7.16E-04	7.16E-04	7.16E-04	7.16E-04	7.16E-04	7.16E-04	
1830	2.17E-02	9.45E-03	4.79E-03	4.79E-03	4.79E-03	2.01E-03	1.50E-03	2.27E-03	1.72E-03	9.36E-03	9.07E-04	5.19E-04	5.19E-04	5.19E-04	5.19E-04	5.19E-04	5.19E-04	5.19E-04	5.19E-04	5.19E-04	5.19E-04
1900	1.87E-02	8.23E-03	3.07E-03	3.09E-03	3.09E-03	1.68E-03	1.56E-03	2.24E-03	1.74E-03	1.18E-03	8.83E-04	5.73E-04	5.73E-04	5.73E-04	5.73E-04	5.73E-04	5.73E-04	5.73E-04	5.73E-04	5.73E-04	5.73E-04
1930	1.93E-02	8.47E-03	6.56E-03	6.56E-03	6.56E-03	3.68E-03	2.27E-03	2.24E-03	1.74E-03	1.18E-03	8.83E-04	5.73E-04	5.73E-04	5.73E-04	5.73E-04	5.73E-04	5.73E-04	5.73E-04	5.73E-04	5.73E-04	5.73E-04
2000	1.91E-02	6.90E-03	7.47E-03	7.51E-03	7.51E-03	3.59E-03	2.12E-03	2.01E-03	1.74E-03	1.18E-03	7.49E-04	5.73E-04	5.73E-04	5.73E-04	5.73E-04	5.73E-04	5.73E-04	5.73E-04	5.73E-04	5.73E-04	5.73E-04
2030	2.14E-02	8.71E-03	8.71E-03	8.71E-03	8.71E-03	3.65E-03	2.06E-03	2.06E-03	1.74E-03	1.18E-03	8.83E-04	7.40E-04	7.40E-04	7.40E-04	7.40E-04	7.40E-04	7.40E-04	7.40E-04	7.40E-04	7.40E-04	7.40E-04
2100	2.38E-02	8.71E-03	9.07E-03	9.07E-03	9.07E-03	3.75E-03	2.02E-03	2.02E-03	1.74E-03	1.18E-03	8.59E-04	7.95E-04	7.95E-04	7.95E-04	7.95E-04	7.95E-04	7.95E-04	7.95E-04	7.95E-04	7.95E-04	7.95E-04
2130	2.15E-02	7.54E-03	6.56E-03	6.56E-03	6.56E-03	3.06E-03	2.06E-03	2.06E-03	1.74E-03	1.18E-03	6.44E-04	6.44E-04	6.44E-04	6.44E-04	6.44E-04	6.44E-04	6.44E-04	6.44E-04	6.44E-04	6.44E-04	6.44E-04
2200	2.11E-02	6.16E-03	6.16E-03	6.16E-03	6.16E-03	3.89E-03	2.01E-03	2.01E-03	1.74E-03	1.18E-03	6.12E-04	4.30E-04	4.30E-04	4.30E-04	4.30E-04	4.30E-04	4.30E-04	4.30E-04	4.30E-04	4.30E-04	4.30E-04
2230	1.53E-02	5.06E-03	4.96E-03	4.96E-03	4.96E-03	3.15E-03	1.72E-03	1.72E-03	1.74E-03	1.18E-03	6.68E-04	2.86E-04	2.86E-04	2.86E-04	2.86E-04	2.86E-04	2.86E-04	2.86E-04	2.86E-04	2.86E-04	2.86E-04
2300	1.53E-02	4.96E-03	4.96E-03	4.96E-03	4.96E-03	3.15E-03	1.72E-03	1.72E-03	1.74E-03	1.18E-03	6.30E-04	2.86E-04	2.86E-04	2.86E-04	2.86E-04	2.86E-04	2.86E-04	2.86E-04	2.86E-04	2.86E-04	2.86E-04
2330	1.53E-02	4.89E-03	4.89E-03	4.89E-03	4.89E-03	3.15E-03	1.72E-03	1.72E-03	1.74E-03	1.18E-03	6.21E-04	2.86E-04	2.86E-04	2.86E-04	2.86E-04	2.86E-04	2.86E-04	2.86E-04	2.86E-04	2.86E-04	2.86E-04
2360	1.53E-02	4.82E-03	4.82E-03	4.82E-03	4.82E-03	3.15E-03	1.72E-03	1.72E-03	1.74E-03	1.18E-03	6.12E-04	2.86E-04	2.86E-04	2.86E-04	2.86E-04	2.86E-04	2.86E-04	2.86E-04	2.86E-04	2.86E-04	2.86E-04
2390	1.53E-02	4.82E-03	4.82E-03	4.82E-03	4.82E-03	3.15E-03	1.72E-03	1.72E-03	1.74E-03	1.18E-03	6.12E-04	2.86E-04	2.86E-04	2.86E-04	2.86E-04	2.86E-04	2.86E-04	2.86E-04	2.86E-04	2.86E-04	2.86E-04
2400	8.64E-02	5.35E-03	5.35E-03	5.35E-03	5.35E-03	4.03E-03	3.29E-03	3.18E-03	3.18E-03	3.18E-03	2.01E-03	1.29E-03	1.29E-03	1.29E-03	1.29E-03	1.29E-03	1.29E-03	1.29E-03	1.29E-03	1.29E-03	1.29E-03
430	1.56E-02	1.22E-02	5.82E-03	7.23E-03	7.23E-03	4.03E-03	3.29E-03	3.18E-03	3.18E-03	3.18E-03	2.01E-03	1.29E-03	1.29E-03	1.29E-03	1.29E-03	1.29E-03	1.29E-03	1.29E-03	1.29E-03	1.29E-03	1.29E-03
500	3.53E-02	2.02E-02	7.32E-03	7.32E-03	7.32E-03	4.26E-03	3.49E-03	3.49E-03	3.49E-03	3.49E-03	2.12E-03	1.32E-03	1.32E-03	1.32E-03	1.32E-03	1.32E-03	1.32E-03	1.32E-03	1.32E-03	1.32E-03	1.32E-03
530	1.74E-02	1.19E-02	6.02E-03	6.02E-03	6.02E-03	4.49E-03	3.75E-03	3.75E-03	3.75E-03	3.75E-03	2.12E-03	1.32E-03	1.32E-03	1.32E-03	1.32E-03	1.32E-03	1.32E-03	1.32E-03	1.32E-03	1.32E-03	1.32E-03
600	2.26E-02	1.26E-02	4.49E-03	4.49E-03	4.49E-03	4.49E-03	3.75E-03	3.75E-03	3.75E-03	3.75E-03	2.12E-03	1.32E-03	1.32E-03	1.32E-03	1.32E-03	1.32E-03	1.32E-03	1.32E-03	1.32E-03	1.32E-03	1.32E-03
630	1.44E-02	1.28E-02	2.58E-03	2.58E-03	2.58E-03	3.41E-03	2.51E-03	2.51E-03	2.51E-03	2.51E-03	1.52E-03	1.32E-03	1.32E-03	1.32E-03	1.32E-03	1.32E-03	1.32E-03	1.32E-03	1.32E-03	1.32E-03	1.32E-03
700	3.91E-02	1.48E-02	5.41E-03	5.41E-03	5.41E-03	4.01E-03	3.23E-03	3.23E-03	3.23E-03	3.23E-03	2.12E-03	1.32E-03	1.32E-03	1.32E-03	1.32E-03	1.32E-03	1.32E-03	1.32E-03	1.32E-03	1.32E-03	1.32E-03
730	4.03E-02	1.03E-02	1.03E-03	1.03E-03	1.03E-03	4.06E-03	3.23E-03	3.23E-03	3.23E-03	3.23E-03	2.12E-03	1.32E-03	1.32E-03	1.32E-03	1.32E-03	1.32E-03	1.32E-03	1.32E-03	1.32E-03	1.32E-03	1.32E-03
800	4.49E-02	1.49E-02	1.49E-03	1.49E-03	1.49E-03	4.06E-03	3.24E-03	3.24E-03	3.24E-03	3.24E-03	2.12E-03	1.32E-03	1.32E-03	1.32E-03	1.32E-03	1.32E-03	1.32E-03	1.32E-03	1.32E-03	1.32E-03	1.32E-03
830	4.37F-02	1.03E-02	1.03E-03	1.03E-03	1.03E-03	4.06E-03	3.24E-03	3.24E-03	3.24E-03	3.24E-03	2.12E-03	1.32E-03	1.32E-03	1.32E-03	1.32E-03	1.32E-03	1.32E-03	1.32E-03	1.32E-03	1.32E-03	1.32E-03
900	4.37F-02	1.03E-02	1.03E-03	1.03E-03	1.03E-03	4.06E-03	3.24E-03	3.24E-03	3.24E-03	3.24E-03	2.12E-03	1.32E-03	1.32E-03	1.32E-03	1.32E-03	1.32E-03	1.32E-03	1.32E-03	1.32E-03	1.32E-03	1.32E-03
1000	2.16E-02	1.61E-02	1.61E-03	1.61E-03	1.61E-03	4.06E-03	3.24E-03	3.24E-03	3.24E-03	3.24E-03	2.12E-03	1.32E-03	1.32E-03	1.32E-03	1.32E-03	1.32E-03	1.32E-03	1.32E-03	1.32E-03	1.32E-03	1.32E-03
1070	2.16E-02	1.61E-02	1.61E-03	1.61E-03	1.61E-03	4.06E-03	3.24E-03	3.24E-03	3.24E-03	3.24E-03	2.12E-03	1.32E-03	1.32E-03	1.32E-03	1.32E-03	1.32E-03	1.32E-03	1.32E-03	1.32E-03	1.32E-03	1.32E-03
1100	1.91E-02	1.91E-02	1.91E-03	1.91E-03	1.91E-03	4.06E-03	3.24E-03	3.24E-03	3.24E-03	3.24E-03	2.12E-03	1.32E-03	1.32E-03	1.32E-03	1.32E-03	1.32E-03	1.32E-03	1.32E-03	1.32E-03	1.32E-03	1.32E-03
1130	4.44E-02	1.03E-02	1.03E-03	1.03E-03	1.03E-03	4.06E-03	3.24E-03	3.24E-03	3.24E-03	3.24E-03	2.12E-03	1.32E-03	1.32E-03	1.32E-03	1.32E-03	1.32E-03	1.32E-03	1.32E-03	1.32E-03	1.32E-03	1.32E-03
1160	4.44E-02	1.03E-02	1.03E-03	1.03E-03	1.03E-03	4.06E-03	3.24E-03	3.24E-03	3.24E-03	3.24E-03	2.12E-03	1.32E-03	1.32E-03	1.32E-03	1.32E-03	1.32E-03	1.32E-03	1.32E-03	1.32E-03	1.32E-03	1.32E-03
1190	1.75E-02	1.75E-02	1.75E-03	1.75E-03	1.75E-03	4.06E-03	3.24E-03	3.24E-03	3.24E-03	3.24E-03	2.12E-03	1.32E-03	1.32E-03	1.32E-03	1.32E-03	1.32E-03	1.32E-03	1.32E-03	1.32E-03	1.32E-03	1.32E-03
1200	1.75E-02	1.75E-02	1.75E-03	1.75E-03	1.75E-03	4.06E-03	3.24E-03	3.24E-03	3.24E-03	3.24E-03	2.12E-03	1.32E-03	1.32E-03	1.32E-03	1.32E-03	1.32E-03	1.32E-03	1.32E-03	1.32E-03	1.32E-03	1.32E-03
1230	1.75E-02	1.75E-02	1.75E-03	1.75E-03	1.75E-03	4.06E-03	3.24E-03	3.24E-03	3.24E-03	3.24E-03	2.12E-03	1.32E-03	1.32E-03	1.32E-03	1.32E-03	1.32E-03	1.32E-03	1.32E-03	1.32E-03	1.32E-03	1.32E-03
1260	1.75E-02	1.75E-02	1.75E-03	1.75E-03	1.75E-03	4.06E-03	3.24E-03	3.24E-03	3.24E-03	3.24E-03	2.12E-03	1.32E-03	1.32E-03	1.32E-03	1.32E-03	1.32E-03	1.32E-03	1.32E-03	1.32E-03	1.32E-03	1.32E-03
1290	1.75E-02	1.75E-02	1.75E-03	1.75E-03	1.75																

NRL REPORT 8618

**Table A2 (Continued)**  
 (PROCESSED ON 08-11-14R-32)

NFMF		L65532		GK		SNI	
		RADIUS	PHOTUS	---	---	---	---
79	121	1.409	1.96E-02	8.78E-03	9.17E-03	4.82E-03	7.88
79	120	1.370	1.93E-02	5.41E-03	4.65E-03	4.44E-03	6.93
79	119	1.339	1.90E-02	5.02E-03	4.19E-03	4.19E-03	5.97
79	118	1.309	1.87E-02	4.64E-03	4.19E-03	4.19E-03	5.03
79	117	1.279	1.84E-02	4.25E-03	4.19E-03	4.19E-03	4.07
79	116	1.249	1.81E-02	3.85E-03	4.19E-03	4.19E-03	3.03
79	115	1.219	1.78E-02	3.46E-03	4.19E-03	4.19E-03	2.03
79	114	1.189	1.75E-02	3.07E-03	4.19E-03	4.19E-03	1.03
79	113	1.159	1.72E-02	2.68E-03	4.19E-03	4.19E-03	0.03
79	112	1.129	1.69E-02	2.30E-03	4.19E-03	4.19E-03	-0.97
79	111	1.099	1.66E-02	1.91E-03	4.19E-03	4.19E-03	-3.97
79	110	1.069	1.63E-02	1.52E-03	4.19E-03	4.19E-03	-7.97
79	109	1.039	1.60E-02	1.13E-03	4.19E-03	4.19E-03	-11.97
79	108	1.009	1.57E-02	7.44E-04	4.19E-03	4.19E-03	-15.97
79	107	9.70E+01	1.54E-02	3.55E-04	4.19E-03	4.19E-03	-19.97
79	106	9.40E+01	1.51E-02	2.16E-04	4.19E-03	4.19E-03	-23.97
79	105	9.10E+01	1.48E-02	1.77E-04	4.19E-03	4.19E-03	-27.97
79	104	8.79E+01	1.45E-02	1.38E-04	4.19E-03	4.19E-03	-31.97
79	103	8.49E+01	1.42E-02	9.99E-05	4.19E-03	4.19E-03	-35.97
79	102	8.19E+01	1.39E-02	6.10E-05	4.19E-03	4.19E-03	-39.97
79	101	7.89E+01	1.36E-02	2.21E-05	4.19E-03	4.19E-03	-43.97
79	100	7.59E+01	1.33E-02	8.32E-06	4.19E-03	4.19E-03	-47.97
79	99	6.29E+01	1.20E-02	3.43E-06	4.19E-03	4.19E-03	-51.97
79	98	5.99E+01	1.17E-02	9.54E-07	4.19E-03	4.19E-03	-55.97
79	97	5.69E+01	1.14E-02	5.75E-07	4.19E-03	4.19E-03	-59.97
79	96	5.39E+01	1.11E-02	2.16E-07	4.19E-03	4.19E-03	-63.97
79	95	5.09E+01	1.08E-02	8.37E-08	4.19E-03	4.19E-03	-67.97
79	94	4.79E+01	1.05E-02	4.58E-08	4.19E-03	4.19E-03	-71.97
79	93	4.49E+01	1.02E-02	2.79E-08	4.19E-03	4.19E-03	-75.97
79	92	4.19E+01	9.9E-03	1.20E-08	4.19E-03	4.19E-03	-79.97
79	91	3.89E+01	9.6E-03	6.21E-09	4.19E-03	4.19E-03	-83.97
79	90	3.59E+01	9.3E-03	3.42E-09	4.19E-03	4.19E-03	-87.97
79	89	3.29E+01	9.0E-03	1.83E-09	4.19E-03	4.19E-03	-91.97
79	88	2.99E+01	8.7E-03	1.04E-09	4.19E-03	4.19E-03	-95.97
79	87	2.69E+01	8.4E-03	6.65E-10	4.19E-03	4.19E-03	-99.97
79	86	2.39E+01	8.1E-03	4.86E-10	4.19E-03	4.19E-03	-103.97
79	85	2.09E+01	7.8E-03	3.87E-10	4.19E-03	4.19E-03	-107.97
79	84	1.79E+01	7.5E-03	2.88E-10	4.19E-03	4.19E-03	-111.97
79	83	1.49E+01	7.2E-03	1.89E-10	4.19E-03	4.19E-03	-115.97
79	82	1.19E+01	6.9E-03	1.10E-10	4.19E-03	4.19E-03	-119.97
79	81	8.9E+00	6.6E-03	6.11E-11	4.19E-03	4.19E-03	-123.97
79	80	5.9E+00	6.3E-03	3.22E-11	4.19E-03	4.19E-03	-127.97
79	79	2.9E+00	6.0E-03	1.33E-11	4.19E-03	4.19E-03	-131.97
79	78	1.9E+00	5.7E-03	7.44E-12	4.19E-03	4.19E-03	-135.97
79	77	1.6E+00	5.4E-03	4.55E-12	4.19E-03	4.19E-03	-139.97
79	76	1.3E+00	5.1E-03	2.66E-12	4.19E-03	4.19E-03	-143.97
79	75	1.0E+00	4.8E-03	1.77E-12	4.19E-03	4.19E-03	-147.97
79	74	7.0E-01	4.5E-03	8.88E-13	4.19E-03	4.19E-03	-151.97
79	73	4.0E-01	4.2E-03	4.99E-13	4.19E-03	4.19E-03	-155.97
79	72	1.0E-01	3.9E-03	2.10E-13	4.19E-03	4.19E-03	-159.97
79	71	6.0E-02	3.6E-03	1.21E-13	4.19E-03	4.19E-03	-163.97
79	70	3.0E-02	3.3E-03	6.22E-14	4.19E-03	4.19E-03	-167.97
79	69	1.0E-01	3.0E-03	3.33E-14	4.19E-03	4.19E-03	-171.97
79	68	6.0E-02	2.7E-03	1.44E-14	4.19E-03	4.19E-03	-175.97
79	67	3.0E-02	2.4E-03	7.55E-15	4.19E-03	4.19E-03	-179.97
79	66	1.0E-01	2.1E-03	4.66E-15	4.19E-03	4.19E-03	-183.97
79	65	6.0E-02	1.8E-03	2.77E-15	4.19E-03	4.19E-03	-187.97
79	64	3.0E-02	1.5E-03	1.88E-15	4.19E-03	4.19E-03	-191.97
79	63	1.0E-01	1.2E-03	1.00E-15	4.19E-03	4.19E-03	-195.97
79	62	6.0E-02	9.8E-04	6.11E-16	4.19E-03	4.19E-03	-199.97
79	61	3.0E-02	7.5E-04	3.22E-16	4.19E-03	4.19E-03	-203.97
79	60	1.0E-01	5.2E-04	1.33E-16	4.19E-03	4.19E-03	-207.97
79	59	6.0E-02	3.9E-04	7.44E-17	4.19E-03	4.19E-03	-211.97
79	58	3.0E-02	2.6E-04	4.55E-17	4.19E-03	4.19E-03	-215.97
79	57	1.0E-01	2.3E-04	2.66E-17	4.19E-03	4.19E-03	-219.97
79	56	6.0E-02	2.0E-04	1.77E-17	4.19E-03	4.19E-03	-223.97
79	55	3.0E-02	1.7E-04	1.00E-17	4.19E-03	4.19E-03	-227.97
79	54	1.0E-01	1.4E-04	6.11E-18	4.19E-03	4.19E-03	-231.97
79	53	6.0E-02	1.1E-04	3.22E-18	4.19E-03	4.19E-03	-235.97
79	52	3.0E-02	8.8E-05	2.00E-18	4.19E-03	4.19E-03	-239.97
79	51	1.0E-01	6.5E-05	1.21E-18	4.19E-03	4.19E-03	-243.97
79	50	6.0E-02	4.2E-05	7.44E-19	4.19E-03	4.19E-03	-247.97
79	49	3.0E-02	2.9E-05	4.55E-19	4.19E-03	4.19E-03	-251.97
79	48	1.0E-01	2.6E-05	3.00E-19	4.19E-03	4.19E-03	-255.97
79	47	6.0E-02	2.3E-05	2.00E-19	4.19E-03	4.19E-03	-259.97
79	46	3.0E-02	2.0E-05	1.33E-19	4.19E-03	4.19E-03	-263.97
79	45	1.0E-01	1.7E-05	9.00E-20	4.19E-03	4.19E-03	-267.97
79	44	6.0E-02	1.4E-05	6.11E-20	4.19E-03	4.19E-03	-271.97
79	43	3.0E-02	1.1E-05	4.55E-20	4.19E-03	4.19E-03	-275.97
79	42	1.0E-01	8.8E-06	3.22E-20	4.19E-03	4.19E-03	-279.97
79	41	6.0E-02	6.5E-06	2.00E-20	4.19E-03	4.19E-03	-283.97
79	40	3.0E-02	4.2E-06	1.33E-20	4.19E-03	4.19E-03	-287.97
79	39	1.0E-01	1.9E-06	9.00E-21	4.19E-03	4.19E-03	-291.97
79	38	6.0E-02	1.6E-06	6.11E-21	4.19E-03	4.19E-03	-295.97
79	37	3.0E-02	1.3E-06	4.55E-21	4.19E-03	4.19E-03	-299.97
79	36	1.0E-01	1.0E-06	3.22E-21	4.19E-03	4.19E-03	-303.97
79	35	6.0E-02	7.7E-07	2.00E-21	4.19E-03	4.19E-03	-307.97
79	34	3.0E-02	5.4E-07	1.33E-21	4.19E-03	4.19E-03	-311.97
79	33	1.0E-01	3.1E-07	9.00E-22	4.19E-03	4.19E-03	-315.97
79	32	6.0E-02	2.8E-07	6.11E-22	4.19E-03	4.19E-03	-319.97
79	31	3.0E-02	2.5E-07	4.55E-22	4.19E-03	4.19E-03	-323.97
79	30	1.0E-01	2.2E-07	3.22E-22	4.19E-03	4.19E-03	-327.97
79	29	6.0E-02	1.9E-07	2.00E-22	4.19E-03	4.19E-03	-331.97
79	28	3.0E-02	1.6E-07	1.33E-22	4.19E-03	4.19E-03	-335.97
79	27	1.0E-01	1.3E-07	9.00E-23	4.19E-03	4.19E-03	-339.97
79	26	6.0E-02	1.0E-07	6.11E-23	4.19E-03	4.19E-03	-343.97
79	25	3.0E-02	7.7E-08	4.55E-23	4.19E-03	4.19E-03	-347.97
79	24	1.0E-01	5.4E-08	3.22E-23	4.19E-03	4.19E-03	-351.97
79	23	6.0E-02	3.1E-08	2.00E-23	4.19E-03	4.19E-03	-355.97
79	22	3.0E-02	1.8E-08	1.33E-23	4.19E-03	4.19E-03	-359.97
79	21	1.0E-01	1.5E-08	9.00E-24	4.19E-03	4.19E-03	-363.97
79	20	6.0E-02	1.2E-08	6.11E-24	4.19E-03	4.19E-03	-367.97
79	19	3.0E-02	9.8E-09	4.55E-24	4.19E-03	4.19E-03	-371.97
79	18	1.0E-01	7.5E-09	3.22E-24	4.19E-03	4.19E-03	-375.97
79	17	6.0E-02	5.2E-09	2.00E-24	4.19E-03	4.19E-03	-379.97
79	16	3.0E-02	3.9E-09	1.33E-24	4.19E-03	4.19E-03	-383.97
79	15	1.0E-01	1.6E-09	9.00E-25	4.19E-03	4.19E-03	-387.97
79	14	6.0E-02	1.3E-09	6.11E-25	4.19E-03	4.19E-03	-391.97
79	13	3.0E-02	1.0E-09	4.55E-25	4.19E-03	4.19E-03	-395.97
79	12	1.0E-01	7.7E-09	3.22E-25	4.19E-03	4.19E-03	-399.97
79	11	6.0E-02	5.4E-09	2.00E-25	4.19E-03	4.19E-03	-403.97
79	10	3.0E-02	3.1E-09	1.33E-25	4.19E-03	4.19E-03	-407.97
79	9	1.0E-01	9.8E-09	9.00E-26	4.19E-03	4.19E-03	-411.97
79	8	6.0E-02	7.5E-09	6.11E-26	4.19E-03	4.19E-03	-415.97
79	7	3.0E-02	5.2E-09	4.55E-26	4.19E-03	4.19E-03	-419.97
79	6	1.0E-01	2.9E-09	3.22E-26	4.19E-03	4.19E-03	-423.97
79	5	6.0E-02	2.6E-09	2.00E-26	4.19E-03	4.19E-03	-427.97
79	4	3.0E-02	2.3E-09	1.33E-26	4.19E-03	4.19E-03	-431.97
79	3	1.0E-01	2.0E-09	9.00E-27	4.19E-03	4.19E-03	-435.97
79	2	6.0E-02	1.7E-09	6.11E-27	4.19E-03	4.19E-03	-439.97
79	1	3.0E-02	1.4E-09	4.55E-27	4.19E-03	4.19E-03	-443.97
79	0	1.0E-01	1.1E-09	3.22E-27	4.19E-03	4.19E-03	-447.97

PROGRAM A49NPL : AEROSOL DISTRIBUTION TABULATION  
NR:6532 ON SNI  
Radius ---> 5.03 5.97 6.93 7.88 8.83 9.78 10.73 11.68 12.63 13.58 14.53

79	122	1298	2.84E-02	1.67E-02	1.44E-02	8.19E-03	8.50E-03	6.18E-03	5.25E-03	3.94E-03	3.01E-03
	1290	2.68E-02	1.59E-02	1.51E-02	1.43E-02	8.93E-03	5.92E-03	5.66E-03	5.18E-03	2.79E-03	2.46E-03
	1300	2.59E-02	1.51E-02	1.59E-02	1.25E-02	8.85E-03	8.78E-03	5.85E-03	4.80E-03	8.62E-03	3.01E-03
	1310	2.52E-02	1.59E-02	1.28E-02	1.28E-02	7.65E-03	8.47E-03	5.19E-03	4.89E-03	2.84E-03	2.34E-03
	1400	2.66E-02	1.41E-02	1.36E-02	1.11E-02	7.45E-03	7.42E-03	4.85E-03	4.54E-03	2.72E-03	2.08E-03
	1430	2.44E-02	1.36E-02	1.36E-02	1.11E-02	7.45E-03	7.42E-03	4.85E-03	3.87E-03	3.51E-03	2.74E-03
	1500	2.32E-02	1.15E-02	1.06E-02	6.60E-03	5.75E-03	3.55E-03	3.55E-03	2.70E-03	2.32E-03	1.81E-03
	1530	2.06E-02	9.74E-02	8.78E-03	6.23E-03	5.97E-03	3.41E-03	3.03E-03	2.05E-03	1.43E-03	1.34E-03
	1600	2.13E-02	9.69E-03	9.21E-03	4.87E-03	6.04E-03	3.41E-03	3.01E-03	1.93E-03	1.65E-03	1.46E-03
	1630	2.53E-02	1.39E-02	1.15E-02	6.90E-03	6.21E-03	4.08E-03	3.07E-03	2.05E-03	1.55E-03	1.79E-03
	1700	2.13E-02	9.45E-02	9.32E-03	6.93E-03	6.28E-03	4.34E-03	4.48E-03	2.48E-03	2.38E-03	8.59E-04
	1730	2.82E-02	1.26E-02	1.08E-02	6.87E-03	6.11E-03	3.87E-03	3.39E-03	2.70E-03	1.89E-03	2.29E-03
	1800	2.83E-02	1.42E-02	1.16E-02	6.78E-03	6.78E-03	4.26E-03	4.42E-03	3.41E-03	2.10E-03	1.67E-03
	1830	3.9E-02	1.54E-02	1.22E-02	7.76E-03	7.42E-03	4.08E-03	4.08E-03	2.27E-03	2.10E-03	1.36E-03
	1900	3.96E-02	1.66E-02	1.52E-02	8.35E-03	8.35E-03	5.49E-03	4.89E-03	3.57E-03	2.36E-03	2.01E-03
	1930	4.94E-02	2.11E-02	2.05E-02	1.08E-02	1.27E-02	9.97E-03	6.92E-03	4.80E-03	4.27E-03	3.65E-03
	2000	4.19E-02	1.90E-02	1.84E-02	1.02E-02	1.02E-02	7.33E-03	6.35E-03	6.35E-03	4.44E-03	3.06E-03
	2030	4.62E-02	1.88E-02	1.88E-02	1.05E-02	1.05E-02	7.13E-03	6.35E-03	4.58E-03	3.08E-03	3.41E-03
	2100	4.29E-02	1.80E-02	1.77E-02	9.29E-03	9.74E-03	6.97E-03	4.94E-03	3.51E-03	3.27E-03	2.94E-03
	2130	4.38E-02	1.95E-02	1.86E-02	1.14E-02	1.21E-02	8.33E-03	6.33E-03	4.82E-03	3.84E-03	3.13E-03
	2200	4.23E-02	2.04E-02	1.85E-02	1.07E-02	1.07E-02	7.1E-03	5.35E-03	4.58E-03	3.17E-03	2.82E-03
	2230	4.62E-02	2.15E-02	2.16E-02	1.29E-02	1.16E-02	7.92E-03	5.75E-03	4.96E-03	3.89E-03	3.82E-03
	2300	4.77E-02	1.89E-02	1.97E-02	1.07E-02	1.07E-02	6.69E-03	6.85E-03	6.11E-03	4.56E-03	2.98E-03
	2330	5.32E-02	2.15E-02	2.03E-02	1.09E-02	1.08E-02	7.73E-03	6.99E-03	4.01E-03	3.17E-03	2.66E-03
79	123	0	5.90E-02	2.42E-02	2.56E-02	1.28E-02	1.30E-02	9.00E-02	6.56E-03	5.04E-03	3.96E-03
	30	6.17E-02	2.63E-02	2.69E-02	1.45E-02	1.32E-02	1.05E-02	1.05E-02	7.09E-03	5.6E-03	3.27E-03
	100	5.83E-02	2.39E-02	2.35E-02	1.26E-02	1.09E-02	9.05E-02	9.12E-02	6.65E-03	5.25E-03	2.51E-03
	130	5.96E-02	2.25E-02	2.44E-02	1.19E-02	1.44E-02	8.04E-02	9.48E-02	6.04E-03	4.24E-03	2.17E-03
	200	5.49E-02	2.07E-02	2.12E-02	1.04E-02	1.04E-02	8.04E-02	5.20E-03	5.20E-03	4.41E-03	2.84E-03
	230	4.84E-02	1.85E-02	1.84E-02	9.57E-03	8.93E-03	6.40E-03	5.18E-03	5.18E-03	2.84E-03	1.91E-03
	300	5.51E-02	1.95E-02	2.15E-02	1.03E-02	1.03E-02	6.46E-03	6.66E-03	3.77E-03	2.68E-03	1.77E-03
	330	5.129E-02	2.02E-02	2.08E-02	1.06E-02	1.06E-02	7.03E-03	5.20E-03	3.41E-03	2.89E-03	1.84E-03
	400	5.63E-02	1.92E-02	2.08E-02	1.07E-02	1.07E-02	6.90E-03	4.39E-03	3.84E-03	2.65E-03	2.27E-03
	450	6.02E-02	2.22E-02	2.31E-02	1.10E-02	1.10E-02	9.19E-03	8.59E-03	4.51E-03	2.48E-03	2.03E-03
	490	6.09E-02	2.32E-02	2.32E-02	1.13E-02	1.13E-02	9.16E-03	8.55E-03	4.58E-03	2.49E-03	2.13E-03
	530	5.75E-02	1.72E-02	1.72E-02	1.03E-02	1.03E-02	7.03E-03	6.95E-03	4.70E-03	2.75E-03	2.29E-03
	600	5.94E-02	1.78E-02	1.78E-02	1.04E-02	1.04E-02	7.15E-03	6.98E-03	4.73E-03	2.78E-03	2.32E-03
	630	4.53E-02	1.45E-02	1.45E-02	8.00E-03	8.00E-03	5.11E-03	5.11E-03	3.01E-03	1.46E-03	1.46E-03
	700	4.51E-02	1.41E-02	1.41E-02	8.04E-03	8.04E-03	5.14E-03	5.14E-03	3.04E-03	9.31E-04	9.31E-04
	730	5.51E-02	2.16E-02	2.16E-02	1.15E-02	1.15E-02	7.16E-03	6.60E-03	3.60E-03	1.74E-03	1.74E-03
	760	5.03E-02	1.83E-02	1.83E-02	2.01E-02	2.01E-02	7.15E-03	6.65E-03	3.62E-03	1.91E-03	1.91E-03
	800	5.74E-02	1.34E-02	1.34E-02	8.78E-03	8.78E-03	5.17E-03	5.17E-03	3.05E-03	9.79E-04	9.79E-04

AD-A121 369      RESULTS OF LASER-CALIBRATED HIGH-RESOLUTION  
TRANSMISSION MEASUREMENTS AND..(U) NAVAL RESEARCH LAB  
WASHINGTON DC   J A DOWLING ET AL. 30 SEP 82 NRL-8618

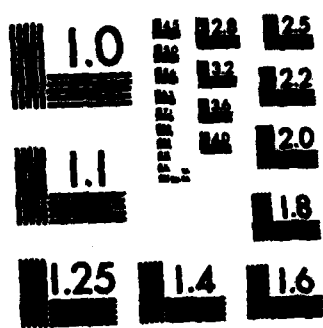
F/G 4/1

272

NL

UNCLASSIFIED





MICROCOPY RESOLUTION TEST CHART  
NATIONAL BUREAU OF STANDARDS-1963-A

Table A2 (Continued)  
(PROCESSED ON 08-MAR-82)

PROGRAM AGNRL : AEROSOL DISTRIBUTION TABULATION													
NPL:6532 ON SNI RADIUS -->		5.03	5.97	6.93	7.88	8.83	9.78	10.73	11.68	12.63	13.58	14.53	
79	123	900	2.84E-02	9.69E-03	4.37E-03	4.08E-03	2.46E-03	1.55E-03	1.15E-03	7.88E-04	4.06E-04	4.06E-04	
79	938	2.58E-02	9.89E-03	1.04E-02	5.15E-03	4.99E-03	4.18E-03	1.91E-03	1.86E-03	1.18E-03	6.12E-04	6.12E-04	
1039	2.73E-02	1.89E-02	1.07E-02	2.28E-02	3.77E-03	3.29E-03	4.51E-03	2.24E-03	2.82E-03	1.79E-03	6.44E-04	6.44E-04	
1039	2.04E-02	8.19E-03	6.55E-03	4.13E-03	5.55E-03	5.28E-03	5.75E-03	3.48E-03	1.50E-03	9.31E-04	5.01E-04	5.01E-04	
1160	1.92E-02	1.99E-02	8.83E-02	1.23E-02	6.83E-03	5.28E-03	5.75E-03	3.48E-03	1.79E-03	1.86E-03	5.35E-04	4.77E-04	
1130	2.47E-02	1.23E-02	1.23E-02	1.23E-02	7.95E-03	7.95E-03	1.91E-02	5.20E-03	3.75E-03	1.17E-03	6.68E-04	4.06E-04	
1260	4.39E-02	1.99E-02	1.99E-02	1.99E-02	8.57E-03	8.57E-03	1.91E-02	5.20E-03	3.75E-03	1.17E-03	6.68E-04	4.06E-04	
1239	7.25E-02	3.32E-02	3.51E-02	1.77E-02	1.77E-02	1.77E-02	1.16E-02	1.16E-02	1.20E-02	7.81E-03	3.89E-03	2.22E-03	
1300	8.79E-02	3.88E-02	4.16E-02	1.99E-02	1.99E-02	1.99E-02	1.62E-02	1.62E-02	1.62E-02	6.80E-03	3.04E-03	1.10E-03	
1338	7.53E-02	2.88E-02	2.88E-02	1.29E-02	1.29E-02	1.29E-02	1.86E-02	1.86E-02	1.86E-02	6.42E-03	3.94E-03	1.58E-03	
1400	4.89E-02	1.56E-02	1.56E-02	1.60E-02	6.35E-03	6.35E-03	6.35E-03	6.35E-03	6.35E-03	2.24E-03	1.65E-03	1.15E-03	
1439	2.50E-02	9.49E-03	9.49E-03	9.52E-03	3.99E-03	3.99E-03	3.99E-03	3.84E-03	3.53E-03	1.62E-03	1.41E-03	1.12E-03	
1539	1.92E-02	7.23E-02	5.51E-02	5.51E-02	3.96E-03	3.96E-03	3.96E-03	3.96E-03	3.96E-03	1.24E-03	6.44E-04	5.73E-04	
1600	1.70E-02	9.33E-02	5.59E-02	5.59E-02	3.39E-03	3.39E-03	2.98E-03	2.98E-03	2.98E-03	1.84E-03	6.00E-03	8.12E-03	
1700	1.42E-02	7.39E-02	4.39E-03	4.39E-03	2.98E-03	2.98E-03	1.72E-03	1.72E-03	1.59E-03	1.77E-04	1.91E-04	1.91E-04	
1739	1.19E-02	6.35E-03	4.30E-03	4.30E-03	3.08E-03	3.08E-03	2.17E-03	1.79E-03	1.24E-03	9.31E-04	7.88E-04	4.77E-04	
1800	1.93E-02	5.55E-03	5.55E-03	3.22E-03	2.91E-03	1.55E-03	1.55E-03	1.55E-03	1.08E-03	5.01E-04	5.01E-04	4.77E-04	
1839	9.32E-03	4.39E-03	5.51E-03	5.51E-03	3.32E-03	2.22E-03	1.95E-03	1.95E-03	1.58E-03	9.87E-04	7.64E-04	2.15E-04	
1900	9.93E-03	5.51E-03	3.03E-03	3.03E-03	2.10E-03	1.10E-03	1.10E-03	1.10E-03	8.59E-04	6.21E-04	2.63E-04	2.63E-04	
1939	8.95E-03	5.15E-03	3.739E-03	3.739E-03	2.41E-03	2.70E-03	1.48E-03	1.48E-03	1.22E-03	8.12E-04	5.49E-04	3.35E-04	
2000	1.40E-02	6.70E-03	4.56E-03	4.56E-03	2.67E-03	2.46E-03	1.46E-03	1.46E-03	1.21E-03	8.12E-04	5.38E-04	4.06E-04	
2039	1.40E-02	6.95E-03	6.95E-03	6.95E-03	3.53E-03	3.63E-03	1.79E-03	1.79E-03	1.62E-03	1.22E-03	8.35E-04	7.88E-04	
2100	1.29E-02	5.68E-03	6.88E-03	6.88E-03	2.65E-03	3.65E-03	1.53E-03	1.53E-03	1.89E-03	1.08E-03	6.92E-04	5.73E-04	
2139	1.11E-02	4.77E-03	4.49E-03	4.49E-03	2.98E-03	2.98E-03	1.34E-03	1.34E-03	1.15E-03	8.19E-04	3.58E-04	3.10E-04	
2200	1.41E-02	5.47E-03	5.54E-03	5.54E-03	3.32E-03	4.15E-03	2.05E-03	2.05E-03	1.27E-03	1.07E-03	5.01E-04	5.01E-04	
2239	1.74E-02	8.00E-03	7.90E-03	7.90E-03	4.08E-03	3.77E-03	2.72E-03	2.32E-03	1.65E-03	1.34E-03	9.39E-04	9.55E-04	
2300	1.61E-02	6.44E-03	5.82E-03	5.82E-03	3.22E-03	3.68E-03	2.58E-03	2.15E-03	1.24E-03	1.07E-03	9.31E-04	6.44E-04	
2339	1.71E-02	7.18E-03	7.14E-03	7.14E-03	3.84E-03	4.46E-03	2.48E-03	2.29E-03	1.77E-03	9.55E-04	6.92E-04	6.92E-04	
79	124	8	2.21E-02	9.15E-02	6.69E-03	5.38E-03	3.44E-03	2.98E-03	2.48E-03	1.60E-03	1.24E-03	1.24E-03	8.59E-04
79	38	8	2.97E-02	1.35E-02	1.89E-02	5.28E-03	5.95E-03	5.95E-03	5.95E-03	5.89E-03	2.48E-03	1.91E-03	2.18E-03
109	2.64E-02	1.15E-02	1.05E-02	1.05E-02	1.15E-02	1.15E-02	5.98E-03	4.03E-03	2.82E-03	1.69E-03	1.74E-03	9.79E-04	
139	2.61E-02	1.05E-02	1.05E-02	1.05E-02	1.15E-02	1.15E-02	5.98E-03	5.1E-03	2.55E-03	1.51E-03	1.43E-03	8.59E-04	
209	2.81E-02	1.65E-02	1.65E-02	1.65E-02	1.89E-02	1.89E-02	5.98E-03	5.08E-03	2.67E-03	1.58E-03	1.43E-03	9.55E-04	
239	2.95E-02	1.23E-02	1.23E-02	1.23E-02	1.35E-02	1.35E-02	6.16E-03	5.88E-03	4.01E-03	2.74E-03	1.36E-03	9.31E-04	
309	2.95E-02	1.23E-02	1.23E-02	1.23E-02	1.35E-02	1.35E-02	6.16E-03	5.88E-03	4.01E-03	2.74E-03	1.36E-03	9.31E-04	
339	3.38E-02	1.23E-02	1.23E-02	1.23E-02	1.43E-02	1.43E-02	6.37E-03	6.04E-03	4.46E-03	3.15E-03	2.10E-03	9.87E-04	
409	3.52E-02	1.18E-02	1.48E-02	6.61E-03	7.92E-03	4.99E-03	7.09E-03	4.99E-03	2.82E-03	1.69E-03	1.22E-03	1.34E-03	
439	4.22E-02	1.49E-02	1.84E-02	7.92E-03	7.92E-03	6.75E-03	7.35E-03	4.13E-03	3.29E-03	2.17E-03	1.72E-03	1.31E-03	
509	4.66E-02	1.61E-02	9.02E-03	9.02E-03	7.56E-03	7.56E-03	6.59E-03	6.59E-03	3.75E-03	2.89E-03	1.96E-03	1.22E-03	
539	4.22E-02	1.49E-02	8.21E-03	8.21E-03	6.21E-03	6.21E-03	4.08E-03	4.08E-03	2.89E-03	2.89E-03	1.48E-03	9.87E-04	
609	3.48E-02	1.16E-02	1.27E-02	6.09E-03	6.09E-03	4.58E-03	4.58E-03	2.65E-03	2.65E-03	2.15E-03	1.22E-03	8.12E-04	

Table A2 (Continued)  
 (PROCESSED ON 08-MAR-82)

PROGRAM A49NRL: AEROSOL DISTRIBUTION TABULATION													
NPL:6532 ON SNI RADIIUS --->		5.03	5.97	6.93	7.88	8.83	9.78	10.73	11.68				
79	124	630	2.09E-02	7.79E-03	8.16E-03	3.70E-03	3.25E-03	2.29E-03	1.43E-03	9.31E-04	6.44E-04	4.54E-04	4.30E-04
79	124	700	2.82E-02	5.04E-02	4.20E-02	5.08E-03	4.27E-03	3.44E-03	2.03E-03	1.74E-03	7.88E-04	9.07E-04	5.01E-04
79	124	730	1.79E-02	5.87E-03	6.28E-03	2.98E-03	2.94E-03	1.98E-03	1.22E-03	6.92E-04	5.73E-04	3.34E-04	
800	2.38E-02	9.26E-03	1.07E-02	5.04E-03	4.70E-03	3.37E-03	1.91E-03	1.58E-03	1.10E-03	6.68E-04	4.06E-04		
830	2.61E-02	1.02E-02	5.39E-03	5.16E-03	4.61E-03	3.15E-03	2.24E-03	1.69E-03	1.01E-03	6.21E-04	5.25E-04		
900	1.39E-02	5.29E-03	6.67E-03	2.36E-03	1.75E-03	1.17E-03	6.44E-04	5.25E-04	3.16E-04	1.91E-04			
930	1.40E-02	5.18E-03	4.73E-03	2.12E-03	1.69E-03	8.83E-04	8.35E-04	5.49E-04	2.39E-04	2.86E-04			
79	127	1230	2.82E-02	1.45E-02	1.11E-02	6.13E-03	6.59E-03	4.49E-03	3.94E-03	2.74E-03	2.44E-03	2.05E-03	1.29E-03
79	1300	2.89E-02	1.68E-02	1.04E-02	8.26E-03	6.87E-03	5.56E-03	4.70E-03	3.72E-03	3.72E-03	2.39E-03	1.69E-03	
1330	2.39E-02	1.79E-02	8.59E-03	9.31E-03	6.47E-03	5.18E-03	4.30E-03	3.15E-03	2.67E-03	2.67E-03	2.05E-03		
1400	2.43E-02	1.39E-02	9.95E-03	7.71E-03	5.75E-03	4.42E-03	3.72E-03	2.98E-03	2.67E-03	2.61E-03	1.50E-03		
1430	2.52E-02	1.62E-02	9.95E-03	8.31E-03	5.96E-03	4.23E-03	3.42E-03	2.68E-03	2.44E-03	2.44E-03	1.79E-03		
1500	2.28E-02	1.31E-02	8.74E-03	6.92E-03	6.92E-03	6.04E-03	6.68E-03	3.93E-03	3.93E-03	3.93E-03	1.41E-03		
1530	1.68E-02	1.11E-02	6.69E-03	5.98E-03	4.51E-03	3.49E-03	2.41E-03	2.55E-03	2.24E-03	2.24E-03	1.22E-03		
1600	1.48E-02	1.03E-02	6.04E-03	4.89E-03	4.15E-03	2.94E-03	2.51E-03	2.51E-03	1.60E-03	1.31E-03	9.31E-04		
1630	1.60E-02	1.15E-02	5.35E-03	5.35E-03	3.39E-03	2.94E-03	2.15E-03	1.41E-03	1.36E-03	7.40E-04	6.59E-04		
1700	1.63E-02	1.18E-02	6.35E-03	6.06E-03	4.44E-03	3.68E-03	6.05E-03	5.55E-03	2.27E-03	1.67E-03			
1730	1.74E-02	1.18E-02	5.85E-03	5.49E-03	4.77E-03	3.76E-03	2.86E-03	2.36E-03	1.79E-03	1.38E-03	1.10E-03		
1800	1.37E-02	1.06E-02	4.87E-03	5.30E-03	3.53E-03	3.51E-03	2.05E-03	2.05E-03	1.69E-03	1.65E-03	9.07E-04		
1830	2.14E-02	1.43E-02	7.39E-03	7.28E-03	5.20E-03	4.88E-03	3.13E-03	2.12E-03	1.84E-03	1.27E-03	1.07F-03		
1900	2.45E-02	1.45E-02	9.26E-03	6.78E-03	6.37E-03	3.82E-03	3.82E-03	2.29E-03	1.91E-03	1.27E-03	1.10E-03		
1930	1.89E-02	1.89E-02	7.47E-03	4.63E-03	5.56E-03	3.29E-03	2.91E-03	1.89E-03	1.46E-03	1.31E-03	9.31E-04		
2000	1.31E-02	8.55E-03	6.61E-03	4.75E-03	3.91E-03	2.96E-03	2.46E-03	1.50E-03	1.29E-03	9.55E-04	1.00E-03		
79	128	930	5.63E-03	4.15E-03	2.03E-03	1.84E-03	1.49E-03	1.17E-03	1.17E-03	6.44E-04	5.73E-04	2.63E-04	
79	960	5.85E-03	5.28E-03	4.93E-03	2.77E-03	2.60E-03	1.65E-03	1.52E-03	1.12E-03	9.79E-04	6.44E-04	3.58E-04	
1030	8.38E-03	7.14E-03	3.75E-03	4.28E-03	2.32E-03	3.75E-03	1.86E-03	1.43E-03	1.10E-03	1.03E-03	6.73E-04		
1100	9.71E-03	8.02E-03	5.11E-03	5.49E-03	4.20E-03	3.46E-03	2.99E-03	2.84E-03	2.27E-03	1.34E-03	1.17E-03		
1130	1.25E-02	1.02E-02	5.92E-03	6.16E-03	4.20E-03	3.99E-03	2.94E-03	2.84E-03	1.84E-03	1.49E-03	1.24E-03		
1200	1.35E-02	9.95E-03	6.95E-03	6.25E-03	4.56E-03	3.99E-03	2.94E-03	2.94E-03	1.84E-03	1.49E-03	1.50E-03		
1230	1.55E-02	1.23E-02	8.28E-03	7.97E-03	6.37E-03	5.44E-03	3.72E-03	3.98E-03	2.34E-03	2.15E-03	1.67E-03		
1300	1.63E-02	1.32E-02	1.07E-02	9.81E-03	6.73E-03	5.18E-03	3.18E-03	3.96E-03	2.03E-03	2.74E-03	2.03E-03		
1330	2.32E-02	1.98E-02	1.44E-02	1.20E-02	9.12E-03	7.69E-03	6.23E-03	5.18E-03	3.99E-03	3.72E-03	2.82E-03		
1400	2.43E-02	1.79E-02	1.57E-02	1.44E-02	1.30E-02	1.05E-02	9.67E-03	6.73E-03	5.30E-03	3.89E-03	3.44E-03		
1430	3.14E-02	2.29E-02	1.95E-02	1.73E-02	1.57E-02	1.32E-02	1.05E-02	9.12E-03	6.59E-03	5.61E-03	5.01E-03		
1500	3.66E-02	2.52E-02	2.32E-02	1.73E-02	1.86E-02	1.37E-02	1.08E-02	7.88E-03	6.44E-03	5.94E-03	5.59E-03		
1530	3.66E-02	2.58E-02	2.45E-02	1.85E-02	1.69E-02	1.33E-02	1.07E-02	7.95E-03	6.82E-03	5.88E-03	5.65E-03		
1600	3.56E-02	3.48E-02	2.87E-02	2.37E-02	1.81E-02	1.66E-02	1.25E-02	1.10E-02	8.83E-03	7.92E-03	6.97E-03		
1630	4.27E-02	3.49E-02	2.87E-02	2.37E-02	1.81E-02	1.66E-02	1.24E-02	1.10E-02	8.21E-03	7.26E-03	8.21E-03		
1700	4.90E-02	3.51E-02	2.39E-02	2.14E-02	1.71E-02	1.17E-02	1.03E-02	1.03E-02	9.00E-03	8.21E-03	7.88E-03		
1730	5.03E-02	3.61E-02	3.39E-02	2.14E-02	1.71E-02	1.17E-02	1.03E-02	1.03E-02	9.00E-03	8.21E-03	7.88E-03		

Table A2 (Concluded)  
(PROCESSED ON 08-MAR-82)

PROGRAM A49NRL: AEROSOL DISTRIBUTION TABULATION		(PROCESSED ON 08-MAR-82)											
NRL:6532 ON SNI RADIUS ->	5.03	5.97	6.93	7.88	8.83	9.78	10.73	11.68	12.63	13.58	14.53		
79 128 1888	4.97E-02	4.08E-02	3.30E-02	2.77E-02	2.05E-02	1.49E-02	1.04E-02	7.78E-03	6.16E-03	4.51E-03	4.82E-03		
79 129 630	4.34E-02	3.55E-02	2.20E-02	1.87E-02	1.56E-02	1.28E-02	9.43E-03	7.54E-03	6.18E-03	5.25E-03	4.46E-03		
79 129 788	4.22E-02	3.22E-02	2.05E-02	1.90E-02	1.80E-02	1.59E-02	1.39E-02	1.24E-02	1.01E-02	8.01E-03	5.32E-03	4.22E-03	
79 129 739	3.87E-02	3.05E-02	2.53E-02	1.96E-02	1.69E-02	1.61E-02	1.42E-02	9.40E-03	6.14E-03	5.94E-03	4.99E-03	3.92E-03	
800 800	3.95E-02	2.52E-02	2.32E-02	1.76E-02	1.37E-02	1.15E-02	9.40E-03	6.18E-03	5.92E-03	4.99E-03	3.92E-03	4.39E-03	
838 838	3.53E-02	2.57E-02	2.34E-02	1.90E-02	1.52E-02	1.49E-02	1.34E-02	9.40E-03	8.26E-03	6.04E-03	4.73E-03	3.39E-03	
908 908	3.97E-02	2.35E-02	1.97E-02	1.87E-02	1.49E-02	1.38E-02	9.21E-03	7.21E-03	5.63E-03	4.99E-03	3.89E-03	3.56E-03	
1000 1000	3.77E-02	2.34E-02	1.62E-02	1.42E-02	1.06E-02	8.04E-03	6.44E-03	5.04E-03	4.54E-03	3.22E-03	2.67E-03		
1030 1030	3.55E-02	2.20E-02	1.56E-02	1.18E-02	9.7E-03	6.83E-03	5.82E-03	4.58E-03	3.63E-03	2.94E-03	2.32E-03		
1198 1198	3.33E-02	2.29E-02	1.46E-02	1.22E-02	9.85E-03	7.14E-03	6.06E-03	4.56E-03	3.75E-03	2.94E-03	2.58E-03		
1130 1130	3.49E-02	2.19E-02	1.68E-02	1.28E-02	9.85E-03	7.14E-03	6.11E-03	6.87E-03	4.59E-03	3.80E-03	2.84E-03	2.01E-03	
1200 1200	3.78E-02	2.54E-02	1.68E-02	1.38E-02	1.10E-02	8.04E-03	6.84E-03	5.18E-03	5.85E-03	4.28E-03	2.53E-03		
1230 1230	4.27E-02	2.59E-02	1.99E-02	1.36E-02	1.36E-02	1.34E-02	9.09E-03	7.38E-03	5.95E-03	4.99E-03	3.60E-03	2.84E-03	
1300 1300	4.29E-02	2.54E-02	1.82E-02	1.38E-02	1.38E-02	1.35E-02	9.02E-03	6.92E-03	5.54E-03	4.63E-03	3.65E-03	2.84E-03	
1330 1330	3.33E-02	2.29E-02	1.55E-02	1.22E-02	1.04E-02	8.57E-03	6.68E-03	5.49E-03	4.92E-03	3.75E-03	3.15E-03		
1400 1400	3.88E-02	2.59E-02	1.81E-02	1.46E-02	1.24E-02	1.04E-02	7.66E-03	5.61E-03	4.56E-03	3.83E-03	3.10E-03		
1430 1430	4.18E-02	2.63E-02	1.90E-02	1.48E-02	1.34E-02	1.06E-02	7.30E-03	6.14E-03	5.28E-03	4.22E-03	3.65E-03		
1500 1500	4.06E-02	2.62E-02	1.78E-02	1.48E-02	1.10E-02	9.67E-03	8.21E-03	5.82E-03	4.94E-03	4.25E-03	3.82E-03		
1530 1530	4.16E-02	2.89E-02	1.88E-02	1.55E-02	1.31E-02	1.31E-02	9.93E-03	7.88E-03	5.54E-03	4.51E-03	3.27E-03		
1600 1600	4.32E-02	2.95E-02	1.95E-02	1.62E-02	1.31E-02	1.05E-02	8.69E-03	6.92E-03	6.92E-03	5.54E-03	4.58E-03	3.60E-03	
1630 1630	4.09E-02	2.63E-02	1.52E-02	1.35E-02	1.35E-02	9.71E-03	7.54E-03	6.92E-03	4.49E-03	3.89E-03	3.60E-03		
1700 1700	3.43E-02	2.37E-02	1.51E-02	1.44E-02	1.21E-02	1.06E-02	8.62E-03	6.92E-03	5.62E-03	4.44E-03	3.99E-03	2.67E-03	
1730 1730	2.96E-02	2.27E-02	1.40E-02	1.27E-02	8.21E-03	7.09E-03	5.59E-03	4.44E-03	3.25E-03	2.60E-03			
1800 1800	3.27E-02	2.46E-02	1.41E-02	1.43E-02	1.08E-02	8.57E-03	6.49E-03	5.32E-03	4.44E-03	2.72E-03	2.79E-03		
1830 1830	3.55E-02	2.54E-02	1.59E-02	1.43E-02	1.10E-02	8.74E-03	6.75E-03	5.28E-03	4.30E-03	3.32E-03	3.06E-03		
1900 1900	3.19E-02	2.33E-02	1.53E-02	1.37E-02	1.09E-02	8.99E-03	7.30E-03	4.82E-03	4.54E-03	3.29E-03	2.70E-03		
1930 1930	3.73E-02	2.43E-02	1.62E-02	1.32E-02	1.05E-02	7.47E-03	6.54E-03	4.44E-03	4.58E-03	3.03E-03	2.63E-03		
2000 2000	3.82E-02	2.26E-02	1.36E-02	1.08E-02	8.19E-03	6.66E-03	5.06E-03	4.42E-03	3.72E-03	2.91E-03	2.74E-03		
2030 2030	3.83E-02	2.35E-02	1.78E-02	1.27E-02	1.02E-02	7.78E-03	6.64E-03	4.42E-03	3.72E-03	2.92E-03	2.81E-03		
79 130 600	1.59E-01	6.93E-02	7.32E-02	3.95E-02	3.42E-02	2.05E-02	1.49E-02	1.66E-02	1.65E-02	1.27E-02	8.45E-03	4.96E-03	
79 130 630	2.19E-01	9.37E-02	9.34E-02	5.02E-02	4.28E-02	3.50E-02	2.08E-02	1.58E-02	1.19E-02	7.02E-02	6.06E-03		
79 130 700	1.86E-01	8.15E-02	8.04E-02	3.60E-02	3.75E-02	2.52E-02	1.69E-02	1.08E-02	1.02E-02	6.68E-03	5.13E-03	2.98E-03	
79 130 730	1.04E-01	4.08E-02	4.05E-02	1.79E-02	1.79E-02	1.16E-02	1.40E-02	1.40E-02	1.12E-02	4.51E-03	2.60E-03	2.36E-03	
79 130 800	5.51E-02	2.11E-02	2.11E-02	8.40E-03	8.41E-03	5.39E-03	5.39E-03	5.39E-03	1.10E-02	1.07E-03	8.59E-04		
79 130 830	2.67E-02	8.45E-03	7.54E-03	2.67E-03	2.61E-03	1.62E-03	1.62E-03	1.62E-03	1.25E-03	1.08E-03	9.07E-04		
79 130 900	2.79E-02	7.85E-03	8.50E-03	2.98E-03	2.95E-03	1.79E-03	1.79E-03	1.79E-03	1.21E-03	1.08E-03	9.57E-04		
79 130 930	2.03E-02	5.66E-03	5.599E-03	2.65E-03	1.62E-03	8.12E-03	8.12E-03	8.12E-03	1.19E-03	1.09E-03	1.67E-04		
1000 1000	2.40E-02	6.92E-03	7.49E-03	2.72E-03	2.36E-03	1.53E-03	1.53E-03	1.53E-03	7.40E-04	6.82E-04	1.67E-04		
1030 1030	2.47E-02	7.95E-03	9.19E-03	2.22E-03	2.88E-03	2.08E-03	2.08E-03	2.08E-03	9.79E-04	6.92E-04	3.58E-04		
1100 1100	1.90E-02	5.85E-03	6.23E-03	2.63E-03	1.86E-03	1.15E-03	6.21E-04	6.92E-04	4.77E-04	2.15E-04	9.55E-05		